

HEAT FLOW IN THE SOLIDIFICATION
OF CASTINGS

by

CLYDE MELVIN ADAMS, JR.

S.B., Massachusetts Institute of Technology

(1949)

M.S., Massachusetts Institute of Technology

(1950)

SUBMITTED IN PARTIAL FULFILLMENT
OF THE REQUIREMENTS FOR THE
DEGREE OF DOCTOR OF
SCIENCE

at the

MASSACHUSETTS INSTITUTE OF
TECHNOLOGY

June, 1953

Signature of Author.....
Department of Metallurgy, May 18, 1953

Certified by.....
Thesis Supervisor

Accepted by.....
Chairman, Departmental Committee
on Graduate Students

HEAT FLOW IN THE SOLIDIFICATION OF CASTINGS

By

Clyde Melvin Adams, Jr.

Submitted to the Department of Metallurgy on May 18, 1953,
in partial fulfillment of the requirements
for the degree of Doctor of Science.

ABSTRACT

A theoretical study has been made of the factors which control the rate of heat flow from solidifying sand and chill castings. The investigation has been focussed on three shapes of high symmetry: spherical, cylindrical, and slab-shaped castings.

An evaluation of Chvorinov's Rule for sand castings (freezing time proportional to the ratio, squared, of volume to surface area) indicates that this simplified relationship is valid only for comparing castings having similar shapes. More precise expressions are presented for the three basic shapes. For purposes of calculation, it is shown that: (1) Superheat may be accurately added, calorifically, to the latent heat of fusion. (2) Alloys which freeze over wide ranges of temperature, and which evolve their latent heat uniformly over this range, have an "effective" melting point one-fifth of the way from the solidus to the liquidus.

For certain idealized boundary conditions, the more complicated

See Adams (Metall.) Feb. 15, 1953

problems of chill castings are amenable to analysis by an iterative procedure, which yields freezing rates in terms of power series. The known, exact solution for one-dimensional solidification may be developed in this fashion, and two- and three-dimensional systems, for which exact solutions are not known, may also be handled. The iterative procedure is further used to study the effect of thermal contact resistance at the mold-metal interface.

In studying practical chill casting problems, the following results are significant: (1) Contact resistance is of controlling importance in small chill castings. (2) Contact resistance ("air-gap" formation) has only a minor effect on freezing rates of large steel ingots. (3) A useful, accurate simplification is permissible for small castings of aluminum-, copper-, and magnesium-base castings, poured in ferrous molds. (4) Under idealized conditions, precise study of alloy solidification from a chill mold is feasible. Such a study indicates that thermal conditions depend largely upon total heat of fusion and thermal conductivity, and only slightly upon the mechanism of solidification.

Thesis Supervisor: Howard F. Taylor

Title: Professor of Metallurgy

TABLE OF CONTENTS

<u>Section No.</u>		<u>Page No.</u>
	Abstract	i
	List of Illustrations.	vi
	List of Tables	viii
	Acknowledgements	ix
I	Introduction	1
II	Review of the Literature	3
III	Analysis of Heat Flow From Sand Castings	8
IV	Analysis of Heat Flow From Chilled Castings:	
	Constant Casting Surface Temperature	25
	A. Solidification From a Plane Chilled Surface. . .	27
	B. Solidification From a Spherical Chilled Surface.	40
	C. Solidification From a Cylindrical Chilled Surface.	45
	D. Numerical Values: Freezing Rates and Times of Spheres and Cylinders.	47
	E. Total Heat Removed During the Solidification of Chilled Castings	52
V	Analysis of Heat Flow From Chilled Castings: Metals Cast Into Metal Molds	76

<u>Section No.</u>		<u>Page No.</u>
	A. Plane Mold Wall	76
	1. Perfect Thermal (Wetted) Contact Between the Metal and the Mold.	76
	2. The Effect of Thermal Contact Resistance Between the Metal and the Mold.	78
	B. Spherical and Cylindrical Mold Walls; Non-Wetting Contact	88
	1. Heat Flow Into Metal Molds.	88
	2. Solidification of Lead in a Cast Iron Cylinder; Conductivities of Metal and of Mold Approximately Equal.	93
	3. Solidification of Copper and Aluminum in a Cast Iron Mold; Conductivity of Metal Much Greater Than Conductivity of Mold	96
VI	Heat Flow During Solidification of Cast Alloys Which Freeze Over Wide Temperature Ranges	109
	A. Chilled Casting: Aluminum - 4 Per Cent Copper Cast Against a Flat Copper Mold Wall	109
	B. Sand Casting	118
VII	Conclusions.	123
VIII	Suggestions For Further Work	126

<u>Section</u> <u>No.</u>		<u>Page</u> <u>No.</u>
	Bibliography	127
	Biographical Note.	129

LIST OF ILLUSTRATIONS

<u>Figure No.</u>		<u>Page No.</u>
1	Deviation Between Exact and Approximate Expressions for Cylindrical Heat Flow	24
2	Linear Freezing Parabolic Rate Constants	61
3	Inverse Freezing Rates of Spheres	62
4	Inverse Freezing Rates of Spheres	63
5	Complete Solidification Times for Spheres	64
6	Inverse Freezing Rates of Cylinders	65
7	Inverse Freezing Rates of Cylinders	66
8	Complete Solidification Times for Cylinders	67
9	Rates of Heat Removal from Solid Portions of Freezing Spheres	68
10	Rates of Heat Removal from Solid Portions of Freezing Spheres	69
11	Ratio of Specific to Latent Heat Removed During Complete Solidification of Spheres	70
12	Rates of Heat Removal from Solid Portions of Freezing Cylinders	71
13	Rates of Heat Removal from Solid Portions of Freezing Cylinders	72
14	Ratio of Specific to Latent Heat Removed During Complete Freezing of Cylinders	73

<u>Figure No.</u>		<u>Page No.</u>
15	Ratio of Specific to Latent Heat Removed from Spheres, Cylinders, and Slabs During Complete Solidification	74
16	One-Dimensional Inverse Freezing Rate with Contact Resistance	101
17	Freezing Times for Partially Frozen Cylinders	102
18	Freezing Times for Partially Frozen Cylinders	103
19	Equation (47): Lead in Cast Iron	104
20	Lead Freezing in Cast Iron Cylinder	105
21	Copper Freezing in Cast Iron Cylinder	106
22	Aluminum Freezing in Cast Iron Cylinder	107
23	Solidification Curves for Duralumin Obtained at Various Pouring Temperatures	108
24	Heat Content of Al - 4% Cu Alloy vs. Temperature	121
25	Temperature Distribution in Aluminum Cast Against a Copper Mold	122

LIST OF TABLES

<u>Table No.</u>		<u>Page No.</u>
I	Definition of Terms	22
II	Definition of Terms Not Included in Table I	59
III	Thermal Properties of Steel	87
IV	Thermal Properties of Cast Metals Used in Calculations	95
IV-A	Thermal Properties of a Cast Iron Mold	95
V	Definition of Terms Not Included in Tables I and II	100
VI	Physical Values for Aluminum - 4 Per Cent Copper Alloy	110
VII	Definition of Terms Not Included in Tables I, II, and	120

ACKNOWLEDGEMENTS

The author would like to express his sincerest appreciation to Professor Howard F. Taylor, and the Foundry group in the Metals Processing Laboratory, for generating the favorable environment in which this unsponsored investigation could be conducted. The author also wishes to thank his wife, Theresa, for her assistance in drafting the numerous Figures which were required.

I. INTRODUCTION

The primary objective of the work has been to collect, clarify, or establish the quantitative relationships which govern the heat flow problems associated with the freezing of metals. Preliminary experimental work and perusal of the literature indicated a greater need for (and profit from) analytical effort than measurement. Some of the basic characteristics of the problems have not been appreciated well enough to permit full interpretation of the vast amount of experimental data obtained in this field.

Mathematical treatments of the problem have, in general, been limited to idealized one-dimensional, semi-infinite systems involving pure metals, which are difficult to assess in terms of experimental results. In particular, the effects of such realistic factors as thermal contact resistance at the mold-metal interface, and the presence of alloying elements, have been the subject of much speculation, experimentation, and dispute. The observation that some data agree well with mathematical solutions (e.g. solidification of steel ingots), whereas others do not (non-ferrous ingots), leads most investigators to regard any mathematical approach with suspicion.

Sections III, IV, and V of the thesis treat of pure metals, or alloys which freeze over a narrow temperature range, while Section VI considers the application of "pure metal" equations to the solidification of alloys having wide freezing ranges. Part of the study merely involves the application of known heat transfer relationships to a

specialized class of problems. This is particularly true of the section on sand castings. The remainder of the investigation is concerned with regions for which general mathematical solutions are not known.

II. REVIEW OF THE LITERATURE

The earliest studies of solidification heat flow problems dealt, analytically, with the rate of polar ice formation. Franz Neumann appears to have been the first to show that the error function solution of the differential equation for linear heat conduction would conform to solidification boundary conditions. Neumann's solution predicts temperature distributions and thickness of ice formed as a function of time, when the surface of a large body of water is lowered to a temperature below the freezing point. The solution predicts that the thickness of ice should be proportional to the square root of time, for unidirectional freezing. Using this relationship in conjunction with observed data on ice formation, Neumann obtained a value for the conductivity of ice within ten per cent of the currently accepted value. Most subsequent solutions of this and related heat flow problems have duplicated, in principle, the technique devised by Neumann; the solution is described in Carslaw and Jaeger.¹

The solidification rate of steel in an ingot mold was first studied by Feild.² The reasoning is difficult to follow, but Feild also arrived at a parabolic relationship (Feild's formula) between thickness solidified and time. Lightfoot³ has obtained solutions for the same problem by considering the solidification front as a moving source of heat, an analytical technique somewhat more general than that of Neumann. Lightfoot's solution was the first to rigorously combine the properties of the metal and the mold. C. Schwarz⁴ has presented a solution identical

with that of Lightfoot, based upon the method of Neumann. The findings of Schwarz and Lightfoot do not agree with those of Feild. All of the above solutions apply for semi-infinite conditions, perfect thermal contact between metal and mold, and unidirectional solidification. All predict a parabolic relationship between thickness of solid metal and time.

Although much simpler, analytically, the heat flow problems in sand casting have only been considered separately by Chvorinov.⁵ Chvorinov simplifies the problem by neglecting any temperature gradients in the casting, and assuming that the heated zone in the sand is relatively shallow (contour effects are neglected). The solution applicable under these conditions is that for heating a semi-infinite solid (the mold) from a constant temperature surface (the casting). On this basis, Chvorinov concludes that the time for complete freezing should be proportional to:

$$\left(\frac{\text{Casting Volume}}{\text{Casting Surface Area}} \right)^2$$

Chvorinov partially verifies his conclusions with temperature measurements in steel castings and sand molds.

In addition to the mathematical studies, three classes of experimental data have been collected, all within the last 25 years. The simplest, most direct, and in some cases the most accurate device has been the widely used pour-out test. For those studies to which pour-out techniques are not applicable, thermal analysis has proved valuable. More recently the use of an electrical analogue has met with moderate

success.⁶ An excellent review of the existing data on sand castings has been made by Ruddle.⁷

Pour-out tests have been employed to study solidification of steel ingots by Matushka,⁸ Nelson,⁹ Chipman and FonDersmith,¹⁰ and Spretnak.¹¹ In general, the findings of these investigators are in agreement for the early stages of solidification. It is found that the relationship,

$$x' = a\sqrt{\theta} - b$$

describes thickness, "x'", as a function of time, "θ". When the units are inches and minutes,

$$0.9 < a < 1.1$$

and

$$0 < b < 0.5$$

Cast iron ingot molds were used in all cases. The constant, "b", is considered to result from a delayed start of solidification due to the presence of superheat. The constant, "a", agrees well with the theoretical values obtained by C. Schwarz⁴ and Lightfoot.³

Alexander¹² has used the pour-out technique to study the solidification of aluminum ingots in cast iron molds. The results of this investigation indicated much larger values for both "a" and "b", and are discussed further in Section V. Heat transfer in the solidification of non-ferrous chill castings has received very little attention.

In the field of sand casting, Briggs and Gezelius,¹³ Troy,¹⁴ Clark,¹⁵ and many others have investigated steel castings by means of

pour-out tests, and Hunsicker¹⁶ has done the same with aluminum. Data obtained in this fashion are not as satisfactory for sand castings as for chill castings. Gradients tend to be much less pronounced in sand castings; thus a very small freezing range can result in an appreciable "mushy" zone. Only poor thermal conductors with high melting points (e.g. steel), or very pure metals, give reliable information from pour-out tests on sand castings. Even with steel, only the early stages of solidification have been successfully investigated, yielding results which agree moderately well with Chvorinov's theoretical relationship. Hunsicker,¹⁶ using 99.8 per cent aluminum, obtained poor agreement between pour-out tests and thermal analysis. With more than one-half per cent nickel, silicon, or copper in aluminum, pour-out tests failed completely.

The only satisfactory experimental means for studying alloys which freeze over wide temperature ranges is provided by thermal analysis. Although several investigators have made limited thermal studies of sand and chill castings,^{5,8,13,16,17} the most extensive contributions have been made by Pellini, et. al.¹⁸ at the Naval Research Laboratory. Of particular value was the NRL work on steel ingots, because, for the first time, reliable information on the final stages of solidification was obtained. An increase in linear freezing rates was observed near the end of solidification. The parabolic rate constant, "a", for the early stages of freezing was about 1.0 inch/ $\sqrt{\text{minutes}}$. Pellini has also presented data on chill and sand cast grey iron, aluminum, and bronze. All of the work was carried out on 7 by 7 by 20 inch rectangular solid castings.

Although the data are very detailed and extensive, they have not been interpreted in other than qualitative terms. Careful study of this data indicates that for high purity metals, chill cast, thermal analysis is not as precise a measurement as the pour-out technique. Thermal analysis is preferable for impure, sand cast metals having high thermal conductivity.

The Heat and Mass Flow Analyzer at Columbia University has been initiated on a long-range program to study casting solidification under the direction of Paschkis.⁶ The analyzer is an analogue device, substituting electrical for thermal resistance, capacitance, and potential. The problems of leakage and manually introducing heat of fusion into the circuit, have interfered seriously with the success of this approach.

In conclusion, it may be observed that the field of solidification heat transfer is currently rich in experimental data, but lacks quantitative interpretation.

III. ANALYSIS OF HEAT FLOW FROM SAND CASTINGS

(Pure metals and alloys which freeze completely within a narrow temperature range.)

In this section, solutions are considered which are all based upon one simplification: it is assumed that the thermal conductivity of a cast metal is much greater than that of a sand mold. In a particular problem, the validity of this assumption may be tested by using relationships obtained in later sections. In this way it can be shown that solutions given below are quite valid for copper- and aluminum-base castings, but that small errors may be introduced in the case of cast steel.

The above assumption greatly reduces the complexity of the heat conduction problems for sand castings in two ways: (1) The temperature gradients in the casting are very small, and thus the surface temperature of the casting is constant and nearly equal to the melting point of the metal. (2) Since, during freezing, the solid part of the casting does not cool appreciably below the melting point, only heat of fusion is removed from the casting. In addition, since the rate of heat flow is very low, there is no temperature drop across the mold-metal interface; i.e. the surface temperature of the mold equals the surface temperature of the casting. None of the above statements would be true, in general, for metals cast into metal molds.

From the present point of view, the essential heat flow problem may

$$\frac{1}{\alpha} \frac{\partial T}{\partial \theta} = \frac{\partial^2 T}{\partial x^2} \quad (1)$$

$$\frac{T_s - T}{T_s - T_\infty} = \operatorname{erf} \frac{x}{2\sqrt{\alpha\theta}} \quad (2)$$

$$\left. \frac{q}{A_s} \right|_{x=0} = -K \left. \frac{\partial T}{\partial x} \right|_{x=0} \quad (3)$$

$$\left. \frac{q}{A_s} \right|_{x=0} = -\frac{K(T_s - T_\infty)}{\sqrt{\pi\alpha\theta}} \quad (4)$$

$$\frac{Q}{A_s} = \frac{2K(T_s - T_\infty)\sqrt{\theta}}{\sqrt{\pi\alpha}} \quad (5)$$

$$\frac{Q}{A_s} = X' \rho' H \quad (6)$$

$$T_s \cong T_m \quad (7)$$

$$X' = \frac{2}{\sqrt{\pi}} \left(\frac{T_m - T_\infty}{\rho' H} \right) \sqrt{K\rho C_p} \sqrt{\theta} \quad (8)$$

be stated as follows: The mold is initially at room temperature, " T_r ". At zero time the surface of the mold cavity is instantly raised to a high temperature, " T_s ", and held constant throughout solidification. Three cases are considered: plane-walled, spherical, and cylindrical mold cavities. Definitions of all symbols used in the analysis are included in Table I.

Consider first the flow of heat from a plane-walled mold cavity (an infinite slab). This is a repetition of the solution used by Chvorinov for mold cavities of all shapes.⁵

Equation (1): The partial differential equation for linear heat flow.

This equation must be satisfied by the temperature in the mold, along with the initial and boundary conditions described above.

Equation (2): The solution valid for these conditions.^{1a} Temperature is given as a function of the distance from the mold-metal interface, " x ", time, " θ ", and the thermal diffusivity of the mold, " α ".

Equation (3): The Fourier conduction equation. Heat flux equals conductivity, " k ", times the temperature gradient.

Equation (4): Substitute (3) into (2).

Equation (5): Integrate (4). This is the solution desired, giving the total heat per unit area which has entered the mold in time, " θ ".

Equation (6): The heat which enters the mold equals the heat of fusion

evolved by the casting, if there is no superheat. (The effect of superheat on sand castings is considered below.)

Equation (8): Substitute (6) and (7) into (5).

Equation (8) reveals the manner in which the thermal properties of the metal and of the mold influence solidification time of a casting. The product of conductivity, density and specific heat is a measure of the "chilling" capacity of the mold material, while the ratio of the melting point to the volumetric heat of fusion is the factor for comparison of the different metals.

$$12. \quad \frac{1}{\alpha} \frac{\partial T}{\partial \theta} = \frac{\partial^2 T}{\partial r^2} + \frac{2}{r} \frac{\partial T}{\partial r} \quad (9)$$

$$\frac{T - T_n}{T_s - T_n} = \frac{R}{r} \left[1 - \operatorname{erf} \frac{r - R}{2\sqrt{\alpha \theta}} \right] \quad (10)$$

$$\left. \frac{q}{A_s} \right|_{r=R} = -K \left. \frac{\partial T}{\partial r} \right|_{r=R} \quad (11)$$

$$\left. \frac{q}{A_s} \right|_{r=R} = K(T_s - T_n) \left[\frac{1}{R} + \frac{1}{\sqrt{\pi \alpha \theta}} \right] \quad (12)$$

$$\frac{Q}{A_s} = K(T_s - T_n) \left[\frac{\theta}{R} + \frac{2\sqrt{\theta}}{\sqrt{\pi \alpha}} \right] \quad (13)$$

$$Q_f = \frac{4}{3} \pi R^3 \rho' H, \quad A_s = 4\pi R^2 \quad (14)$$

$$\frac{Q_f}{A_s} = \frac{\rho' H R}{3}$$

$$\frac{\rho' H}{3} = K(T_m - T_n) \left[\frac{\theta_f}{R^2} + \frac{2}{\sqrt{\pi \alpha}} \frac{\sqrt{\theta_f}}{R} \right] \quad (15)$$

$$\frac{R}{\sqrt{\theta_f}} = \frac{3}{\sqrt{\pi}} \left(\frac{T_m - T_n}{\rho' H} \right) \sqrt{K \rho C_p} \left(1 + \sqrt{1 + \frac{\pi \alpha \rho' H}{3K(T_m - T_n)}} \right) \quad (16)$$

Consider next the flow of heat from a spherical mold cavity. The solution of this problem parallels closely the preceding solution for the slab.

Equation (9): The partial differential equation for heat flow in spherically symmetrical coordinates.

Equation (10): The solution of (9) for the present boundary conditions.^{1b}

Equation (11): The Fourier equation at the mold-metal interface relating surface flux to the temperature gradient.

Equation (12): Substitute (10) into (11).

Equation (13): Integrate (12).

Equation (15): Assuming no superheat, the heat of fusion evolved during complete solidification equals the heat absorbed by the mold. Attention is focussed here upon the time required for complete solidification, " θ_f ".

Equation (16): Solve (15) (quadratic) for $\frac{R}{\sqrt{\theta_f}}$.

14.

$$\frac{1}{\alpha} \frac{\partial T}{\partial \theta} = \frac{\partial^2 T}{\partial r^2} + \frac{1}{r} \frac{\partial T}{\partial r} \quad (17)$$

$$\frac{T_s - T}{T_s - T_\infty} = -\frac{2}{\pi} \int_0^\infty e^{-\alpha u^2 \theta} \left[\frac{J_0(ur) Y_0(uR) - Y_0(ur) J_0(uR)}{J_0^2(uR) + Y_0^2(uR)} \right] \frac{du}{u} \quad (18)$$

$$\left. \frac{q}{A_s} \right)_{r=R} = -K \left. \frac{\partial T}{\partial r} \right)_{r=R}$$

$$\left. \frac{q}{A_s} \right)_{r=R} = \frac{4K(T_s - T_\infty)}{\pi^2 R} \int_0^\infty e^{-\alpha u^2 \theta} \left[\frac{1}{J_0^2(uR) + Y_0^2(uR)} \right] \frac{du}{u} \quad (19)$$

CYLINDER:

$$A = 2\pi R L$$

$$A_s = 2\pi R_c L$$

$$\left. \frac{1}{A_s} \frac{dA}{dn} \right)_{n=R_c} = \frac{1}{R_c} \quad (20)$$

SPHERE:

$$A = 4\pi r^2$$

$$A_s = 4\pi R_s^2$$

$$\left. \frac{1}{A_s} \frac{dA}{dn} \right)_{n=R_s} = \frac{2}{R_s} \quad (21)$$

$$\therefore R_s = 2R_c \quad (22)$$

The solution for heat flow from a cylindrical mold cavity is more cumbersome than either of the preceding problems. Although the procedure is the same, in principle, an approximation is used to simplify the resulting expressions.

Equation (17): The partial differential equation for heat flow in cylindrical coordinates.

Equation (18): The solution valid for these conditions.^{1c}

Equation (19): The resulting expression for the heat flux at the mold-metal interface.^{1c}

Numerical values for the integral in (19) have been tabulated by Jaeger and Clarke,¹⁹ and the right-hand side of (19) may thus be integrated planimetrically. However, a convenient approximation is possible at this point, which provides a solution of much greater practical value, and which may be more easily compared with corresponding expressions for the slab and the sphere. The validity of the approximation may be checked by comparison with the exact solution. The quantity which is of interest is the rate at which heat enters the mold surface, and this rate is determined by (1) the thermal properties of the mold material, and (2) the rate with which the cross-sectional area of the heat flow path changes with depth of penetration into the mold. For example, comparison of Equations (4) and (12) reveals that one square inch of concave, spherical mold surface can absorb heat more rapidly than a square inch of plane mold surface, because the cross-section of the heat flow path increases with depth of penetration. In this respect, a concave

cylindrical mold surface is intermediate between plane and concave spherical mold surfaces. The objective is to find an approximate expression for the cylinder which is similar in form to the simple sphere equation. This is done by finding the size relationship between a spherical and a cylindrical mold cavity which have equivalent heat absorbing abilities per unit area. Consider that the "heated zone" in the mold is fairly shallow, and that the following development is accurate for regions near the mold surfaces:

Equation (20): The fractional rate of change of the cross-sectional area of the heat flow path with radius, at the mold-metal interface -- for a cylinder.

Equation (21): Repeat for a sphere.

Equation (22): Equate (20) and (21). The condition of "equivalent divergence" of the heat flow paths is that the radius of the sphere is twice that of the cylinder.

$$\left. \frac{q}{A_s} \right)_{n=R} \cong K(T_s - T_n) \left[\frac{0.5}{R} + \frac{1}{\sqrt{\pi \alpha \theta}} \right] \quad (24)$$

$$\frac{R}{K(T_s - T_n)} \left. \frac{q}{A_s} \right)_{n=R} \cong m + \frac{R}{\sqrt{\pi \alpha \theta}} \quad (25)$$

$$\frac{R}{K(T_s - T_n)} \left. \frac{q}{A_s} \right)_{n=R} = \frac{4}{\pi^2} (I) \quad (26)$$

$$\Delta = \frac{4}{\pi^2} (I) - \frac{R}{\sqrt{\pi \alpha \theta}} - m \quad (27)$$

$$\frac{Q}{A_s} = K(T_s - T_n) \left[\frac{m \theta}{R} + \frac{2\sqrt{\theta}}{\sqrt{\pi \alpha}} \right] \quad (28)$$

$$Q_f = \pi R^2 L P' H, \quad A_s = 2\pi R L$$

$$\frac{Q_f}{A_s} = \frac{R P' H}{2} \quad (29)$$

$$\frac{P' H}{2} = K(T_m - T_n) \left[\frac{m \theta_f}{R^2} + \frac{2}{\sqrt{\pi \alpha}} \frac{\sqrt{\theta_f}}{R} \right] \quad (30)$$

$$\frac{R}{\sqrt{\theta_f}} = \frac{2(T_m - T_n)}{\sqrt{\pi} \left(\frac{P' H}{R} \right)} \sqrt{K P C_p \left(1 + \sqrt{1 + \frac{m \pi \alpha P' H}{2 K (T_m - T_n)}} \right)} \quad (31)$$

Equation (24): Combine (12) and (22) to get approximate expression for cylindrical heat flow, accurate within one per cent for the solution of casting problems. Since (22) is strictly valid only at the mold surface, (24) is increasingly accurate for very early times.

Equation (25): Rewrite (24) replacing the constant with "n".

Equation (26): Rewrite (19), the exact expression for the heat flux, replacing the integral with "I".

Equation (27): Subtract (25) from (26) to obtain the arithmetical error inherent in (25).

Using the values given by Jaeger and Clarke,¹⁹ the deviation, " Δ ", is plotted as a function of time in Figure 1, for different assumed values of "n". Since areas are proportional to heat on this diagram, for a given length of time the best average value for "n" is obtained by selecting the curve which balances the areas above (positive) and below (negative) the axis. In this manner, for precise work, Equation (19) may be accurately integrated. Such a refinement is not necessary for casting heat flow work; the value 0.5 is quite adequate, although, for complete solidification of most sand castings, 0.47 is more exact. Figure 1 constitutes a verification of Equation (24).

Using a development exactly paralleling that for the sphere, starting with Equation (25), the following results are obtained:

Equation (28): Heat which enters the mold as a function of time.

Equation (31): Time for complete solidification of a cylinder cast with
no superheat.

SLAB:

$$\frac{V_s}{A_s} \frac{1}{\sqrt{\theta_f}} = \left(\frac{T_m - T_\infty}{\rho' H} \right) \sqrt{K \rho C_p} \left[\frac{2}{\sqrt{\pi}} \right] \quad (32)$$

CYLINDER:

$$\frac{V_s}{A_s} \frac{1}{\sqrt{\theta_f}} = \left(\frac{T_m - T_\infty}{\rho' H} \right) \sqrt{K \rho C_p} \left[\frac{1 + \sqrt{1 + \frac{m \pi \alpha \rho' H}{2 K (T_m - T_\infty)}}}{\sqrt{\pi}} \right] \quad (33)$$

SPHERE:

$$\frac{V_s}{A_s} \frac{1}{\sqrt{\theta_f}} = \left(\frac{T_m - T_\infty}{\rho' H} \right) \sqrt{K \rho C_p} \left[\frac{1 + \sqrt{1 + \frac{\pi \alpha \rho' H}{3 K (T_m - T_\infty)}}}{\sqrt{\pi}} \right] \quad (34)$$

The results of the analysis on sand castings may be conveniently summarized and compared by expressing casting dimensions in terms of volume and surface area. In this way, Equations (8), (31), and (16) become (32), (33), and (34) for the slab, cylinder, and sphere, respectively. It may be seen that for each shape, the time required for complete solidification is proportional to the square of the linear dimensions. Although the equations were derived on the basis of no superheat, a moderate amount of superheat may be accurately taken into account by adding it, calorifically, to the latent heat (justification for this procedure is given in Section VI).

The right-hand side of Equation (32) is the constant used by Chvorinov⁵ to describe the freezing of castings having any shape. The effect of shape is shown by the factor enclosed in brackets at the end of each equation; this factor is largest for the sphere, and smallest for the slab. For most metals, the expression is between 10 and 15 per cent higher for the sphere than for the slab. Since this term must be squared to calculate freezing times, substantial deviations from Chvorinov's relationship may be expected. However, the expressions for the sphere and for the cylinder agree within 4 per cent, so that Chvorinov's rule should apply accurately in comparing the freezing times of "chunky" or prismoidal castings, i.e. castings having not more than one relatively long dimension.

TABLE I.

Definition of Terms

Units: B.T.U. - Hr. - Ft. - °F - Lb.

- α = Thermal diffusivity of mold, (Ft.)²/Hr.
 k = Thermal conductivity of mold, B.T.U./Ft.Hr.°F.
 ρ = Density of mold, Lb./(Ft.)³.
 ρ' = Density of metal.
 C_p = Specific heat of mold, B.T.U./Lb.°F.
 q = Heat flow rate, B.T.U./Hr.
 Q = Total heat which enters mold (leaves casting) in time, "θ", B.T.U.
 Q_f = Total heat which must be removed to freeze casting.
 H = Heat of fusion, B.T.U./Lb.
 T = Temperature, °F.
 T_s = Surface temperature of mold or of casting or of mold-metal interface.
 T_r = Room temperature.
 T_m = Melting temperature.
 x = Distance from mold-metal interface, Ft.
 x^* = Thickness of solid metal layer which freezes in time, "θ" (one-dimensional freezing).
 r = Radial distance from center of spherical or cylindrical mold cavity.
 l = Half-thickness of slab mold cavity.
 R = Radius of spherical or cylindrical mold cavity or casting.
 R_c = Radius of cylindrical mold cavity.

R_s = Radius of spherical mold cavity.

L = Length of cylindrical mold cavity.

A_s = Area of mold-metal interface, (Ft.)².

A = Cross-sectional area of heat flow path; area of isothermal surface of radius, "r".

V_s = Volume of mold cavity, (Ft.)³.

$$\operatorname{erf} u = \frac{2}{\sqrt{\pi}} \int_0^u e^{-x^2} dx$$

$\operatorname{erfc} u = 1 - \operatorname{erf} u$

J_0, Y_0 = Bessel functions of the first and second kind, respectively, of order zero.

n = Dimensionless constant in cylindrical heat flow approximations = 0.5.

I = Integral in Equation (20).

= Difference between exact and approximate cylindrical heat flow rates, Equation (27).

DEVIATION BETWEEN EXACT
AND APPROXIMATE EXPRESSIONS
FOR CYLINDRICAL HEAT FLOW
EQUATION (27)

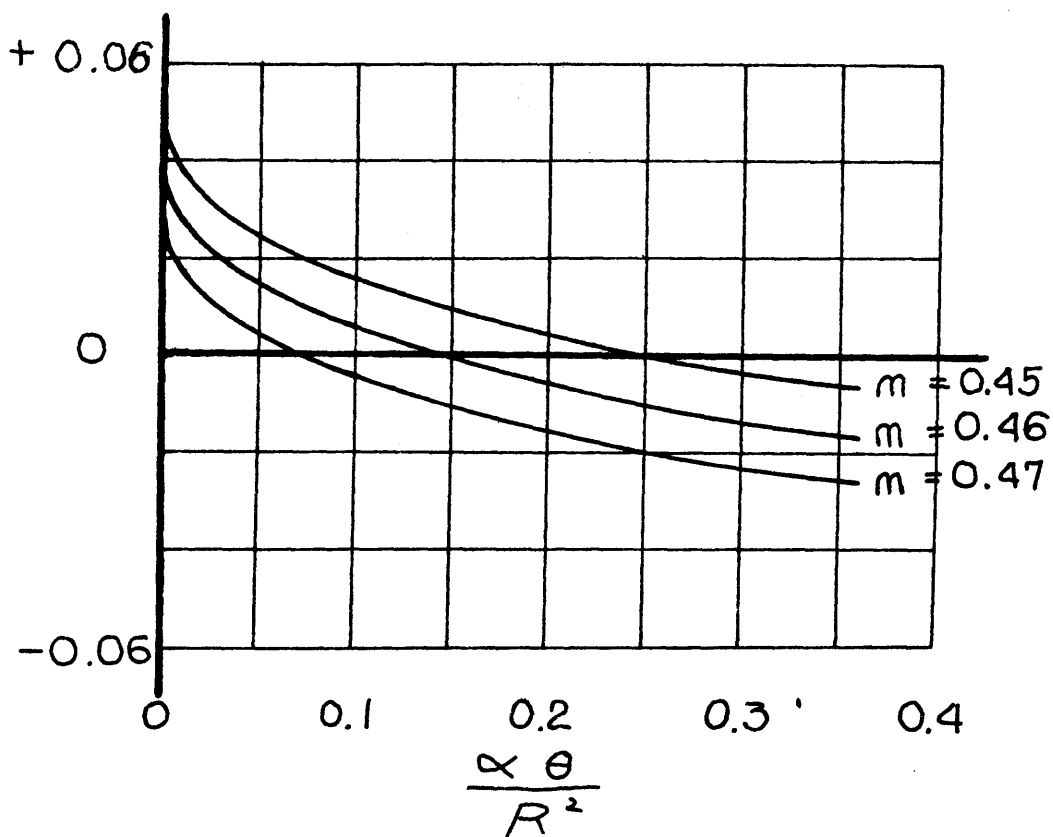


FIGURE 1

IV. ANALYSIS OF HEAT FLOW FROM CHILLED CASTINGS:
CONSTANT CASTING SURFACE TEMPERATURE

(Pure metals and alloys which freeze completely within a narrow temperature range.)

Chilled castings present a class of heat flow problems fundamentally much more complex than those considered in the previous section. The first step in analyzing the over-all picture is to isolate the metal from the mold, and consider heat flow in the metal separately, using the simplest possible boundary condition: constant casting surface temperature. The question of heat flow in the chill mold is considered in Section V. The essential features of chilled castings, which differ from those of sand castings, are: (1) The surface temperature is appreciably lower than the melting point of the metal, and moderate to steep temperature gradients exist in the solid metal. (2) Heat removed in cooling the solid metal is a significant fraction of the total heat removed from the casting during solidification. (3) The conductivity of the cast metal is a controlling factor influencing the rate of solidification.

In the following analysis certain initial and boundary conditions are adhered to throughout. A mass of liquid metal, initially at the melting temperature, has its surface suddenly cooled to " T_s " at zero time. The effect of superheat is not considered in this section. Although it would be quite possible to consider superheat, at least in the one-dimensional case, the results so obtained are unrealistic, because

$$26. \quad \frac{1}{\alpha'} \frac{\partial T}{\partial \theta} = \frac{\partial^2 T}{\partial x^2} \quad (1)$$

$$\frac{T - T_s}{T' - T_s} = \operatorname{erf} \frac{x}{2\sqrt{\alpha'\theta}} \quad (2)$$

$$A_T \quad x = x', \quad T = T_m \quad (3)$$

$$K' \frac{\partial T}{\partial x} = \rho' H \frac{dx'}{d\theta} \quad (4)$$

$$\frac{x'}{2\sqrt{\alpha'\theta}} \equiv \beta \quad (5)$$

$$T' - T_s = \frac{T_m - T_s}{\operatorname{erf} \beta} \quad (6)$$

$$\frac{c_p'(T_m - T_s)}{H} = \sqrt{\pi} \beta e^{\beta^2} \operatorname{erf} \beta \quad (7)$$

$$\frac{c_p'(T_m - T_s)}{H} = 2\beta^2 + \frac{4}{3}\beta^4 + \frac{8}{15}\beta^6 + \dots \quad (8)$$

$$2\beta^2 = \frac{x'}{\alpha'} \frac{dx'}{d\theta} \quad (9)$$

$$\frac{c_p'(T_m - T_s)}{H} = \frac{x'}{\alpha'} \frac{dx'}{d\theta} + \frac{1}{3} \left(\frac{x' dx'}{\alpha' d\theta} \right)^2 + \frac{1}{15} \left(\frac{x' dx'}{\alpha' d\theta} \right)^3 + \dots \quad (10)$$

they depend upon semi-infinite conditions. It has been demonstrated experimentally, and would be expected theoretically, that nearly all of the superheat leaves a finite chill casting very early in the solidification process;¹⁸ thus most of the freezing takes place with the liquid phase at or near its melting point.

All symbols used in the analysis, which did not appear in the previous section, are defined in Table II.

A. Solidification From a Plane Chilled Surface.

The solution presented here is based on the method of Neumann,¹ except that Neumann considered a body of liquid initially above its melting point. The solution, in the absence of superheat, is somewhat more simple, since there are no temperature gradients in the liquid.

Equation (1): The partial differential equation for linear heat flow which must be satisfied in the layer of solid metal.

Equation (2): A particular solution of (1). T^* is an arbitrary constant.

Equation (3,4): At the liquid-solid interface, the temperature must be equal to the melting point, and the temperature gradient is proportional to the rate of solidification.

Equation (5): When condition (3) is imposed on (2), the left-hand side of (2) is seen to be constant, and so the right-hand side is also constant. Equation (5) defines " β ".

Equation (6): Combine (2) and (3).

Equation (7): Substitute (6) into (2), and (2) into (4).

Equation (8): Expand (7) in terms of a power series.

Equation (9): Differentiate (5).

Equation (10): Substitute (9) into (8).

The above procedure consists of assuming the form of the solution, inserting the boundary conditions, and determining whether the boundary conditions and the assumed form are compatible. Since (7) may be solved for a real value of " β ", and all the required conditions are met, (7), (6), and (2) constitute the solution. This technique is used because condition (4) is not linear and homogeneous, and ordinary means for building up solutions of heat flow problems do not apply. The method is not systematic, and cannot be extended to the solidification of other shapes. The reason for putting (7) into the form of (10) is that the power series in (10) may also be built, term by term, by using an iterative procedure demonstrated in the following paragraphs. This procedure is systematic and may be applied to other shapes.

It should be noted that the first term in (10) corresponds to the solution which would apply if the specific heat of cooling the solid metal were small enough to be neglected. The subsequent terms may then be thought of as "specific heat" terms.

$$q = -\rho' H A \frac{dx'}{d\theta} + \rho' C_p' A \int_x^{x'} \frac{\partial T}{\partial \theta} dx \quad (11)$$

$$\frac{\partial T}{\partial x} = -\frac{q}{K'A}, \quad \alpha' = \frac{K'}{\rho' C_p'} \quad (12)$$

$$\frac{\partial T}{\partial x} = \frac{H}{C_p' \alpha'} \frac{dx'}{d\theta} - \frac{1}{\alpha'} \int_x^{x'} \frac{\partial T}{\partial \theta} dx \quad (13)$$

$$\int_{T_s}^T dT = \int_0^x \frac{\partial T}{\partial x} dx \quad (14)$$

$$T - T_s = \frac{H}{C_p' \alpha'} \frac{dx'}{d\theta} x - \frac{1}{\alpha'} \int_0^x \int_x^{x'} \frac{\partial T}{\partial \theta} dx dx \quad (15)$$

$$\frac{(T_m - T_s) C_p'}{H} = \frac{x' dx'}{\alpha' d\theta} - \frac{C_p'}{H \alpha'} \int_0^{x'} \int_x^{x'} \frac{\partial T}{\partial \theta} dx dx \quad (15A)$$

Equation (11): The rate of heat flow at a location, "x", in the solid metal is equal to the rate at which latent heat is being liberated, plus the rate at which specific heat of cooling is being liberated between "x" and "x'".

Equation (12): The Fourier conduction equation.

Equation (13): Substitute (11) into (12).

Equations (14,15): Integration of the gradient in (13) to obtain the temperature drop between "x" and the chilled surface.

Equation (15A): Rewrite (15) to obtain the total temperature drop between the chilled surface and the liquid-solid interface.

Equation (15) may be verified by showing that it satisfies all of the boundary conditions as well as (1). The first term in (15) is the latent heat term and the integral is the specific heat term. The procedure to be followed in the ensuing paragraphs is one of successive approximations. For the first approximation, the integral is neglected, a value obtained for " $\frac{\partial T}{\partial \theta}$ ", and this value is introduced into the integral to obtain the second approximation. Although the expressions become increasingly cumbersome, the operation may be repeated as many times as desired.

$$T_0 - T_s = \frac{H}{C_p' \alpha'} \frac{dx'}{d\theta} X \quad (16)$$

$$\left. \frac{\partial T}{\partial \theta} \right|_0 = \frac{H}{C_p' \alpha'} \frac{d^2 x'}{d\theta^2} X \quad (17)$$

$$\int_0^x \int_0^{x'} x dx dx = \frac{x'^2 X}{2} - \frac{X^3}{6} \quad (18)$$

$$\text{FROM (16):} \begin{cases} T_m - T_s = \frac{H}{C_p' \alpha'} \frac{dx'}{d\theta} X' & (19) \\ 0 = \left(\frac{dx'}{d\theta} \right)^2 + X' \frac{d^2 X'}{d\theta^2} & (20) \\ \left. \frac{d^2 X'}{d\theta^2} \right|_0 = -\frac{1}{X'} \left(\frac{dx'}{d\theta} \right)^2 & (21) \end{cases}$$

$$T_i - T_s = \frac{H}{C_p' \alpha'} \frac{dx'}{d\theta} X + \left(\frac{1}{\alpha'} \right)^2 \frac{H}{C_p'} \left(\frac{dx'}{d\theta} \right)^2 \left(\frac{X' X}{2} - \frac{X^3}{6 X'} \right) \quad (22)$$

$$\frac{C_p' (T_m - T_s)}{H} = \frac{X'}{\alpha'} \frac{dx'}{d\theta} + \frac{1}{3} \left(\frac{X' dx'}{\alpha' d\theta} \right)^2 + \dots \quad (23)$$

32.

$$\Delta T_i \equiv T_i - T_0 \quad (24)$$

$$\Delta T_i = \left(\frac{1}{\alpha'}\right)^2 \frac{H}{C_p'} \left(\frac{dx'}{d\theta}\right)^2 \left(\frac{x'x}{2} - \frac{x^3}{6x'}\right) \quad (25)$$

$$\frac{\partial \Delta T_i}{\partial \theta} = \left(\frac{1}{\alpha'}\right)^2 \frac{H}{C_p'} \left[\left(\frac{x}{2} + \frac{x^3}{6x'^2}\right) \left(\frac{dx'}{d\theta}\right)^3 + \left(\frac{x'x}{2} - \frac{x^3}{6x'}\right) 2 \left(\frac{dx'}{d\theta}\right) \frac{d^2x'}{d\theta^2} \right] \quad (26)$$

$$\text{From (23):} \begin{cases} x' \frac{dx'}{d\theta} = \text{CONSTANT} \\ \frac{d^2x'}{d\theta^2} = -\frac{1}{x'} \left(\frac{dx'}{d\theta}\right)^2 \end{cases} \quad (27)$$

$$\frac{\partial \Delta T_i}{\partial \theta} = \left(\frac{1}{\alpha'}\right)^2 \frac{H}{C_p'} \left(\frac{dx'}{d\theta}\right)^3 \left(\frac{x^3}{2x'^2} - \frac{x}{2}\right) \quad (28)$$

$$\int_0^{x'} \int_x^{x'} \left(\frac{x^3}{2x'^2} - \frac{x}{2}\right) dx dx = -\frac{x'^3}{15} \quad (29)$$

$$\frac{(T_m - T_s) C_p'}{H} = \frac{x'}{\alpha'} \frac{dx'}{d\theta} + \frac{1}{3} \left(\frac{x' dx'}{\alpha' d\theta}\right)^2 + \frac{1}{15} \left(\frac{x' dx'}{\alpha' d\theta}\right)^3 + \dots \quad (30)$$

Equation (16): The first approximation for the temperature distribution.

Equation (17): Differentiate (16) with respect to time.

Equation (18): Operate as indicated in (15) upon the factor in (17) containing "x".

Equation (19): Write (16) at $x = x'$.

Equation (20,21): Differentiate (19) with respect to time to obtain the first approximation for the second derivative of "x'" with respect to time.

Equation (22): Substitute (17), (18), and (21) into (15).

Equation (23): Rewrite (22) at $x = x'$, and so obtain the first two terms of (10).

For the bulk of the numerical work in following sections, only the first two terms of a given power series development are used. For this simple case, in which the exact solution is known, the first and second approximations and the exact solution are reproduced in Figure 2, covering the practical range of solidification problems.

For documentary purposes, Equations (24) through (30) represent a repetition of the iterative procedure to obtain the third term in Equation (10). To avoid unnecessary repetition, only the second term in Equation (22) is carried through the operation. Equation (23) is used to evaluate the second derivative of "x'" with respect to time. It may be seen that Equations (10) and (30) are identical.

$$q = -\rho' H 4\pi n'^2 \frac{dn'}{d\theta} - \rho' C_p' 4\pi \int_{n'}^n n^2 \frac{\partial T}{\partial \theta} dn \quad (31)$$

$$\frac{\partial T}{\partial n} = -\frac{q}{4\pi n^2 K'} \quad (32)$$

$$\frac{\partial T}{\partial n} = \frac{H}{\alpha' C_p'} \frac{n'^2}{n^2} \frac{dn'}{d\theta} + \frac{1}{\alpha' n^2} \int_{n'}^n n^2 \frac{\partial T}{\partial \theta} dn \quad (33)$$

$$T_s \int_{R}^T dT = \int_{R}^n \frac{\partial T}{\partial n} dn = - \int_n^R \frac{\partial T}{\partial n} dn \quad (34)$$

$$T - T_s = -\frac{H}{\alpha' C_p'} \left(\frac{R-n}{Rn} \right) n'^2 \frac{dn'}{d\theta} - \frac{1}{\alpha'} \left[\int_{n'}^R \int_{n'}^n n^2 \frac{\partial T}{\partial \theta} dn \right] \frac{dn'}{n^2} \quad (35)$$

$$\frac{(T_m - T_s) C_p'}{H} = -\frac{n'}{R} \left(\frac{R-n'}{\alpha'} \frac{dn'}{d\theta} \right) - \frac{C_p'}{\alpha' H} \left[\int_{n'}^R \int_{n'}^n n^2 \frac{\partial T}{\partial \theta} dn \right] \frac{dn'}{n^2} \quad (36)$$

$$T_0 - T_s = -\frac{H}{\alpha' C_p} \left(\frac{R-n}{Rn} \right) n'^2 \frac{dn'}{d\theta} \quad (37)$$

$$\left. \frac{\partial T}{\partial \theta} \right|_0 = -\frac{H}{\alpha' C_p} \left(\frac{R-n}{Rn} \right) n' \left[n' \frac{d^2 n'}{d\theta^2} + 2 \left(\frac{dn'}{d\theta} \right)^2 \right] \quad (38)$$

$$\int_n^R \left[\int_{n'}^n \left(\frac{R-n}{n} \right) n^2 dn \right] \frac{dn}{n^2} = +\frac{R}{2} (R-n) - \frac{n'^2}{2} \left(\frac{R}{n} - 1 \right) - \frac{1}{6} (R^2 - n^2) + \frac{n'^3}{3} \left(\frac{1}{n} - \frac{1}{R} \right) \quad (39)$$

FROM (37):

$$\frac{(T_m - T_s) \alpha' C_p R}{H} = -(Rn' - n'^2) \frac{dn'}{d\theta}$$

$$0 = (Rn' - n'^2) \frac{d^2 n'}{d\theta^2} + \frac{dn'}{d\theta} \left(R \frac{dn'}{d\theta} - 2n' \frac{dn'}{d\theta} \right)$$

$$\left. \frac{d^2 n'}{d\theta^2} \right|_0 = - \left(\frac{R-2n'}{R-n'} \right) \frac{1}{n'} \left(\frac{dn'}{d\theta} \right)^2 \quad (40)$$

$$\left. \frac{\partial T}{\partial \theta} \right|_0 = -\frac{H}{\alpha' C_p'} \left(\frac{R-n}{n} \right) \left(\frac{n'}{R-n'} \right) \left(\frac{dn'}{d\theta} \right)^2 \quad (41)$$

$$T_i - T_s = -\frac{H}{\alpha' C_p'} \left(\frac{R-n}{Rn} \right) n'^2 \frac{dn'}{d\theta} \quad (42)$$

$$+\left(\frac{1}{\alpha'} \right)^2 \frac{H}{C_p'} \left(\frac{n'}{R-n'} \right) \left(\frac{dn'}{d\theta} \right)^2 \left[\begin{array}{l} +\frac{R}{2}(R-n) \\ -\frac{n'^2}{2} \left(\frac{R}{n} - 1 \right) \\ -\frac{1}{6}(R^2 - n^2) \\ +\frac{n'^3}{3} \left(\frac{1}{n} - \frac{1}{R} \right) \end{array} \right]$$

$$\frac{(T_m - T_s) C_p'}{H} = \frac{n'}{R} \left| \frac{R-n'}{\alpha'} \frac{dn'}{d\theta} \right| + \frac{1}{3} \frac{n'}{R} \left| \frac{R-n'}{\alpha'} \frac{dn'}{d\theta} \right|^2 + \dots (43)$$

$$\Delta T_i = +\left(\frac{1}{\alpha'}\right)^2 \frac{H}{C_p'} \left(\frac{r'}{R-r'}\right) \left(\frac{dr'}{d\theta}\right)^2 \left[\begin{array}{l} +\frac{R}{2} (R-r) \\ -\frac{r'^2}{2} \left(\frac{R}{r} - 1\right) \\ -\frac{1}{6} (R^2 - r^2) \\ +\frac{r'^3}{3} \left(\frac{1}{r} - \frac{1}{R}\right) \end{array} \right] \quad (44)$$

$$\Delta T_i = +\left(\frac{1}{\alpha'}\right)^2 \frac{H}{C_p'} \left(\frac{r'}{R-r'}\right) \left(\frac{dr'}{d\theta}\right)^2 [\nabla] \quad (45)$$

$$\frac{\partial \Delta T_i}{\partial \theta} = +\left(\frac{1}{\alpha'}\right)^2 \frac{H}{C_p'} \left[\begin{array}{l} -\left(\frac{R}{r} - 1\right) \frac{r'^2}{R} \left(\frac{dr'}{d\theta}\right)^3 \\ +[\nabla] \frac{R}{(R-r')^2} \left(\frac{dr'}{d\theta}\right)^3 \\ +[\nabla] 2 \left(\frac{r'}{R-r'}\right) \frac{dr'}{d\theta} \frac{d^2 r'}{d\theta^2} \end{array} \right] \quad (46)$$

$$\int_{r'}^R \left[\int_{r'}^R [\nabla] r^2 dr \right] \frac{dr}{r^2} = \frac{(R-r')^5 (R+5r')}{45 R^2} \quad (47)$$

38.

COMBINING (39), (46), (47):

$$\frac{C_p'}{\alpha' H} \int_{n'}^R \left[n^2 \frac{\partial(\Delta T_i)}{\partial \theta} dn \right] \frac{dn}{n^2} = \quad (48)$$

$$\left(\frac{1}{\alpha'} \right)^3 \left[- \frac{(R-n')^3 n'^2}{3R^2} \left(\frac{dn'}{d\theta} \right)^3 + \frac{(R-n')^3 (R+5n')}{45R} \left(\frac{dn'}{d\theta} \right)^3 \right. \\ \left. + \frac{2(R-n')^4 (R+5n') n'}{45R^2} \frac{dn'}{d\theta} \frac{d^2 n'}{d\theta^2} \right]$$

FROM (43):

$$\frac{(T_m - T_s) C_p' R \alpha'}{H} = -n'(R-n') \frac{dn'}{d\theta} + \frac{1}{3\alpha'} n'(R-n')^2 \left(\frac{dn'}{d\theta} \right)^2 \quad (49)$$

$$0 = -n'(R-n') \frac{d^2 n'}{d\theta^2} - (R-2n') \left(\frac{dn'}{d\theta} \right)^2 \\ + \frac{2}{3\alpha'} n'(R-n')^2 \frac{dn'}{d\theta} \frac{d^2 n'}{d\theta^2} + \frac{1}{3\alpha'} (R-n')(R-3n') \left(\frac{dn'}{d\theta} \right)^3$$

$$\frac{d^2 n'}{d\theta^2} = \frac{\left[(R-2n') - \frac{1}{3} (R-3n') \left(\frac{R-n'}{\alpha'} \frac{dn'}{d\theta} \right) \right]}{\left[1 - \frac{2}{3} \left(\frac{R-n'}{\alpha'} \frac{dn'}{d\theta} \right) \right]} \frac{1}{n'(R-n')} \left(\frac{dn'}{d\theta} \right)^2$$

COMBINING (43, 48, 49, 36):

$$\frac{(T_m - T_s)C_p'}{H} = + \left| \frac{R - n' \frac{dn'}{d\theta}}{\alpha'} \right| \frac{n'}{R} \quad (50)$$

$$+ \left| \frac{R - n' \frac{dn'}{d\theta}}{\alpha'} \right|^2 \frac{1}{3} \frac{n'}{R}$$

$$+ \left| \frac{R - n' \frac{dn'}{d\theta}}{\alpha'} \right|^3 \left\{ -\frac{1}{3} \left(\frac{n'}{R} \right)^2 + \left(\frac{R + 5n'}{45R} \right) - \frac{2}{45} \left(\frac{R + 5n'}{R^2} \right) \left[\frac{(R - 2n') - \left(\frac{R - 3n'}{3} \right) \left(\frac{R - n' \frac{dn'}{d\theta}}{\alpha'} \right)}{1 - \frac{2}{3} \left(\frac{R - n' \frac{dn'}{d\theta}}{\alpha'} \right)} \right] \right\}$$

B. Solidification From a Spherical Chilled Surface.

The technique illustrated in the preceding analysis may also be applied to other symmetrical shapes. Although this device is unnecessary in the case of one-dimensional freezing, where an exact solution is available, the development of an exact solution for the freezing of a sphere or cylinder is of very doubtful feasibility.

Equations (31) through (36) correspond to the one-dimensional Equations (11) through (15A).

Equation (31): Heat flow rate at a location, "r", is the sum of a latent heat and a specific heat term.

Equation (32): Fourier conduction equation for the gradient at "r".

Equation (33): Substitute (31) into (32).

Equations (34,35): Integration of the temperature gradient to get the temperature drop between "r" and the chilled surface of the casting.

Equation (36): Rewrite (35) at $r = r^*$ to obtain the total temperature drop between the liquid-solid interface and the chilled surface.

Equation (35) is put through the same iterative operations as was Equation (15). The resulting second approximation is given by (43). Equation (43) bears some resemblance to (23), and so the iteration was carried one step further in the hope of developing a power series which would approach a recognizable analytical result. The third approximation is given by Equation (50). The indication is that even if the

exact solution were known, it would not be a convenient relationship like (7). The term within the braces in Equation (50) approaches $1/15$ when r' approaches R , or in other words when freezing is essentially one-dimensional.

$$q = -\rho' H 2\pi r' L \frac{dr'}{d\theta} - \rho' C_p' 2\pi L \int_{r'}^R r \frac{\partial T}{\partial \theta} dr \quad (51)$$

$$\frac{\partial T}{\partial r} = -\frac{q}{2\pi r L k'} \quad (52)$$

$$\frac{\partial T}{\partial r} = \frac{H}{C_p' \alpha'} \frac{r' dr'}{r d\theta} + \frac{1}{\alpha' r} \int_{r'}^R r \frac{\partial T}{\partial \theta} dr \quad (53)$$

$$\int_{T_s}^T dT = \int_R^r \frac{\partial T}{\partial r} dr = - \int_r^R \frac{\partial T}{\partial r} dr \quad (54)$$

$$T - T_s = -\frac{H}{C_p' \alpha'} \ln\left(\frac{R}{r}\right) r' \frac{dr'}{d\theta} - \frac{1}{\alpha'} \int_{r'}^R \left[\int_{r'}^r r \frac{\partial T}{\partial \theta} dr \right] \frac{dr}{r} \quad (55)$$

$$\frac{(T_m - T_s) C_p'}{H} = -\frac{1}{\alpha'} \ln\left(\frac{R}{r'}\right) r' \frac{dr'}{d\theta} - \frac{C_p'}{H \alpha'} \int_{r'}^R \left[\int_{r'}^r r \frac{\partial T}{\partial \theta} dr \right] \frac{dr}{r} \quad (56)$$

$$T_0 - T_s = -\frac{H}{C_p' \alpha'} \ln\left(\frac{R}{r'}\right) r' \frac{dr'}{d\theta} \quad (57)$$

$$\left(\frac{\partial T}{\partial \theta}\right)_0 = -\frac{H}{C_p' \alpha'} \ln\left(\frac{R}{r'}\right) \left[r' \frac{d^2 r'}{d\theta^2} + \left(\frac{dr'}{d\theta}\right)^2 \right] \quad (58)$$

$$\int_{r'}^R \left[\int_{r'}^R r \ln\left(\frac{R}{r}\right) dr \right] \frac{dr}{r} =$$

$$\left[1 - \left(\frac{r'}{R}\right)^2 - 2\left(\frac{r'}{R}\right)^2 \ln \frac{R}{r'} \left(1 + \ln \frac{R}{r'}\right) \right] \frac{R^2}{4} \quad (59)$$

FROM (57):

$$\frac{(T_m - T_s) C_p' \alpha'}{H} = -\ln\left(\frac{R}{r'}\right) r' \frac{dr'}{d\theta}$$

$$0 = -\ln\left(\frac{R}{r'}\right) r' \frac{d^2 r'}{d\theta^2} - \ln\left(\frac{R}{r'}\right) \left(\frac{dr'}{d\theta}\right)^2 + \left(\frac{dr'}{d\theta}\right)^2$$

$$\left(\frac{d^2 r'}{d\theta^2}\right)_0 = \frac{\left(\frac{dr'}{d\theta}\right)^2 \left(1 - \ln \frac{R}{r'}\right)}{r' \ln \frac{R}{r'}} \quad (60)$$

$$\left. \frac{\partial T}{\partial \theta} \right|_0 = - \frac{H}{c_p' \alpha'} \frac{\ln\left(\frac{R}{r'}\right)}{\ln\left(\frac{R}{r'}\right)} \left(\frac{dr'}{d\theta} \right)^2 \quad (61)$$

$$\frac{(T_m - T_s) c_p'}{H} = \frac{r'}{R} \ln\left(\frac{R}{r'}\right) \left| \frac{R}{\alpha'} \frac{dr'}{d\theta} \right|$$

$$+ \left(\frac{1 - \left(\frac{r'}{R}\right)^2 - 2 \left(\frac{r'}{R}\right)^2 \ln \frac{R}{r'} \left(1 + \ln \frac{R}{r'}\right)}{4 \ln \frac{R}{r'}} \right) \left| \frac{R}{\alpha'} \frac{dr'}{d\theta} \right|^2$$

+ - - -

(62)

C. Solidification From a Cylindrical Chilled Surface.

The problem of the solidification of a cylinder is handled exactly the same as that for a sphere. Equations (51) through (56) are completely analogous to Equations (31) through (36). Using Equation (55), in this case only the second approximation is obtained; for this reason, in Equation (59), the second integration is carried out over the entire range from r' to R , and substitutions made directly into Equation (56). The resulting second approximation is given by Equation (62).

$$V' \equiv \frac{r'}{R} \quad (63)$$

SPHERE:

$$\left| \frac{\alpha' d\theta}{R^2 dV'} \right| = \frac{HV'(1-V')}{2(T_m - T_s)C_p'} \left(1 + \sqrt{1 + \frac{4}{3V'} \frac{(T_m - T_s)C_p'}{H}} \right) \quad (64)$$

CYLINDER:

$$\left| \frac{\alpha' d\theta}{R^2 dV'} \right| = \frac{HV' \ln \frac{1}{V'}}{2(T_m - T_s)C_p'} \left(1 + \sqrt{1 + G \frac{(T_m - T_s)C_p'}{H}} \right) \quad (65)$$

$$G = \frac{1 - V'^2 - 2V'^2 \ln \frac{1}{V'} (1 + \ln \frac{1}{V'})}{V'^2 (\ln \frac{1}{V'})^3} \quad (66)$$

D. Numerical Values: Freezing Rates and Times of Spheres and Cylinders.

The second approximations obtained in the foregoing analyses were quadratic expressions of the linear freezing rates. Equations (43) and (62) may be solved for the freezing rate, and integrated either graphically or analytically to obtain freezing times.

Equation (63): Definition of v^* .

Equation (64): Inverse freezing rate of sphere from Equation (43).

Equation (65): Inverse freezing rate of cylinder from Equation (62).

Equation (66): Definition of "G", which appears in (65).

Equation (64) has been used to prepare Figures 3 and 4. Inverse rate is shown as a function of v^* for various values of $C_p^*(T_m - T_s)/H$. The area under the curves is proportional to time, and graphical integration of the curves over the entire range gives times for complete solidification. Solidification time of spheres as a function of $C_p^*(T_m - T_s)/H$ is given in Figure 5.

Similarly, Equation (65) has been used to prepare Figures 6 and 7, inverse rates for the freezing of cylinders. Planimetric integration of Figures 6 and 7 leads to Figure 8, which shows the time for complete solidification of cylinders as a function of $C_p^*(T_m - T_s)/H$.

$$\frac{\alpha' \theta}{R^2} = \frac{2}{3B} \left[\begin{aligned} & \frac{1}{6} + \frac{2+3B}{12} \sqrt{(1+B)^3} \\ & - \frac{B(B+2)}{8} \sqrt{1+B} \\ & - \frac{B^2(B+2)}{8} \ln \frac{1+\sqrt{1+B}}{\sqrt{B}} \end{aligned} \right] \quad (67)$$

$$B = \frac{4}{3} \frac{C_p' (T_m - T_s)}{H} \quad (68)$$

It has proved possible, in the case of the sphere, to integrate the inverse rate expression analytically. The result (for complete solidification) is represented by Equation (67).

In assessing the inverse rate curves, Figures 3, 4, 6, and 7, several points are of interest. The linear freezing rate for both spheres and cylinders, and presumably other finite shapes, goes through a minimum during solidification. High freezing rates occur near the beginning and end of solidification. Furthermore, the increase in freezing rate near the end of solidification is much less pronounced for cylinders than for spheres; this increase is also less pronounced for high values of $C_p^*(T_m - T_s)/H$.

$$q)_{n=R} = -\rho' H 4\pi n'^2 \frac{dn'}{d\theta} - \rho' C_p' 4\pi \int_{n'}^R n'^2 \frac{\partial T}{\partial \theta} dx \quad (70)$$

$$\frac{dQ_c}{d\theta} = -\rho' C_p' 4\pi \int_{n'}^R n'^2 \frac{\partial T}{\partial \theta} dx \quad (71)$$

$$\left. \frac{\partial T}{\partial \theta} \right|_0 = -\frac{H}{\alpha' C_p'} \left(\frac{R-n}{n} \right) \left(\frac{n'}{R-n'} \right) \left(\frac{dn'}{d\theta} \right)^2 \quad (41)$$

$$\int_{n'}^R \left(\frac{R-n}{n} \right) n'^2 dx = \frac{(R-n')^2 (R+2n')}{6} \quad (72)$$

$$\frac{dQ_c}{d\theta} \frac{d\theta}{dn'} = \frac{dQ_c}{dn'} \quad , \quad \bar{Q}_H = \frac{4}{3} \pi R^3 \rho' H \quad (73, 74)$$

$$\frac{1}{\bar{Q}_H} \frac{dQ_c}{dv'} = \left(\frac{R^2}{\alpha'} \frac{dv'}{d\theta} \right) \frac{v'(1-v')(1+2v')}{2} \quad (75)$$

$$\frac{1}{\bar{Q}_H} \left| \frac{dQ_c}{dv'} \right| = \frac{(T_m - T_s) C_p'}{H} \left(\frac{1+2v'}{1 + \sqrt{1 + \frac{4}{3v'} \frac{(T_m - T_s) C_p'}{H}}} \right) \quad (76)$$

$$g)_{r=R} = -\rho' H 2\pi r' L \frac{dr'}{d\theta} - \rho' c_p' 2\pi L \int_{r'}^R r \frac{\partial T}{\partial \theta} dr \quad (77)$$

$$\frac{dQ_c}{d\theta} = -\rho' c_p' 2\pi L \int_{r'}^R r \frac{\partial T}{\partial \theta} dr \quad (78)$$

$$\left. \frac{\partial T}{\partial \theta} \right|_0 = -\frac{H}{c_p' \alpha'} \frac{\ln\left(\frac{R}{r}\right)}{\ln\left(\frac{R}{r'}\right)} \left(\frac{dr'}{d\theta}\right)^2 \quad (61)$$

$$\int_{r'}^R r \ln\left(\frac{R}{r}\right) dr = \frac{R^2 - r'^2 - 2r'^2 \ln \frac{R}{r'}}{4} \quad (79)$$

$$\bar{Q}_H = \pi R^2 L \rho' H \quad (80)$$

$$\frac{1}{\bar{Q}_H} \frac{dQ_c}{dV'} = \left(\frac{R^2}{\alpha'} \frac{dV'}{d\theta} \right) \left(\frac{1 - V'^2 - 2V'^2 \ln \frac{1}{V'}}{2 \ln \frac{1}{V'}} \right) \quad (81)$$

E. Total Heat Removed During the Solidification of Chilled Castings.

When heat flow into a chill mold is to be considered, as well as heat flow through the casting (next section), it becomes necessary to know the total heat (latent heat plus specific heat) which leaves the casting. This problem may be handled in the framework of equations which have already been developed in studying freezing rates.

Consider first the case of the sphere.

Equation (70): Rewrite (31) for $r = R$. This is the rate at which heat is flowing across the chilled surface of the casting, or the total rate of heat flow from the casting.

Equation (71): Subtract the latent heat contribution from (70). This is the rate at which the solid part of the casting is losing heat.

Equation (41): Repeat the first approximation of the cooling rate at "r".

Equation (72): Perform the integration indicated in (71) upon the factor containing "r".

Equation (75): Substitute (41), (72), (73), (74) into (71).

Equation (76): Substitute (64) into (75). This is the amount of specific heat which leaves the casting per linear increment of solid metal.

The above procedure is repeated in Equations (77) through (81) for a cylinder. However, in Equation (81) it is not convenient to substitute

$$\frac{\bar{Q}_c}{Q_H} = \frac{3B}{4} \left[-\frac{7}{6} + \frac{(7-3B)(1+B)^{\frac{3}{2}}}{6} + \frac{B(B-1)\sqrt{1+B}}{4} + \frac{B^2(B-1)}{4} \ln \frac{1+\sqrt{1+B}}{\sqrt{B}} \right] \quad (82)$$

the analytical expression for the freezing rate as was done in (76). Instead, for numerical work the appropriate values for the freezing rates may be read from Figures 6 and 7.

Equation (76) is represented graphically in Figures 9 and 10. The total area under any one curve corresponds to the heat removed in cooling the solid portion of the sphere during complete solidification. Planimetric integration of Figures 9 and 10 leads to Figure 11: the ratio of specific heat to latent heat removed during complete solidification of a sphere is plotted as a function of $C_p^*(T_m - T_r)/H$.

Equation (81) was used in conjunction with Figures 6 and 7 to prepare Figures 12 and 13, for the cooling of cylinders during solidification. Figures 12 and 13 were integrated graphically to get Figure 14, which, as in Figure 11 above, gives the ratio of specific to latent heat removed during complete solidification of a cylinder.

In the case of the sphere, Equation (76) has been integrated analytically to give Equation (82), the equation of the curve in Figure 11.

$$\frac{T - T_s}{T' - T_s} = \operatorname{erf} \frac{x}{2\sqrt{\alpha'\theta}} \quad (2)$$

$$q = -AK' \frac{\partial T}{\partial x} \quad (85)$$

$$q|_{x=0} = \frac{AK'(T' - T_s)}{\sqrt{\pi\alpha'\theta}} \quad (86)$$

$$Q = \frac{2AK'(T' - T_s)\sqrt{\theta}}{\sqrt{\pi\alpha'}} \quad (87)$$

$$Q_c = \frac{2AK'(T' - T_s)\sqrt{\theta}}{\sqrt{\pi\alpha'}} - x'AP'H \quad (88)$$

$$\sqrt{\theta} = \frac{x'}{2\beta\sqrt{\alpha'}} \quad , \quad T' - T_s = \frac{T_m - T_s}{\operatorname{erf} \beta} \quad (5, 6)$$

$$\frac{c_p'(T_m - T_s)}{H} = \sqrt{\pi} \beta e^{\beta^2} \operatorname{erf} \beta \quad (7)$$

$$\frac{Q_c}{Q_H} = e^{\beta^2} - 1 \quad (89)$$

$$\frac{Q_c}{Q_H} = \frac{x'^2}{4\alpha'\theta} + \frac{1}{2} \left(\frac{x'^2}{4\alpha'\theta} \right) + \dots \quad (90)$$

$$\frac{X'^2}{\alpha'\theta} = \frac{4C_p'(T_m - T_s)}{H} \left(\frac{1}{1 + \sqrt{1 + \frac{4C_p'(T_m - T_s)}{3H}}} \right) \quad (92)$$

$$\frac{Q_c}{Q_H} = \frac{C_p'(T_m - T_s)}{H} \left(\frac{1}{1 + \sqrt{1 + \frac{4C_p'(T_m - T_s)}{3H}}} \right) \quad (93)$$

$$\left. \frac{Q_c}{Q_H} \right|_p = \frac{X'^2}{4\alpha'\theta} \quad (94)$$

As before, to assess the validity of the total heat approximation, the exact and approximate results for the one-dimensional case are compared graphically. Consider the exact development below for unidirectional freezing.

Equation (2): Repeated, the temperature distribution in the solid portion of the casting.

Equation (85): The Fourier equation.

Equation (86): Combine (2) and (85).

Equation (87): Integrate (86).

Equation (88): Subtract the latent heat contribution. This is the integrated heat which has been removed from the solid metal.

Equation (89): Substitute (5), (6), and (7) into (88), and divide by Q_c .

Equation (90): Expand (89) in power series.

Using procedures already illustrated for the sphere and the cylinder, corresponding approximate solutions for the one-dimensional case are given by Equations (91), (92), and (93). The result in (93) is the same as the first term of the power series, Equation (90).

The results of this section on total heats are summarized in Figure 15, in which solidification time is related to the ratio of specific to latent heat. Four curves are shown, an approximate curve for the slab, sphere, and cylinder, and the exact curve for the slab. The degree

of approximation is not as accurate as in the case of freezing rates, but for moderate levels of $C_p^*(T_m - T_s)/H$ errors in total heats estimated by means of this chart will not be large.

TABLE II.

Definition of Terms Not Included in Table I.

k'	= Thermal conductivity of solid cast metal.
ρ'	= Density of solid cast metal.
C_p'	= Specific heat of solid cast metal.
α'	= Thermal diffusivity of solid cast metal.
Q_H	= Latent heat which leaves casting in time, " θ ".
Q_C	= Specific heat (total heat minus latent heat) which leaves casting in time, " θ ".
\bar{Q}_H	= Total heat of fusion of casting.
\bar{Q}_C	= Total specific heat which leaves casting during complete solidification.
T'	= Integration constant in Equation (2).
ΔT	= $(T_m - T_s)$, used in Figures 3 - 15.
ΔT_1	= Defined by Equation (24).
r'	= Radius of liquid-solid interface in a freezing spherical or cylindrical casting.
	=
V	= Defined by Equations (44) and (45).
v'	= r'/R
G	= Defined by Equation (66).
B	= Defined by Equation (68).

Subscript numerals indicate the order of approximation:

T_0 = First approximation of temperature distribution in solid metal layer.

T_1 = Second approximation, etc.

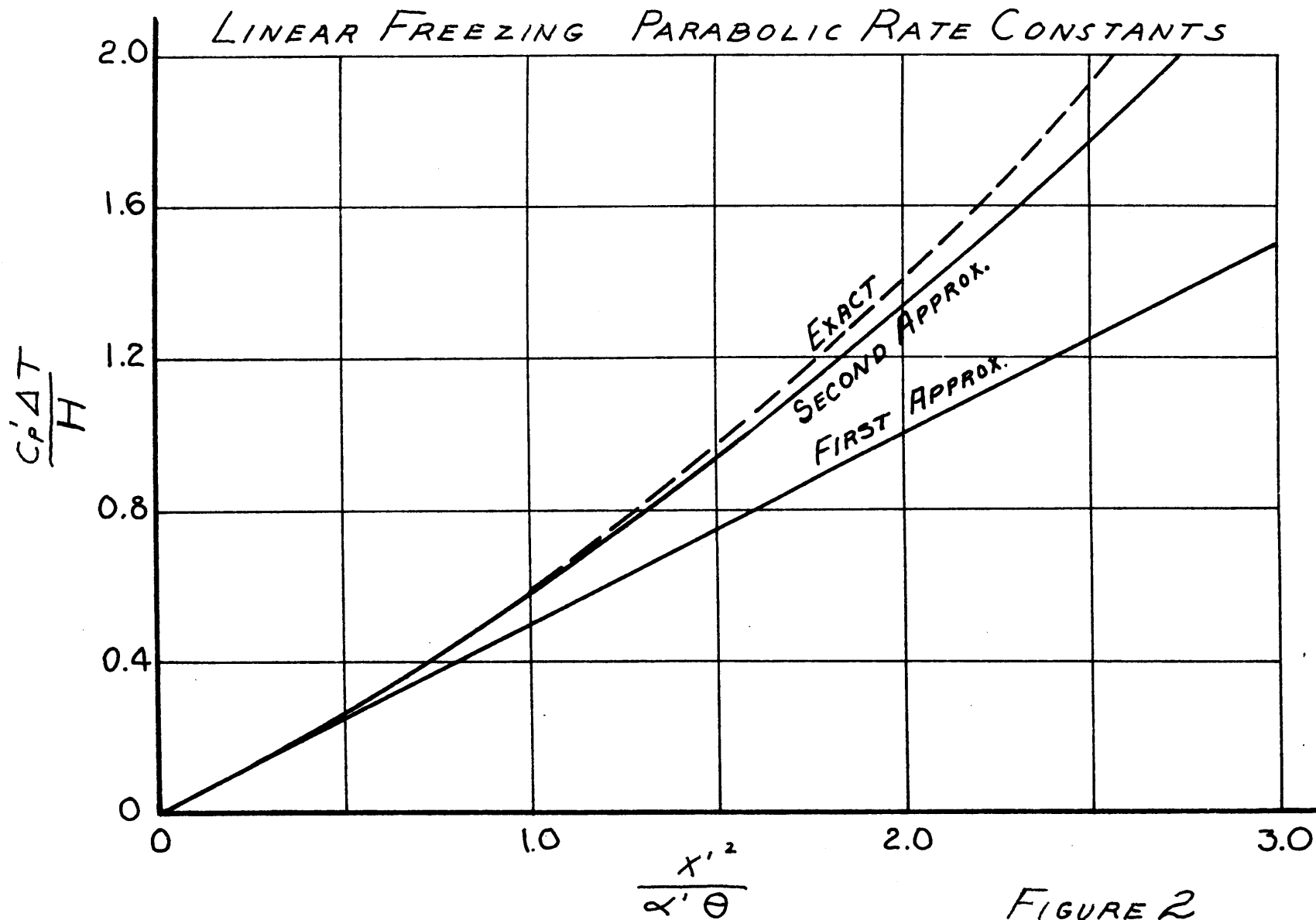


FIGURE 2

INVERSE FREEZING RATES
OF SPHERES

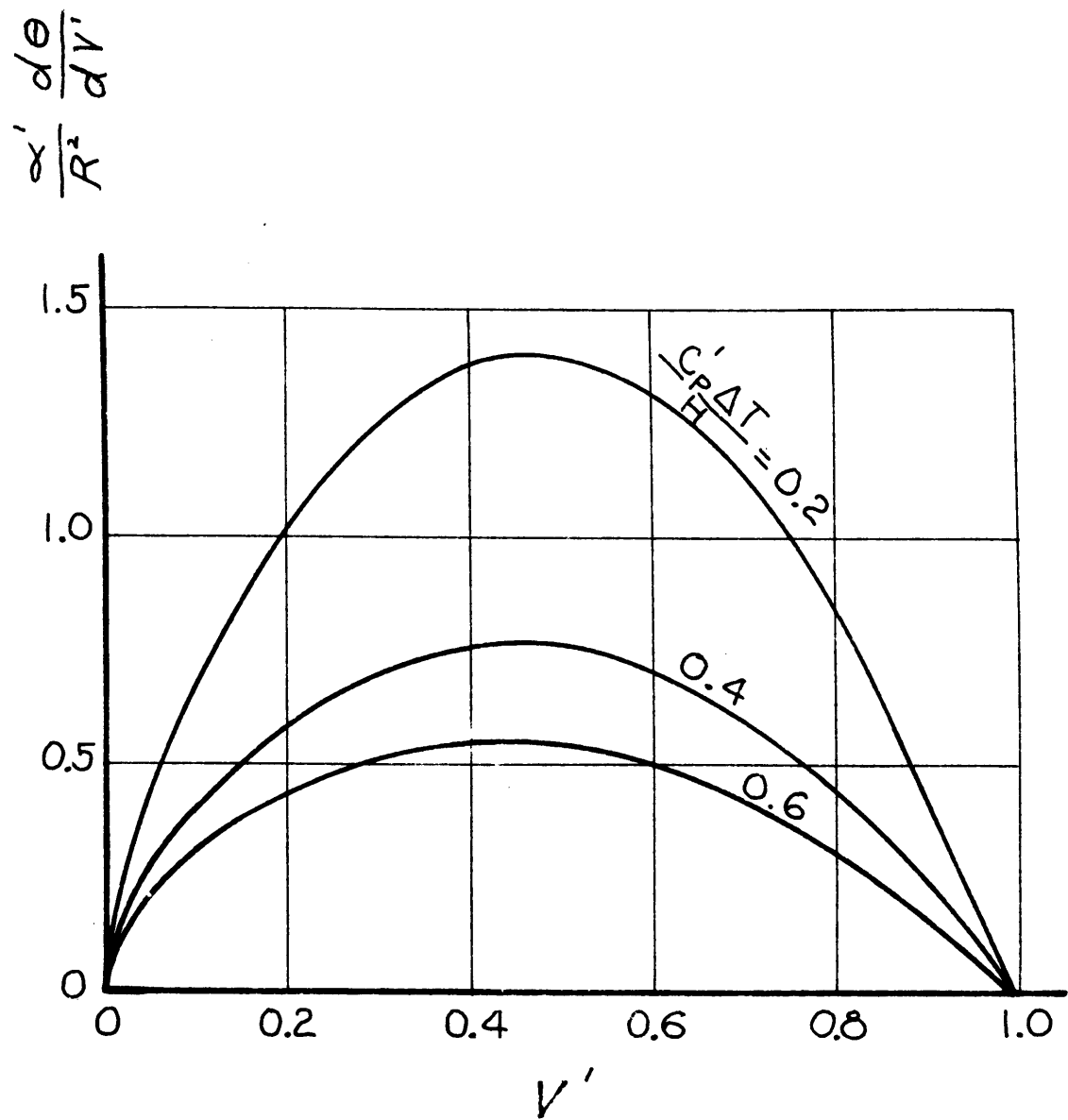
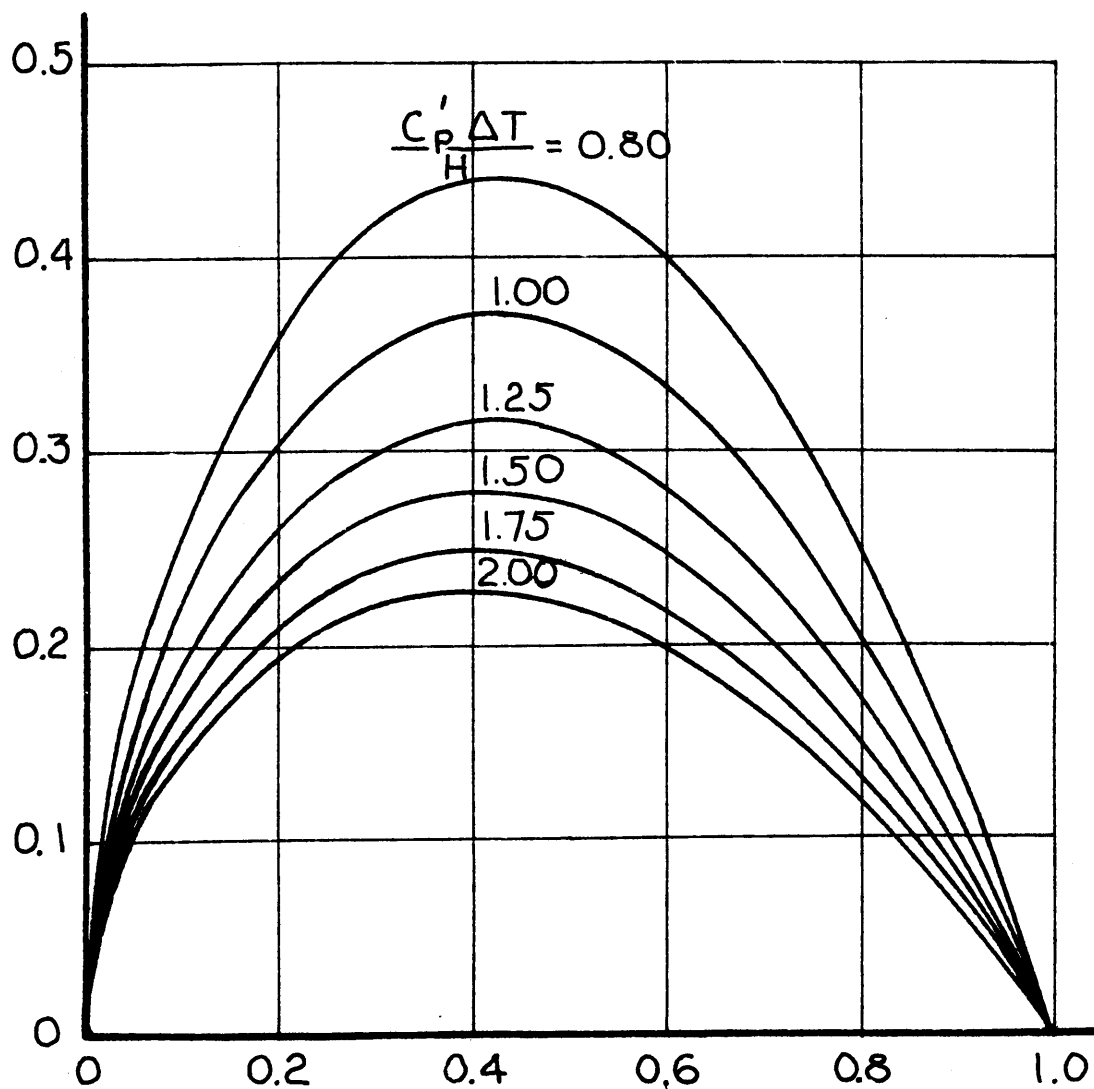


FIGURE 3

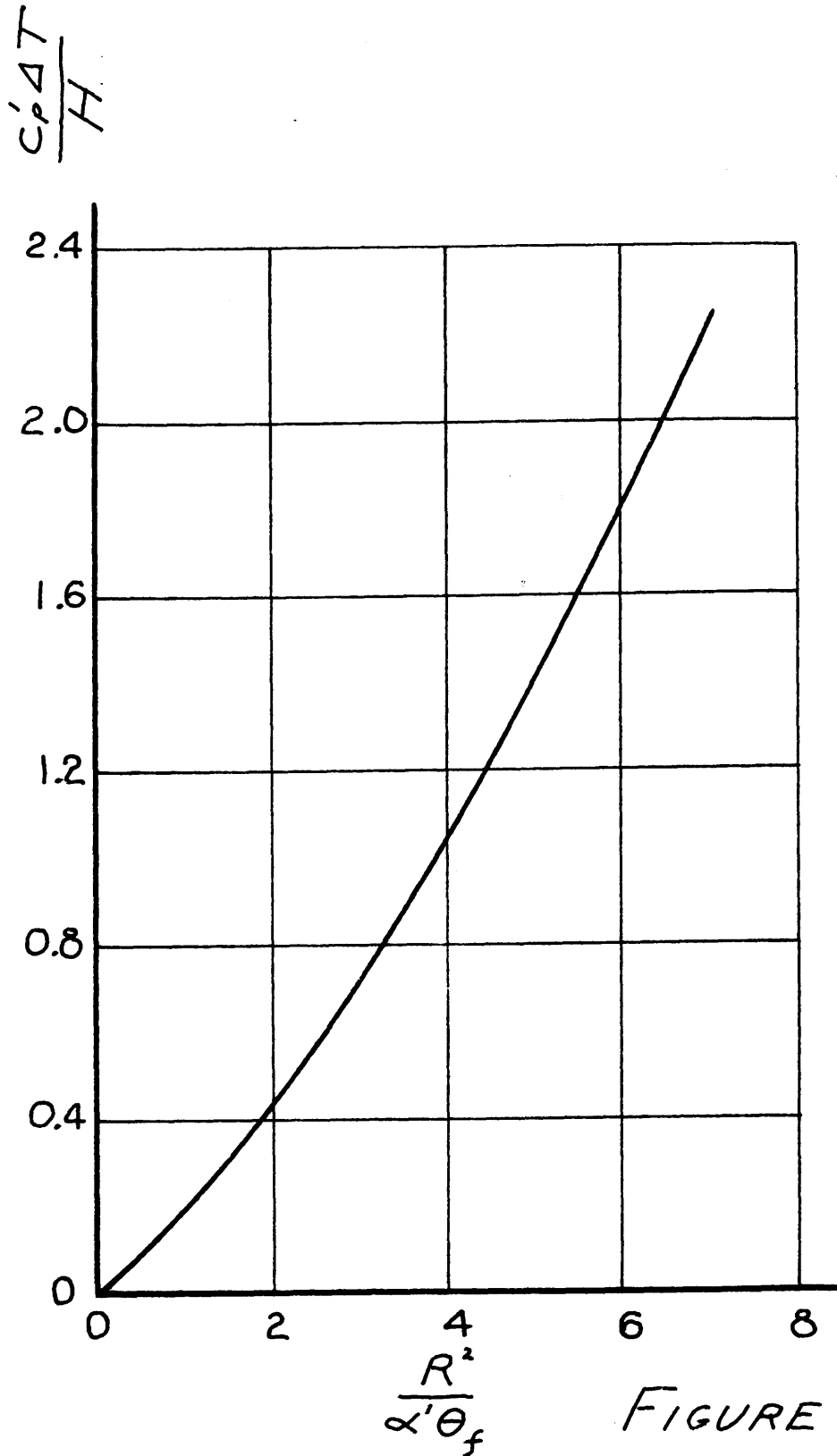
INVERSE FREEZING RATES
OF SPHERES

$$\frac{d\theta}{\delta' R^2} \frac{dV'}{dV'}$$



V' FIGURE 4

COMPLETE SOLIDIFICATION
TIMES FOR SPHERES



INVERSE FREEZING RATES
OF CYLINDERS

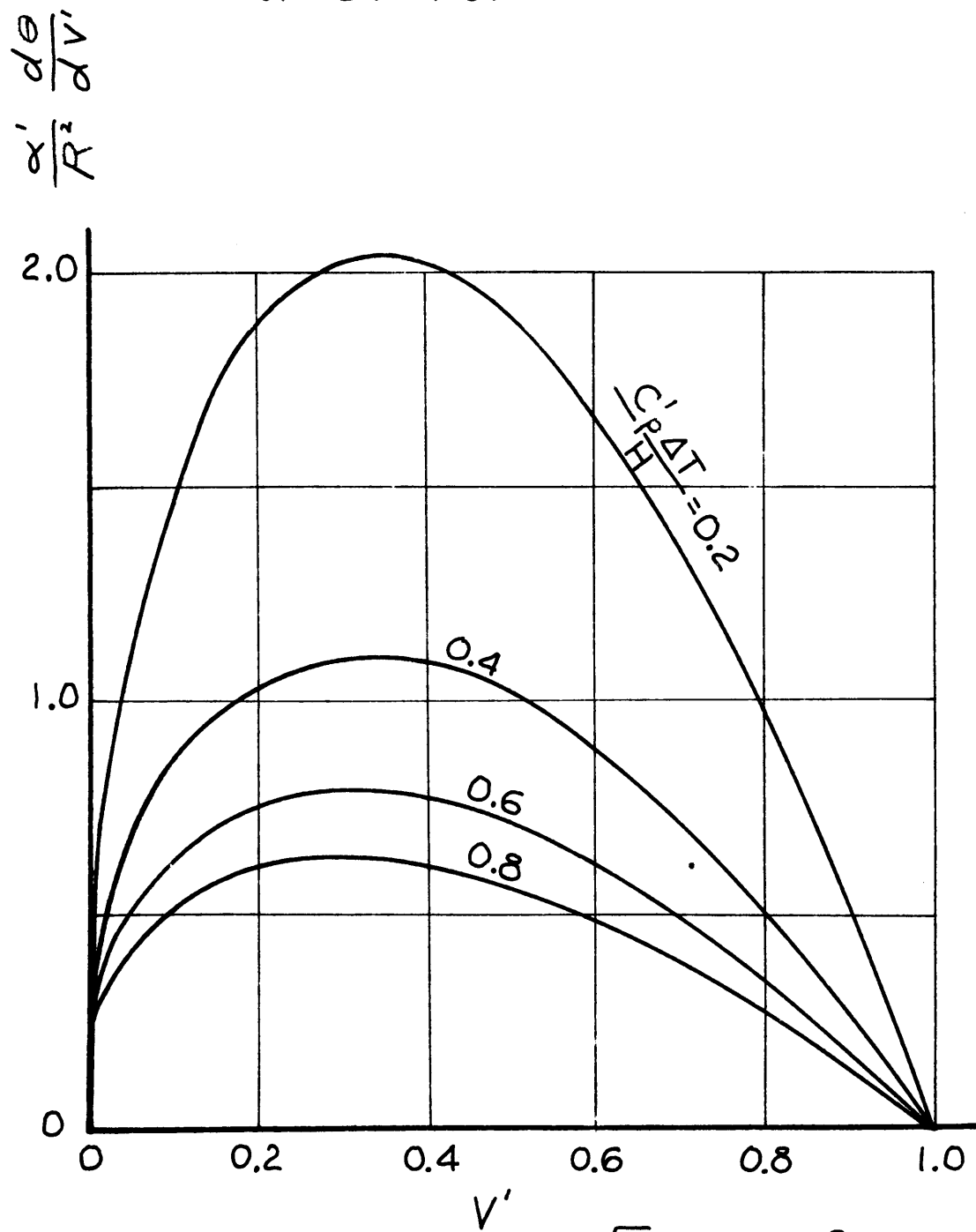
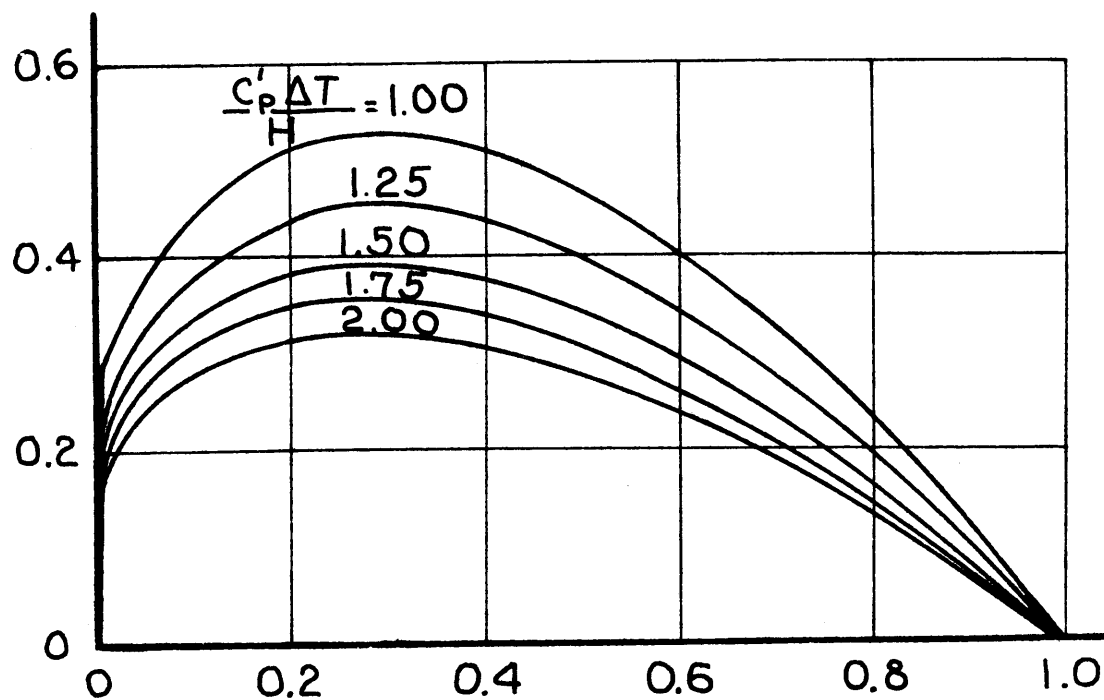


FIGURE 6

INVERSE FREEZING RATES
OF CYLINDERS

$$\frac{d\theta}{dV'}$$

$$\frac{\gamma}{R^2}$$



V' FIGURE 7

COMPLETE SOLIDIFICATION TIMES
FOR CYLINDERS

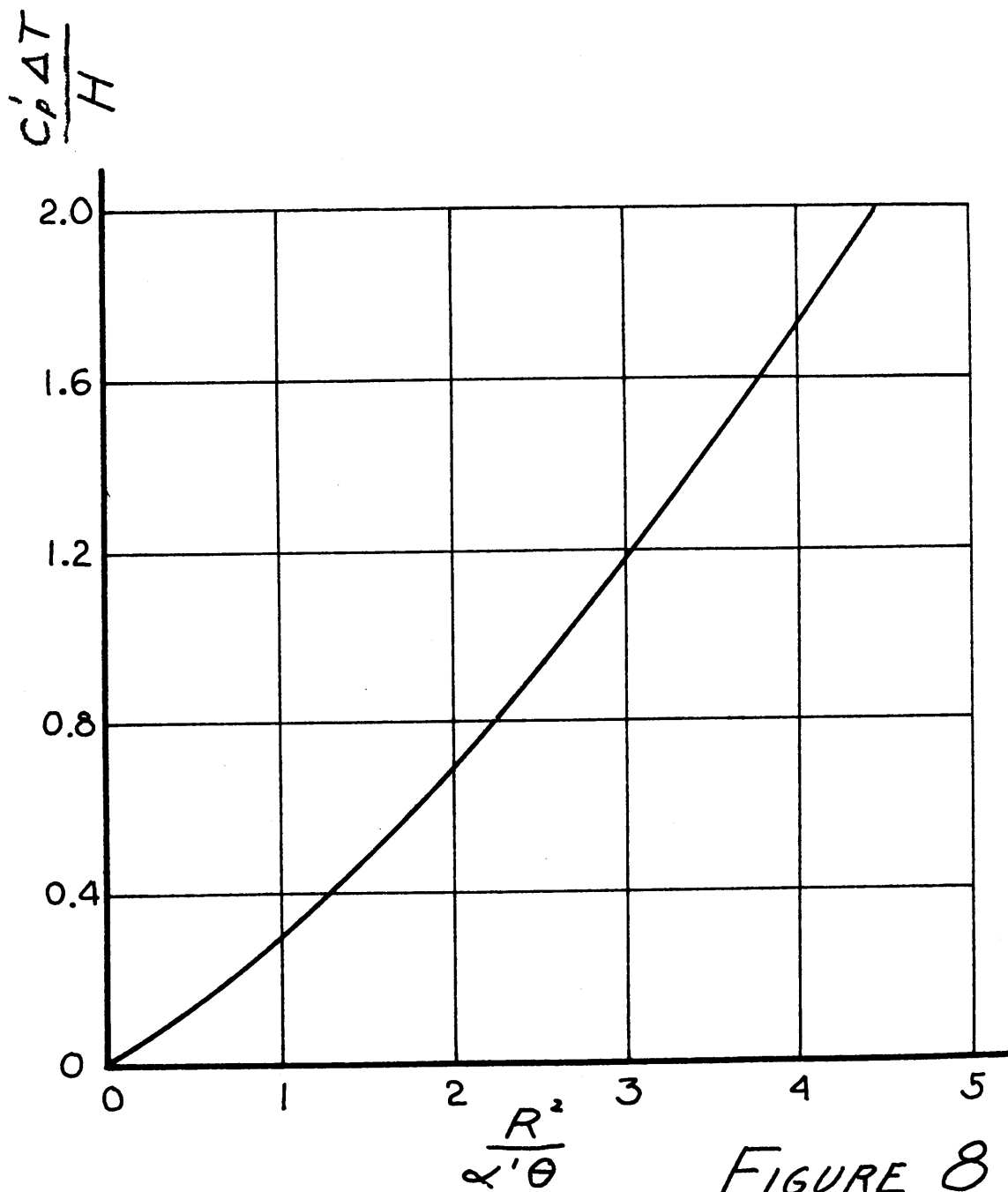


FIGURE 8

$$\frac{dQ_c}{dV'} \frac{3}{4\pi R^3 \rho' H}$$

RATES OF HEAT REMOVAL FROM
SOLID PORTIONS OF FREEZING
SPHERES

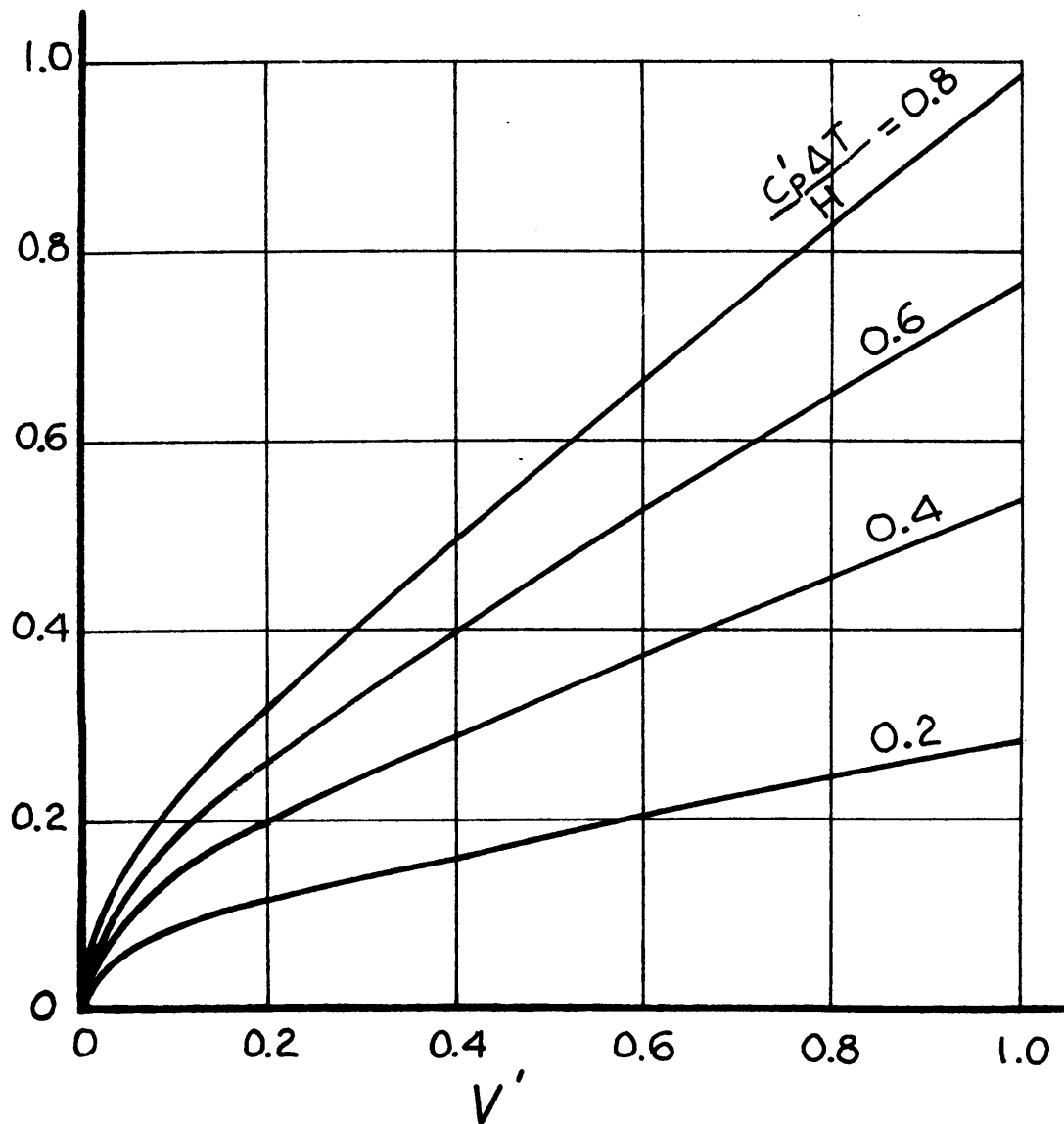


FIGURE 9

$$\frac{dQ_c}{dV'} \frac{3}{4\pi R^3 \rho' H}$$

RATE OF HEAT REMOVAL
FROM SOLID PORTIONS OF
FREEZING SPHERES

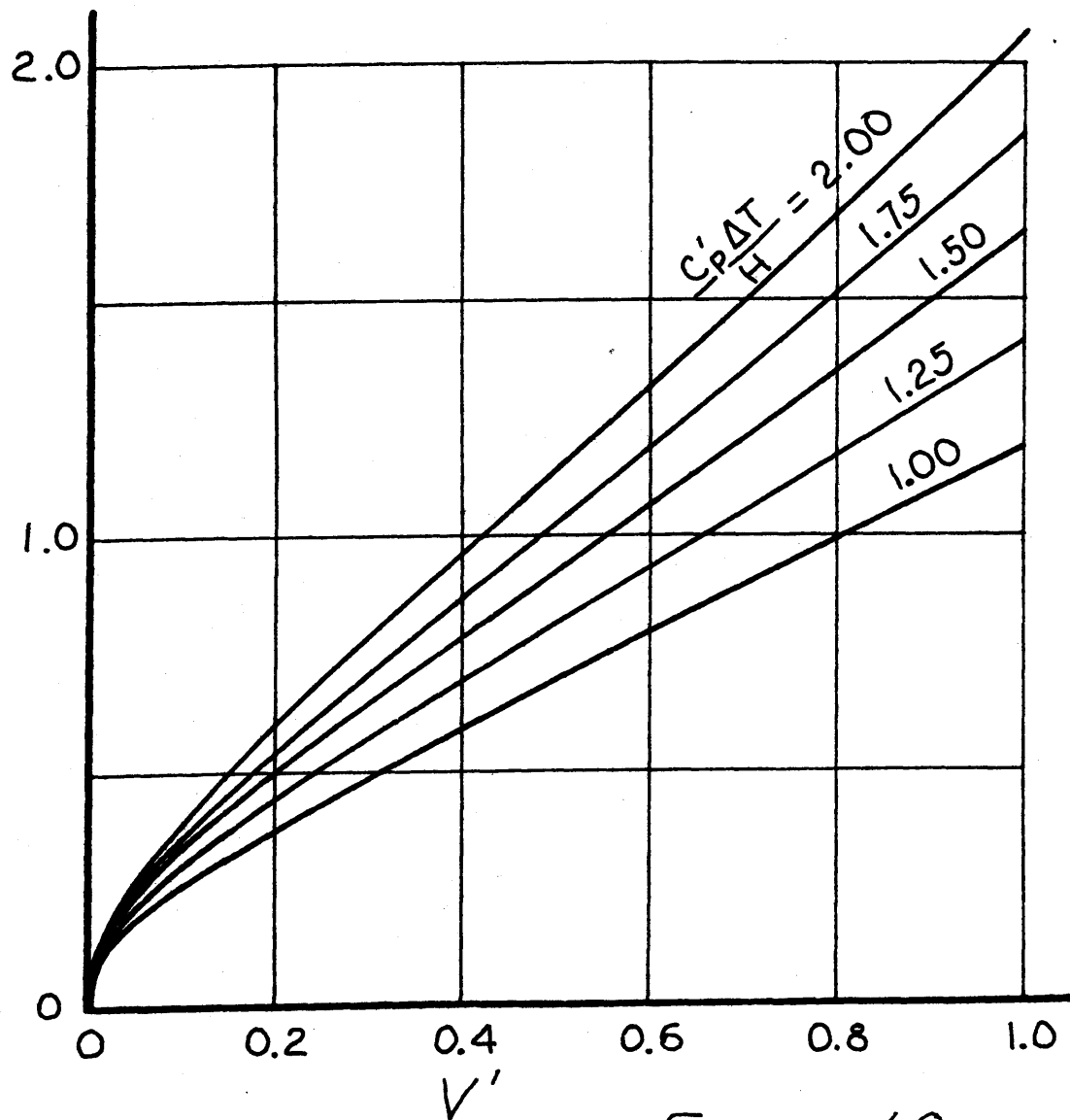


FIGURE 10

RATIO OF SPECIFIC TO LATENT
HEAT REMOVED DURING
COMPLETE SOLIDIFICATION
OF SPHERES

$$\frac{c_p \Delta T}{H}$$

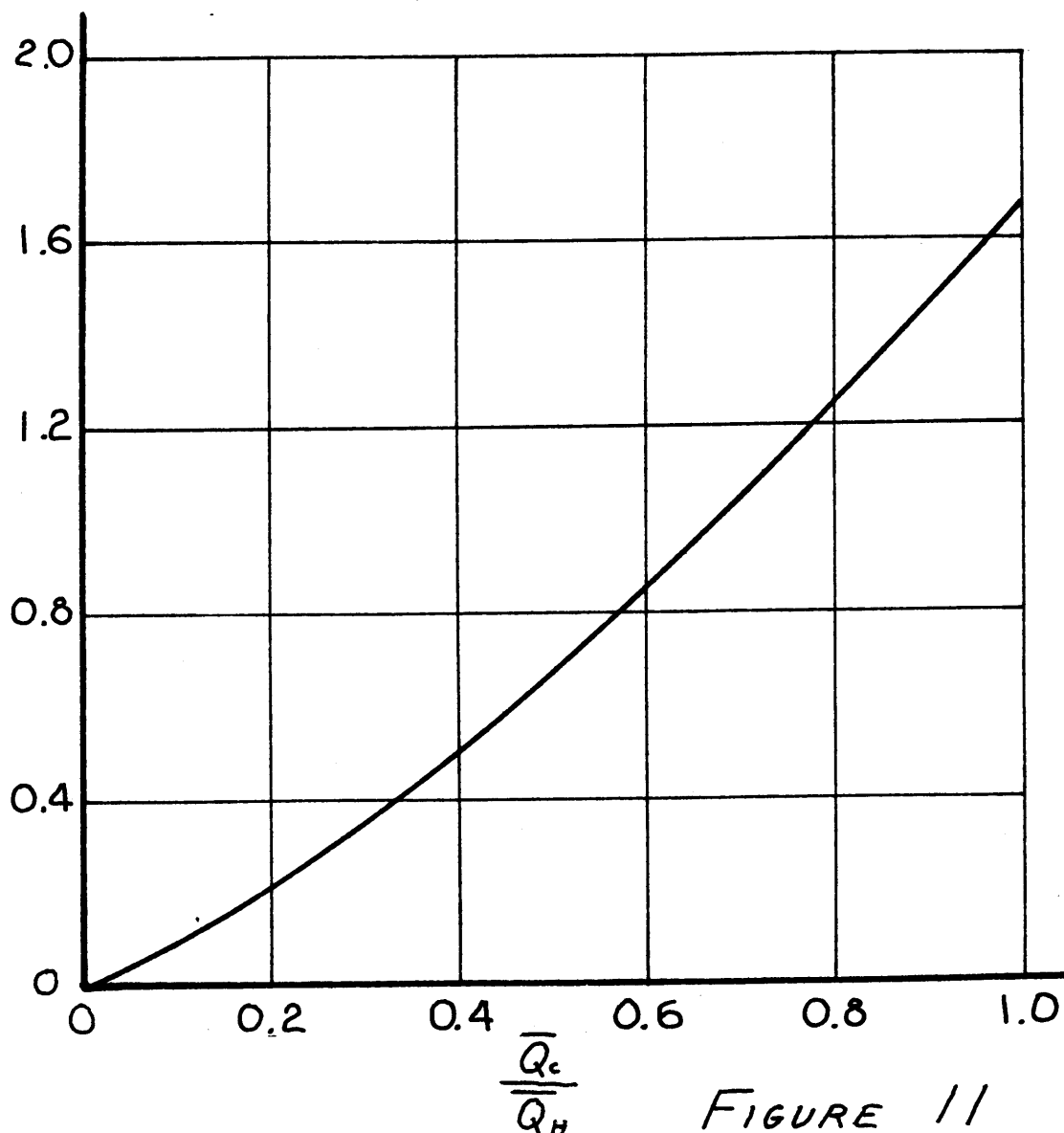


FIGURE 11

RATES OF HEAT REMOVAL
FROM SOLID PORTIONS OF
FREEZING CYLINDERS

$$\frac{dQ_c}{dV'}$$

$$\frac{1}{\pi L \rho' H R^2}$$

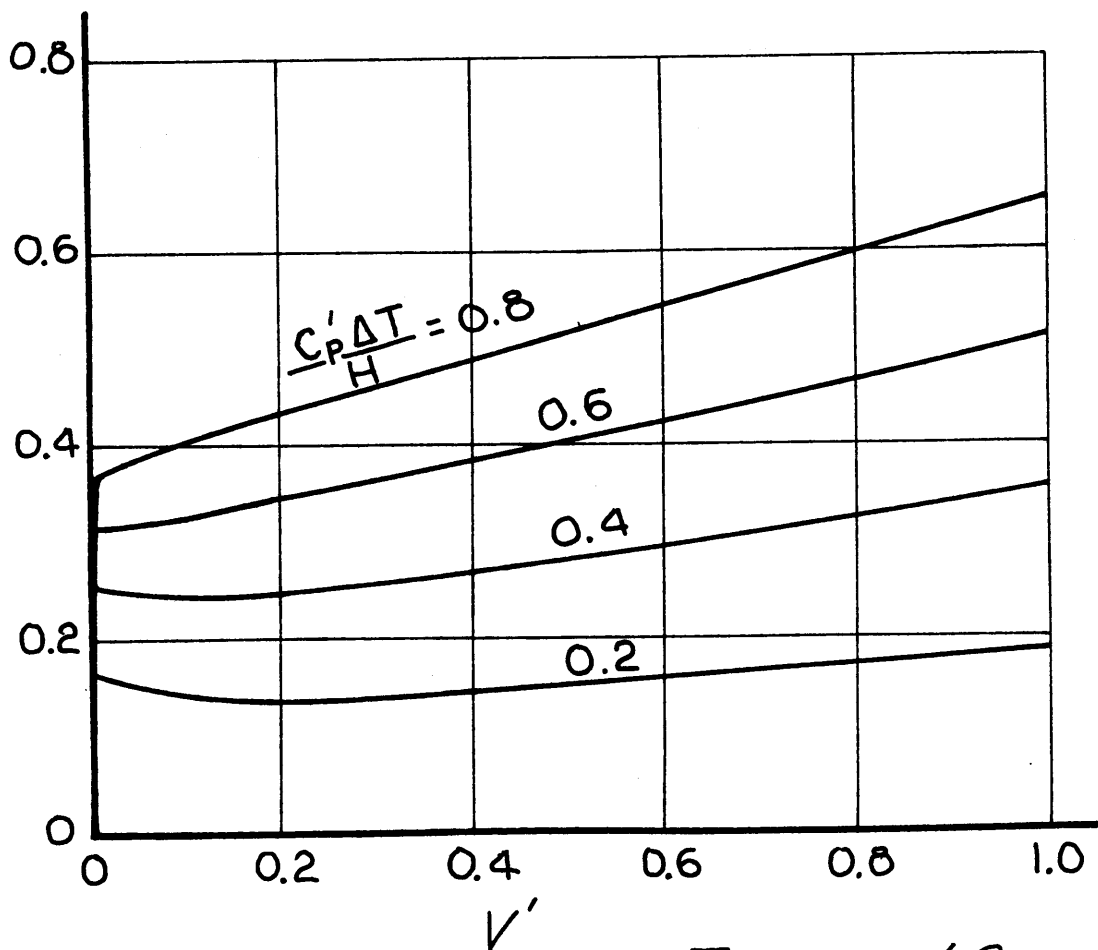


FIGURE 12

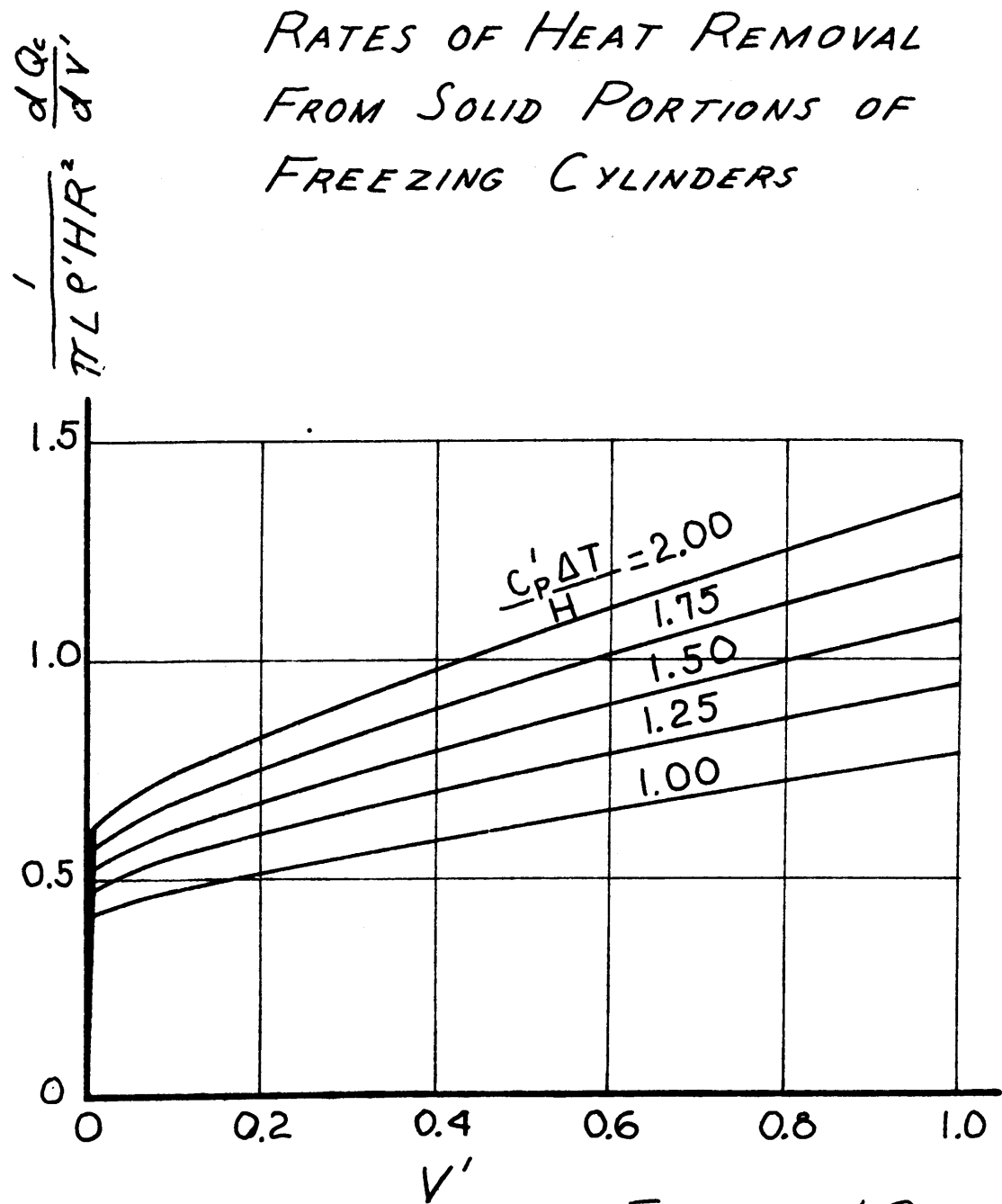
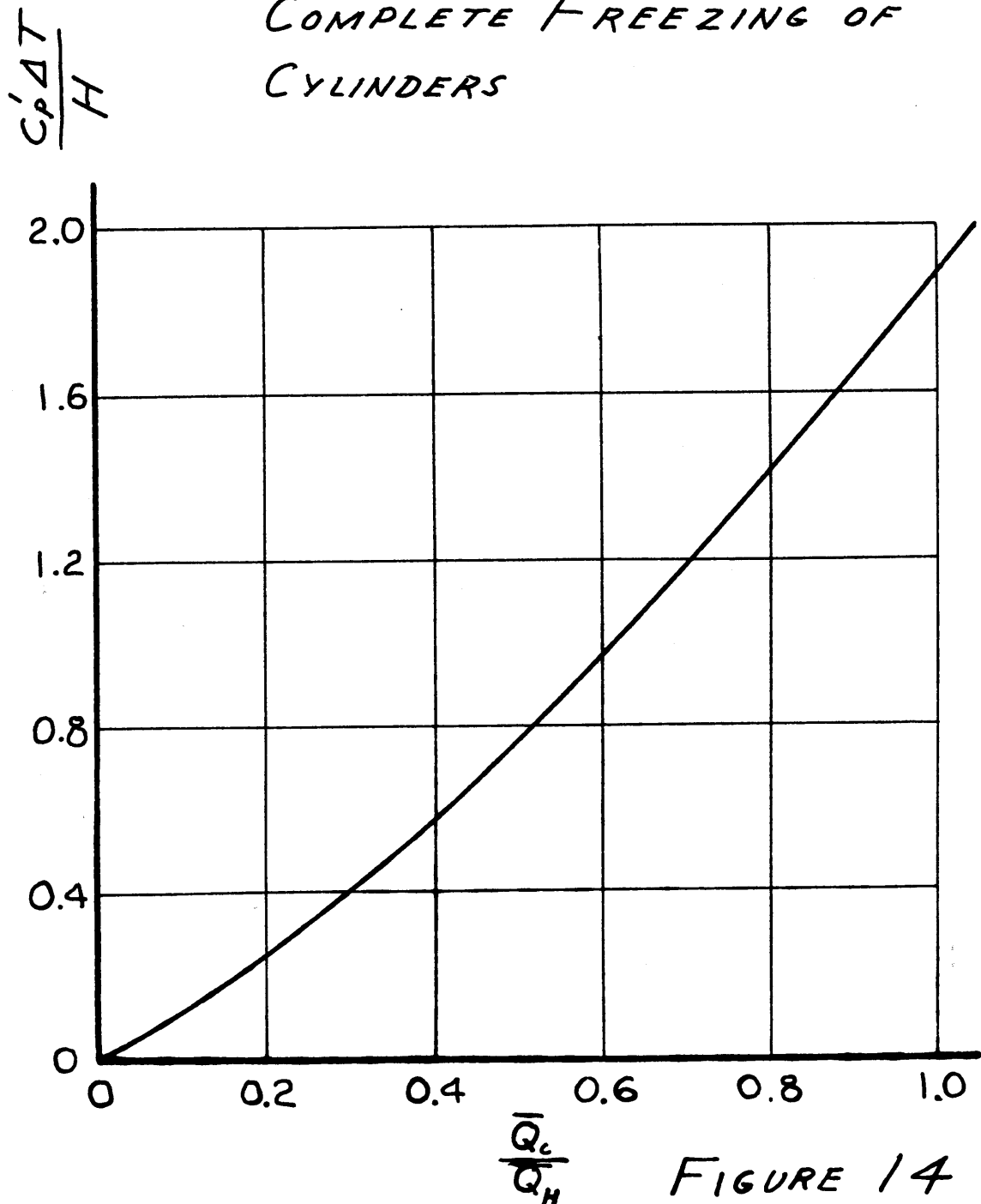


FIGURE 13

RATIO OF SPECIFIC TO LATENT
HEAT REMOVED DURING
COMPLETE FREEZING OF
CYLINDERS



RATIO OF SPECIFIC TO LATENT
HEAT REMOVED FROM SPHERES,
CYLINDERS, AND SLABS DURING
COMPLETE SOLIDIFICATION

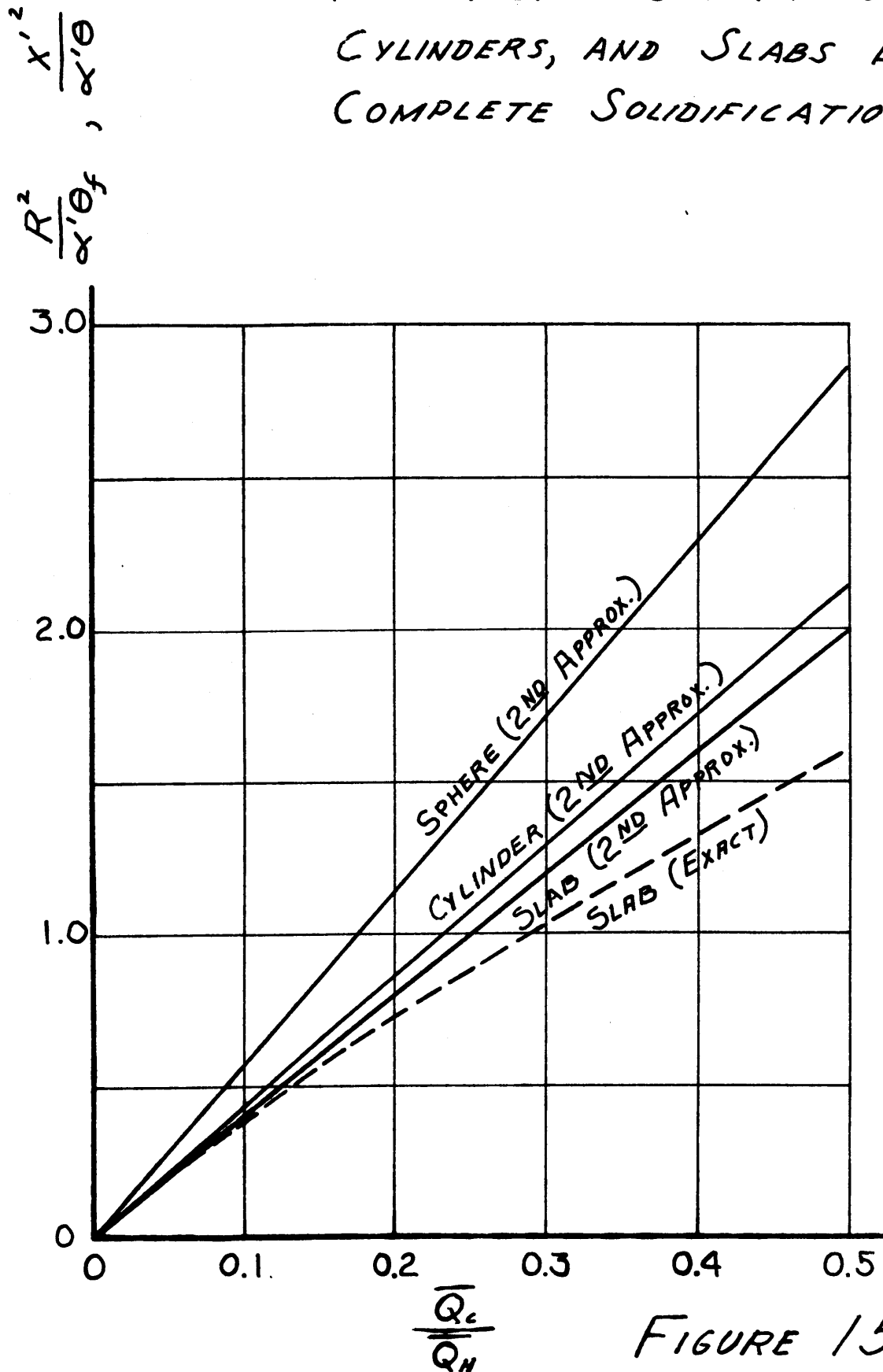


FIGURE 15

$$\frac{1}{\alpha} \frac{\partial T_a}{\partial \theta} = \frac{\partial^2 T_a}{\partial x^2} \quad (1)$$

$$\frac{1}{\alpha_b} \frac{\partial T_b}{\partial \theta} = \frac{\partial^2 T_b}{\partial x^2} \quad (2)$$

$$\frac{T_s - T_a}{T_s - T_\infty} = - \operatorname{erf} \frac{x}{2\sqrt{\alpha}\theta} \quad (3)$$

$$\frac{T_b - T_s}{T_b' - T_s} = \operatorname{erf} \frac{x}{2\sqrt{\alpha'}\theta} \quad (4)$$

$$A_T \quad x=0, \quad K_a \frac{\partial T_a}{\partial x} = K_b \frac{\partial T_b}{\partial x} \quad (5)$$

$$A_T \quad x=x' \quad T_b = T_m \quad (6)$$

$$K_b \frac{\partial T_b}{\partial x} = \rho' H \frac{dx'}{d\theta} \quad (7)$$

$$\beta = \frac{x'}{2\sqrt{\alpha'}\theta} \quad (8)$$

V. ANALYSIS OF HEAT FLOW FROM CHILLED CASTINGS:
 METALS CAST INTO METAL MOLDS

(Pure metals and alloys which freeze completely
 within a narrow temperature range.)

A. Plane Mold Wall.

1. Perfect Thermal (Wetted) Contact Between the Metal and the Mold.

The solution given here is essentially that of Lightfoot³ and Schwarz,⁴ and is based on the method of Neumann.¹ As in the previous section, superheat is not yet considered. The new features of this problem are that the properties of the mold and the metal play a part, and the concept of a mold-metal interface temperature is introduced. Consider that the mold is zone "a" and the solid part of the metal is zone "b". The mold is initially at room temperature, and the liquid metal at its melting point. At zero time, the metal and the mold are brought into intimate contact, and solidification begins. "x" is considered to be positive in the metal, zero at the mold-metal interface, and negative in the mold.

Equations (1,2): The partial differential equation for linear heat flow must be satisfied in zones "a" and "b".

Equations (3,4): Particular solutions of (1) and (2). T_b' is an arbitrary constant and T_s , the mold-metal interface temperature, is unknown. (3) and (4) are based upon the assumption that T_s is constant. (3) and (4) conform with the boundary conditions stated above, and it must now be determined whether they are compatible

$$\frac{(T_m - T_s) C_p'}{H} = \sqrt{\pi} \beta e^{\beta^2} \operatorname{erf} \beta \quad (9)$$

$$\frac{(T_m - T_x) C_p'}{H} = \sqrt{\pi} \beta e^{\beta^2} \left(\sqrt{\frac{K' \rho' C_p'}{K \rho C_p}} + \operatorname{erf} \beta \right) \quad (10)$$

$$\frac{(T_b' - T_s) C_p'}{H} = \sqrt{\pi} \beta e^{\beta^2} \quad (11)$$

$$\frac{T_s - T_x}{T_b' - T_s} = \sqrt{\frac{K' \rho' C_p'}{K \rho C_p}} \quad (12)$$

$$h' = \left(1 + \sqrt{\frac{K' \rho' C_p'}{K \rho C_p}} \right) \bar{h} \quad (13)$$

$$h = \left(1 + \sqrt{\frac{K \rho C_p}{K' \rho' C_p'}} \right) \bar{h} \quad (14)$$

with the remaining boundary conditions.

Equation (5): At the mold-metal interface, the heat flux must be continuous.

Equations (6,7): At the liquid-solid interface, the temperature must equal the melting point, and the gradient must be proportional to the rate of solidification.

Equation (8): When condition (6) is inserted into (4), the left-hand side is constant. Therefore, the argument on the right-hand side must be constant, and is defined as " β ".

Equations (9,10,11): Insert (3) and (4) into boundary conditions (5), (6), and (7).

Since a real value for " β " satisfies Equation (10), and all other requirements are met, (3) and (4) are the desired solutions. " β " is determined from Equation (10), T_s from Equation (9), and T_b^* from Equation (11). The constant, T_b^* , has the following physical meaning: The cast metal behaves like a mass having the same thermal properties, but exhibiting no latent heat, which is initially at T_b^* . T_b^* is higher than T_m . This is basically the reason such a simple solution is possible.

2. The Effect of Thermal Contact Resistance Between the Metal and the Mold.

In order to handle this problem, it has been found necessary to extend the concept of the mold-metal interface temperature, introduced

in the preceding paragraphs. The following statements are intended to clarify how and why this extension is made.

Consider two solids, A and B, initially at different, uniform temperatures, which are suddenly brought into intimate contact (no contact resistance). The initial temperature of A is T_A , and the initial temperature of B is T_B . A has properties: k , ρ , and C_p ; B has properties: k' , ρ' , and C_p' . It can be shown that the interface will immediately assume a temperature, T_S , constant, which will conform to Equation (12).^{1d} With the aid of this interface temperature, the problem can be separated into two individual problems -- the heating or cooling of a semi-infinite solid.

Now consider the same two solids, A and B, initially at the same two temperatures, respectively, which are suddenly brought into poor contact (i.e. there is a film-type thermal contact resistance between the two solids). Mathematically, this contact resistance may be thought of as a "Newton's Law" type of boundary condition wherein the heat flux across the interface is proportional to the temperature drop across the interface. Carslaw^{1e} gives the complete, rather cumbersome solution for this problem. In this case there is no constant, physical interface temperature; there are two surface temperatures, neither of which are constant. However, the solution given by Carslaw may be considerably simplified, algebraically, by using the following procedure: Consider an imaginary reference plane, between the abutting surfaces, which is at T_S , where T_S is constant, and determined as before using Equation (12). If the contact resistance is then apportioned on either

side of the imaginary plane in accordance with Equations (13) and (14), this problem may also be split rigorously into two halves. Each half consists of the heating or cooling of a semi-infinite solid with a "Newton's Law" type of boundary condition. In Equations (13) and (14), \bar{h} is the total coefficient of heat transfer across the interface, h is the coefficient on the "A" side of the plane, and h' is the coefficient on the "B" side of the plane.

Thus the interface temperature which prevails in the absence of contact resistance, still has physical meaning when contact resistance is in effect. The interface temperature is independent of the magnitude of the contact resistance, and is dependent only upon the thermal properties of the two solids.

With the foregoing justification, casting problems will be handled as follows: (a) The problem will first be solved as if there were no contact resistance. (b) Using the interface temperature obtained in (a), and applying Equations (13) and (14), the casting-half of the problem will be isolated and studied separately, using the results of the analysis given below.

$$q)_{x=0} = -\rho' H A \frac{dx'}{d\theta} + \rho' c_p' A \int_0^{x'} \frac{\partial T}{\partial \theta} dx \quad (15)$$

$$T - T_{sc} = \frac{H}{c_p' \alpha'} \frac{dx'}{d\theta} x - \frac{1}{\alpha'} \int_0^x \int_x^{x'} \frac{\partial T}{\partial \theta} dx dx \quad (16)$$

$$-(T_{sc} - T_s) h' A = q)_{x=0} \quad (17)$$

$$T - T_s = \frac{H}{c_p' \alpha'} \frac{dx'}{d\theta} \left(x + \frac{k'}{h'} \right) \quad (18)$$

$$-\frac{k'}{h' \alpha'} \int_0^{x'} \frac{\partial T}{\partial \theta} dx - \frac{1}{\alpha'} \int_0^x \int_x^{x'} \frac{\partial T}{\partial \theta} dx dx$$

$$\frac{c_p' (T_m - T_s)}{H} = \frac{1}{\alpha'} \frac{dx'}{d\theta} \left(x' + \frac{k'}{h'} \right) \quad (19)$$

$$-\frac{c_p' k'}{h' H \alpha'} \int_0^{x'} \frac{\partial T}{\partial \theta} dx - \frac{c_p'}{H \alpha'} \int_0^x \int_x^{x'} \frac{\partial T}{\partial \theta} dx dx$$

$$T_0 - T_s = \frac{H}{c_p' \alpha'} \frac{dx'}{d\theta} \left(x' + \frac{\kappa'}{h'} \right) \quad (20)$$

$$\left. \frac{\partial T}{\partial \theta} \right|_0 = \frac{H}{c_p' \alpha'} \frac{d^2 x'}{d\theta^2} \left(x' + \frac{\kappa'}{h'} \right) \quad (21)$$

$$\int_0^{x'} \left(x + \frac{\kappa'}{h'} \right) dx = x' \left(\frac{x'}{2} + \frac{\kappa'}{h'} \right) \quad (22)$$

$$\int_0^{x'} \int_0^{x'} \left(x + \frac{\kappa'}{h'} \right) dx dx = x'^2 \left(\frac{x'}{3} + \frac{\kappa'}{2h'} \right) \quad (23)$$

$$\frac{\alpha' c_p' (T_m - T_s)}{H} = \frac{dx'}{d\theta} \left(x' + \frac{\kappa'}{h'} \right)$$

$$\left. \frac{d^2 x'}{d\theta^2} \right|_0 = - \left(\frac{dx'}{d\theta} \right)^2 \left(\frac{1}{x' + \frac{\kappa'}{h'}} \right) \quad (24)$$

$$\frac{C_p'(T_m - T_s)}{H} = \left(\frac{k' dx'}{h'\alpha' d\theta} \right) \left(\frac{h'x'}{k'} + 1 \right) \quad (25)$$

$$+ \left(\frac{k' dx'}{h'\alpha' d\theta} \right)^2 \left(\frac{\frac{h'x'}{k'}}{\frac{h'x'}{k'} + 1} \right) \left[\frac{\left(\frac{h'x'}{k'} \right)^2 + 3 \frac{h'x'}{k'} + 3}{3} \right]$$

$$\frac{h'\alpha' d\theta}{k' dx'} = \quad (26)$$

$$\frac{H Z}{2 C_p'(T_m - T_s)} \left(1 + \sqrt{1 + \frac{4 C_p'(T_m - T_s)}{3 H} \left[\frac{Z^3 - 1}{Z^3} \right]} \right)$$

$$Z \equiv \frac{h'x'}{k'} + 1 \quad (27)$$

The problem to be solved is that of a semi-infinite mass of liquid metal, initially at its melting point, which at zero time, begins to lose heat from a plane boundary exposed to a medium at temperature, T_s , constant. The discontinuous temperature drop across the cooling surface is proportional to the heat flux at the surface (Newton's Law of Cooling). The coefficient of heat transfer at the surface is symbolized by h' . The surface temperature of the casting, T_{sc} , is not constant.

It has not been found possible to obtain the exact analytical solution for this one-dimensional problem, but the iterative procedure used in the previous section may be applied to this case as well.

Equations (15,16): Surface heat flux and temperature distribution in the solid metal. The same expressions were obtained for constant casting surface temperature.

Equation (17): Newton's Law of Cooling.

Equation (18): Combine (15), (16), and (17).

Equation (19): Rewrite (18) at $x = x'$.

As before, the first term in Equation (18) is used as the first approximation for the temperature, the indicated operations are performed, and the second approximation, Equation (25), is the result.

Equation (26): Solve (25) for the linear freezing rate.

Equation (27): Definition of Z .

APPROXIMATE INTEGRATION:

$$\frac{z^3 - 1}{z^3} \cong 1 \quad (28)$$

$$E \equiv \frac{H}{2 C_p' (T_m - T_s)} \left(1 + \sqrt{1 + \frac{4 C_p' (T_m - T_s)}{3 H}} \right) \quad (29)$$

$$\frac{h' \alpha'}{k'} \frac{d\theta}{dx'} = E Z = E \left(\frac{h' x'}{k'} + 1 \right) \quad (30)$$

$$\theta = \frac{E}{2 \alpha'} x'^2 + \frac{k' E}{h' \alpha'} x' \quad (31)$$

FORM:

$$\theta = a x'^2 + b x' \quad (32)$$

$$x' = \frac{1}{\sqrt{a}} \sqrt{\theta + \frac{b^2}{4a}} - \frac{b}{2a} \quad (33)$$

$$\theta \gg \frac{b^2}{4a} \quad (34)$$

$$x' = \sqrt{\frac{2 \alpha' \theta}{E}} - \frac{k'}{h'} \quad (35)$$

STEEL Poured IN STEEL MOLD

$$x' = 0.71 \sqrt{\theta} - \frac{k'}{2h'} \quad (\text{FEET, HOURS}) \quad (36)$$

Equation (30): Approximate expression for the inverse freezing rate.

Comparison of the approximate freezing rate, Equation (30), with Equation (26) is provided by Figure 16. Since the curve must be integrated to yield thickness, x^θ , as a function of time, θ , it may be seen in Figure 16 that the area under the straight line is an excellent approximation of this integral, except at very early times.

Equation (31): Integrate (30).

Equation (32): Rewrite (31), using "a" and "b" for the constant coefficients.

Equation (33): Solve (32) for x^θ .

Equations (34,35): Another approximation valid for large values of time, or large values of h^θ .

Equation (35) is useful in understanding problems where contact resistance is not of controlling importance; for large contact resistances, Equation (31) must be used, and for very large contact resistance, an approximate treatment is possible which neglects temperature drop in the casting.

Equation (35) becomes applicable for large castings of a poor conducting metal. The most important and most thoroughly studied problem of this sort is the solidification of steel ingots. Using the assumed values shown in Table III, Equation (35) has been rewritten for the case of steel solidifying in a steel (or cast iron) mold. The

units are feet and hours. The slope is somewhat higher (1.1 in./ $\sqrt{\text{min.}}$) than that reported by most investigators.^{9,10,11}

TABLE III.

Thermal Properties of Steel

(B.T.U. - Ft. - Hr. - °F. - Lb.)

<u>Quantity</u>	<u>Value</u>	<u>Reference</u>
C_p	0.171	Kelley ²¹
H	119	Kelley ²¹
k	18	McAdams ²⁰
ρ	468	
T_m	2700	
T_r	70	

The disparity may be due to an error in the assumed properties, or to the assumption that the mold is initially at room temperature. When the findings of Chipman and FonderSmith,¹⁰ Spretnak,¹¹ and Pellini¹⁸ are plotted showing thickness as a function of the square root of time, the best straight line through the points may be extrapolated to zero time. The intercept on the x⁰ axis gives an estimate of the total coefficient of heat transfer, \bar{h} , at the mold-metal interface. The values so obtained range from 200 to 800 B.T.U. per Ft.²Hr.°F. If the sole mechanism of heat transfer across the mold-metal interface were radiation, the value would be approximately 100; this would be the case only if a very wide air-gap were to form. It is of importance that a variation in \bar{h} over the entire range indicated above would result in a very

minor shift in the solidification curve.

Two important conclusions may be drawn in connection with steel ingots: (1) The experimental observations of several investigators agree in form and magnitude with the theoretical relationship expressed by Equation (35). (2) The sudden formation of an air-gap during solidification would not markedly change the rate of solidification, although temperature distributions would be noticeably affected.

B. Spherical and Cylindrical Mold Walls; Nonwetting Contact.

To complete the picture of heat flow in solidification, it is necessary to consider the solidification of finite shapes cast into metal molds. This class of problems presents the greatest difficulties of all, but is of paramount practical importance.

1. Heat Flow Into Metal Molds.

Before proceeding with the solidification of finite shapes, there remains a heat flow problem not yet outlined: the transfer of heat through a contact resistance into a thick-walled spherical or cylindrical metal mold. The solution to this problem, in conjunction with the results of the previous section, can then be used to arrive at approximate solutions to practical solidification problems. At this point, consider an infinite region bounded internally by a sphere (thick-walled spherical mold), the region being initially at T_r . At zero time, the temperature of the medium within the cavity is raised to T_{sc} , and held constant. Newton's Law governs the flow of heat from the medium to the mold, and the coefficient of heat transfer is \bar{h} .

$$D' \equiv \frac{\bar{h}}{K} \quad (37)$$

$$D \equiv D' + \frac{1}{R} \quad (38)$$

$$\frac{T - T_n}{T_{sc} - T_n} = \frac{R D'}{n D} \left[\operatorname{erfc} \frac{n - R}{2\sqrt{\alpha \theta}} - e^{D(n-R) + D^2 \alpha \theta} \operatorname{erfc} \left(\frac{n - R}{2\sqrt{\alpha \theta}} + D\sqrt{\alpha \theta} \right) \right] \quad (39)$$

$$\frac{Q}{KA} = - \int_0^\theta \left(\frac{\partial T}{\partial n} \right)_{n=R} d\theta \quad (40)$$

$$- \frac{D}{D'} \frac{R}{(T_{sc} - T_n)} \left(\frac{\partial T}{\partial n} \right)_{n=R} = 1 + R D' e^{D^2 \alpha \theta} \operatorname{erfc} D\sqrt{\alpha \theta} \quad (41)$$

$$\frac{D^3}{D'^2} \frac{\alpha Q}{KA(T_{sc} - T_n)} \quad (42)$$

$$= \frac{D^2 \alpha \theta}{D' R} + \frac{2D\sqrt{\alpha \theta}}{\sqrt{\pi}} - \left(1 - e^{D^2 \alpha \theta} \operatorname{erfc} D\sqrt{\alpha \theta} \right)$$

Equations (37,38): Definition of D and D'' .

Equation (39): The solution to the problem outlined in the above paragraph, from Carslaw.^{1f}

Equation (40): Integrated Fourier Conduction Equation at the mold-metal interface.

Equation (41): Differentiate (39) with respect to " r ".

Equation (42): Integrate (41) as indicated in (40).

Equation (42) is the desired solution, giving the total heat which has entered the mold in time, θ . The solution to the corresponding problem for a cylindrical mold cavity is far too cumbersome to be practical. To handle this situation, the same artifice is used as in the case of sand castings: A square inch of a cylindrical mold surface is considered approximately equivalent to that of a spherical mold surface, if the sphere has twice the radius of the cylinder. In the following equations, " n " is approximately 0.5.

$$D = D' + \frac{m}{R} \quad (43)$$

$$\frac{D^3}{D'^2} \frac{\alpha Q}{KA(T_{sc} - T_r)} \quad (44)$$

$$= \frac{D^2 m \alpha \theta}{D' R} + \frac{2D\sqrt{\alpha\theta}}{\sqrt{\pi}} - \left(1 - e^{D^2 \alpha \theta} \operatorname{erfc} D\sqrt{\alpha\theta}\right)$$

APPROXIMATE SOLUTION

$$Q = KA(T_{sm} - T_r) \left(\frac{m\theta}{R} + \frac{2\sqrt{\theta}}{\sqrt{\pi\alpha}} \right) \quad (45)$$

$$Q = \bar{h} A (T_{sc} - T_{sm}) \theta \quad (46)$$

$$\frac{\alpha Q}{KAR(T_{sc} - T_r)} = \frac{\frac{\alpha\theta}{R^2} \left(m + \frac{2}{\sqrt{\pi}} \frac{R}{\sqrt{\alpha\theta}} \right)}{1 + \frac{k}{\bar{h}R} \left(m + \frac{2}{\sqrt{\pi}} \frac{R}{\sqrt{\alpha\theta}} \right)} \quad (47)$$

$$\frac{Q_c}{Q_H} = \frac{(1-V')^2}{4} \left(\frac{R^2}{\alpha'\theta} \right) \quad (48)$$

Equation (43): Rewrite (37) for a cylinder.

Equation (44): Rewrite (42) for a cylinder.

Justification for making the above approximation comes from two sources: (1) The freezing times of castings in metal molds are short enough to fall in the left-hand region of Figure 1, indicating that the "heated zone" is about as shallow as for sand castings. (2) If (39) is rewritten at $r = R$, an expression for the mold-surface temperature as a function of time is obtained for a sphere. Substituting (38) gives the approximate surface temperature for a cylinder. Carslaw^{1c} has plotted the exact surface temperature, and the approximate expression checks perfectly within the accuracy of the plot, for the times encountered in the freezing of castings.

It is convenient and informative to derive a relatively simple relation which closely approximates Equation (44). Assume that the mold surface has, during the time, " θ ", an average effective value, " T_{sm} ", constant and unknown. Then the heat which has entered the mold during this time is given by Equation (45), which was derived in Section III. The same amount of heat has crossed the mold-metal interface during the same length of time, giving Equation (46). The unknown "average" mold surface temperature may be eliminated between Equations (45) and (46), yielding Equation (47). Equation (47) is much more useful than (44), because the coefficient of heat transfer may be solved for algebraically. Equation (44) is transcendental in \bar{h} . Numerical problems may be solved using the simpler relation, and the results checked by Equation (44).

In all cases considered, (47) and (44) have been found to be in very close numerical agreement.

The concept of an average effective temperature has been carried one step further, and the casting surface temperature is considered to be constant and unknown during time, " θ ". This step makes it possible to combine the results of Section IV with those above to obtain freezing curves of thickness versus time. The procedure for doing this is outlined below, and exemplified for the case of lead freezing in a cylindrical cast iron mold. To facilitate numerical work, Figures 6 and 7, the cylindrical inverse rate curves, have been planimetrically integrated for fractional amounts of solidification, and the results are given in Figures 17 and 18. It was not necessary to treat the total-heat curves, Figures 12 and 13, the same way, for inspection of Figure 15 leads to Equation (48). Equation (48) estimates the ratio of specific to latent heat which has left a partially solidified cylinder.

2. Solidification of Lead in a Cast Iron Cylinder: Conductivities of Metal and of Mold Approximately Equal.

The procedure for developing a freezing curve for lead in a cast iron cylinder in stepwise fashion is as follows:

- a. Plot Equation (47) for the given combination of metal, mold, and contact resistance. This has been done in Figure 19.
- b. Select a value for v' , the radius of the liquid-solid interface. The problem is to solve for the time.

- c. Guess at T_{sc} .
- d. Use Figure 17 or 18 with (c) to get a value for time.
- e. Use Equation (48) to get a ratio of specific to latent heat.
- f. Use the above trial information to determine a point on the coordinates of Figure 19.
- g. Repeat (c) through (f) several times. Connect the points so obtained with a curve. Where the curve intersects Equation (47) represents the solution. These intersections are shown in Figure 19.
- h. Repeat (b) through (g) for other values of v^* , and so obtain the desired freezing curve. The time for each value of v^* is the solution of an independent problem.

The procedure described above amounts to the solution of three equations in three unknowns. The unknowns are (1) the time required for a given portion of the cylinder to freeze, (2) the total amount of heat removed during this time, and (3) the average effective casting surface temperature during this period of time. The casting surface temperature is a reference point in the relaxation system: it is the temperature which will cause a given amount of metal to freeze in the length of time required to deliver the correct amount of heat into the mold.

A calculated freezing curve for lead in cast iron is shown in Figure 20. The values for the thermal properties which were used are

listed in Table IV. The points on Figure 20 represent experimental data obtained from pour-out tests. The value of the heat transfer coefficient was chosen to give the best fit between theory and experiment; thus the experimental data represent a measurement of the heat transfer coefficient between lead and cast iron.

TABLE IV.

Thermal Properties of Cast Metals Used in Calculations

(B.T.U. - Ft. - Hr. - °F - Lb.)

<u>Quantity</u>	<u>Value</u>			<u>Reference</u>
	<u>Pb</u>	<u>Cu</u>	<u>Al</u>	
k°	18	200	155	20
ρ°	707	556	169	22
C_p°	0.0329	0.113	0.187	21
H	10.6	88.4	171	21
T_m	621	1983	1217	21

TABLE IV-A.

Thermal Properties of a Cast Iron Mold

<u>Quantity</u>	<u>Value</u>	<u>Reference</u>
k	28	20
ρ	450	22
C_p	0.130	21

The pour-out tests were conducted in an open-ended cast iron

cylinder, having a 2.25 inch inside diameter and 4.25 inch outside diameter. That this wall thickness is large enough to be considered infinite may be verified by comparison with the work of Pellini.¹⁸ In all tests, the metal was poured with zero superheat; the metal was poured from the melting crucible into a cold container, and after partial solidification, the remaining metal was poured into the test mold. High purity metals were used to obtain the smoothest possible liquid-solid interfaces. The open, bottom end of the mold rested upon a gypsum insulator during solidification, and after a specified time interval, the liquid was released by simply lifting the mold. Since the liquid-solid interface was not always a perfect cylinder, its radius was measured by measuring the area of the cross-section of the hole left in the casting.

In the calculation of the curve in Figure 20, a constant value of the heat transfer coefficient was used. Actually, the coefficient decreases (the contact resistance increases) as solidification progresses, since the mold tends to expand upon heating, and the solid portion of the casting tends to contract. The experimental points shown on Figure 20 indicate that the early stages of solidification were slightly more rapid than the calculated curve.

3. Solidification of Copper and Aluminum in a Cast Iron Mold; Conductivity of Metal Much Greater Than Conductivity of Mold.

Under this heading falls a very important variety of solidification problems, as yet very little studied. The following treatment applies to many small non-ferrous chill castings: permanent mold and

die castings and small ingots of aluminum, copper, and magnesium-base alloys.

A somewhat simpler procedure than that used for studying lead castings is applicable to this case. Assume, tentatively, that the gradients in the casting are small, and that most of the temperature drop takes place across the interface and in the mold. If this be true, little error will be introduced by assuming that the surface temperature of the casting is constant, and Equation (47) may be used directly to obtain freezing curves. The result may be checked with the aid of Figures 17 and 18.

Before using Equation (47), a suitable value for the casting surface temperature must be found. As a first approximation, the surface temperature of the casting is taken as the melting point. Equation (47) is then used to estimate the time for complete solidification, and a second approximation for the surface temperature is read from Figure 8. In many instances, the second approximation for the surface temperature will be only slightly below the melting point. Equation (47) may then be used with accuracy to determine the entire freezing curve of thickness as a function of time. This procedure has been applied to the solidification of copper and aluminum in a cast iron mold.

Pour-out tests have been used to study the solidification of copper in a cast iron mold, the procedure being identical with that described above for lead. The data are compared in Figure 21 with a

curve computed from Equation (47). The agreement between the curve and the experimental points is poorer than for the case of lead; the change in contact resistance during solidification appears to be greater with copper. Copper, with its high melting point, would be expected to cause a greater thermal expansion of the mold than lead. The value of the heat transfer coefficient which best fits the data, and for which the curve was drawn, was $350 \text{ B.T.U./}(\text{Ft.})^2(\text{°F.})(\text{Hr.})$. This value is higher than that for lead, because of the higher rate of radiation heat transfer across the gap between the metal and the mold. In making the calculation, the average temperature drop in the casting was found to be only 100°F .

In addition to copper, aluminum has been studied theoretically and experimentally by means of the techniques described above. The simple solution, using Equation (47) directly, may be justified for this case as well. The experimental points and computed curve for aluminum are presented in Figure 22. The value of the heat transfer coefficient, used to obtain the curve which best fits the data, is $930 \text{ B.T.U./}(\text{Ft.})^2(\text{Hr.})(\text{°F.})$. This value is much higher than that for either lead or copper, and the agreement between theory and experiment is quite good. Both of these observations suggest that the contact resistance does not markedly increase during solidification. Aluminum heats the mold less than copper and is a much better conductor than lead; as a result, neither expansion of the mold nor contraction of the casting is pronounced, and good physical contact is maintained for a longer time.

An important observation, which stems from the computations

made for copper and aluminum, is that the magnitude of the contact resistance is of controlling importance in determining the rate of solidification of small non-ferrous chill castings.

In Figure 23, the results of Alexander¹² for aluminum in a small cast iron mold are presented. The form and magnitude of the freezing curves agree well with the smaller casting studied in the subject investigation. In addition, the effect of very large amounts of superheat is seen to be quite minor. Alexander's curves may be used to verify a means for estimating the influence of superheat upon the time required for complete solidification: The superheat is added calorifically to the latent heat, and the calculation carried out as above.

TABLE V.

Definition of Terms Not Included in Tables I and II.

- \bar{h} = Heat transfer coefficient across mold-metal interface,
B.T.U./ $(\text{Ft.})^2(\text{Hr.})(^{\circ}\text{F})$.
- h' = Heat transfer coefficient between imaginary interface "plane" and casting surface.
- h = Heat transfer coefficient between imaginary interface "plane" and mold surface.
- $D^{\circ} = \bar{h}/k$
- $D = D^{\circ} + 1/R$
- T_a = Temperature in (metal) mold.
- T_b = Temperature in solid layer of metal during solidification.
- T_b° = Integration constant in Equation (2).
- T_{sc} = Temperature of casting surface.
- T_{sm} = Temperature of mold surface.
- $Z = h'x'/k' + 1$
- $E = \text{Constant defined by Equation (29)}$.
- $a, b = \text{Constants in Equation (32)}$.

ONE-DIMENSIONAL INVERSE
FREEZING RATE WITH CONTACT
RESISTANCE

$$\frac{h'x'}{k'} \frac{d\theta}{dx'}$$

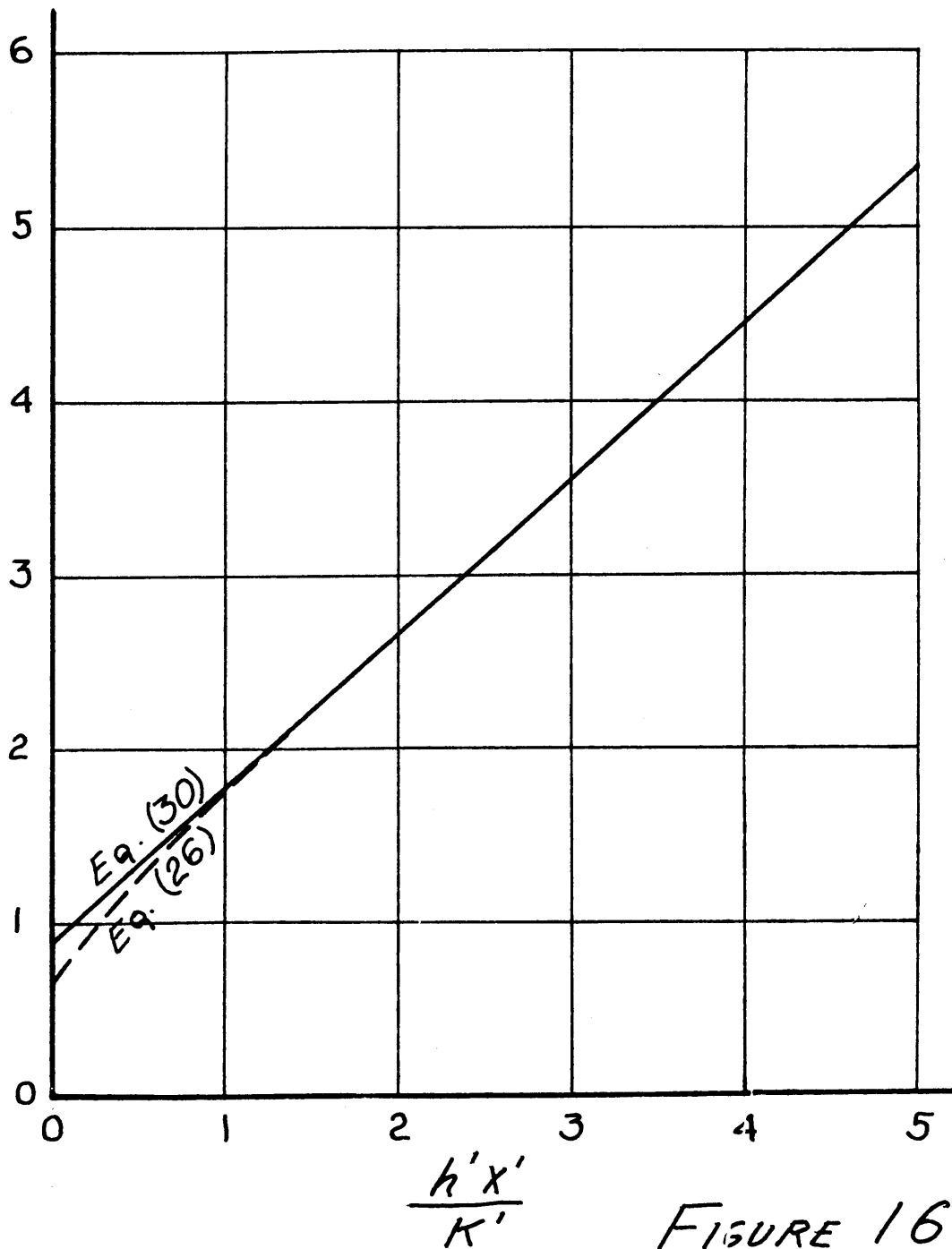


FIGURE 16

FREEZING TIMES FOR
PARTIALLY FROZEN
CYLINDERS

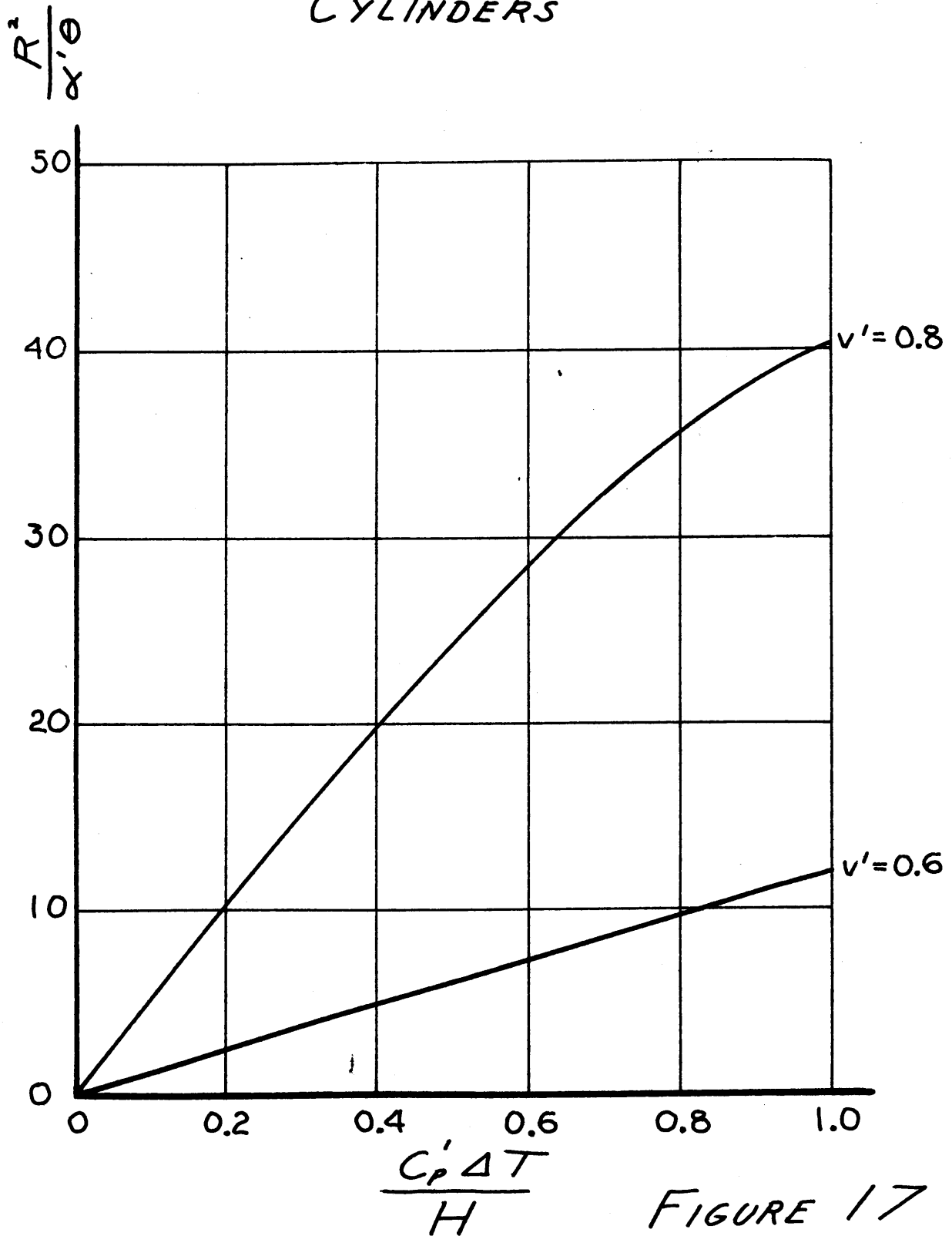
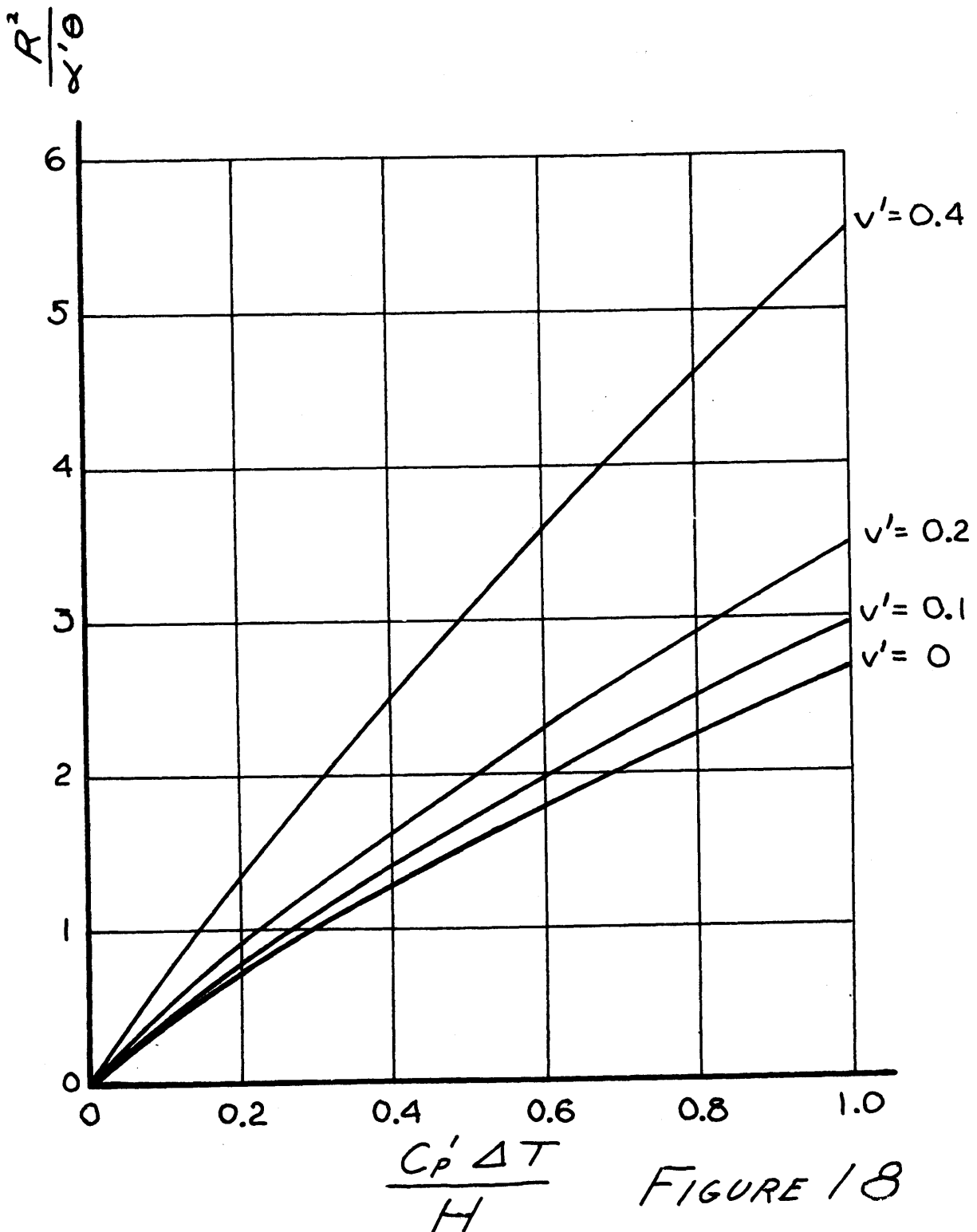


FIGURE 17

FREEZING TIMES FOR
PARTIALLY FROZEN
CYLINDERS



EQUATION (47): LEAD IN CAST IRON
CYLINDER

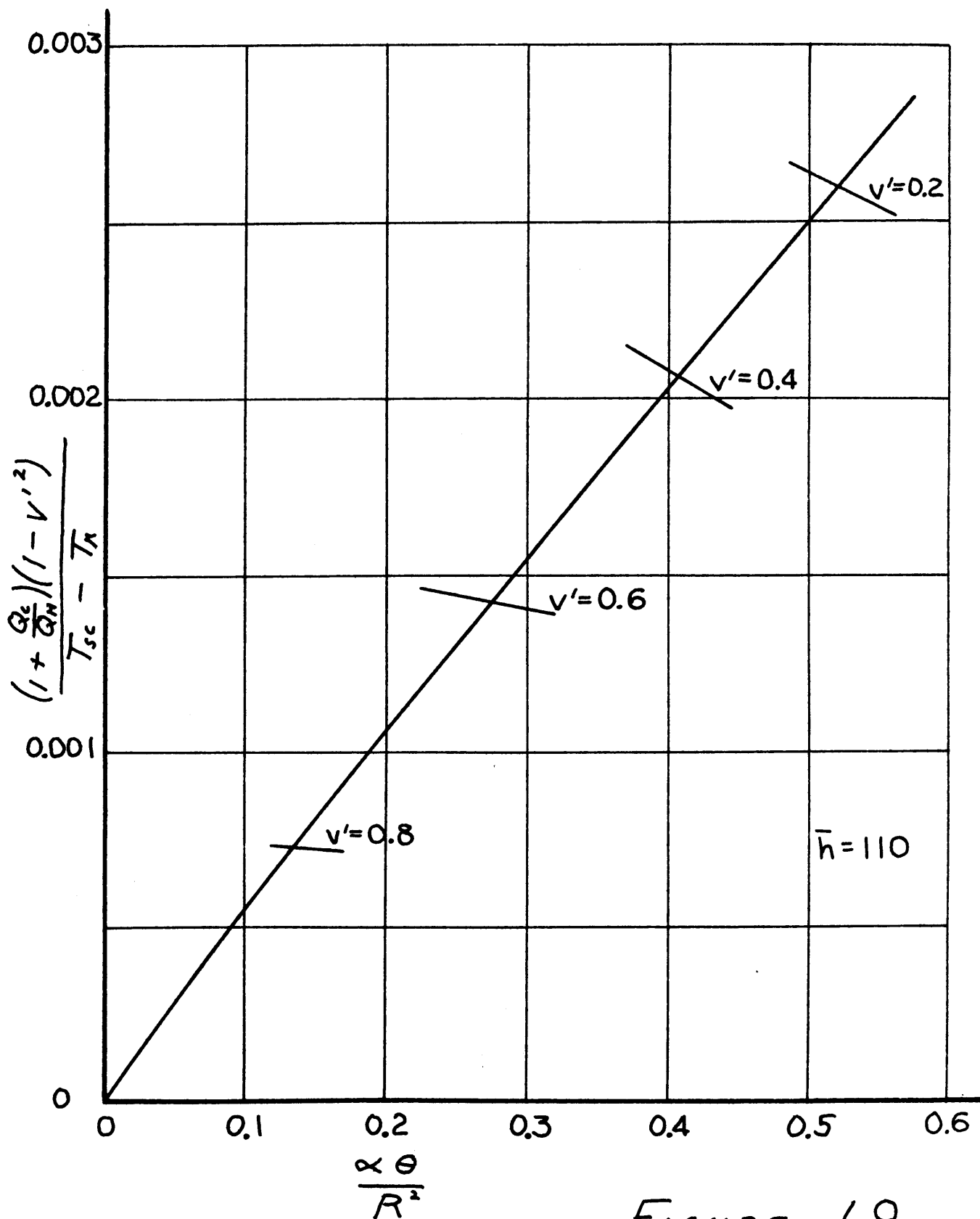


FIGURE 19

LEAD FREEZING IN CAST IRON
CYLINDER

THICKNESS VS. \sqrt{TIME}

$(R-r)$, INCHES

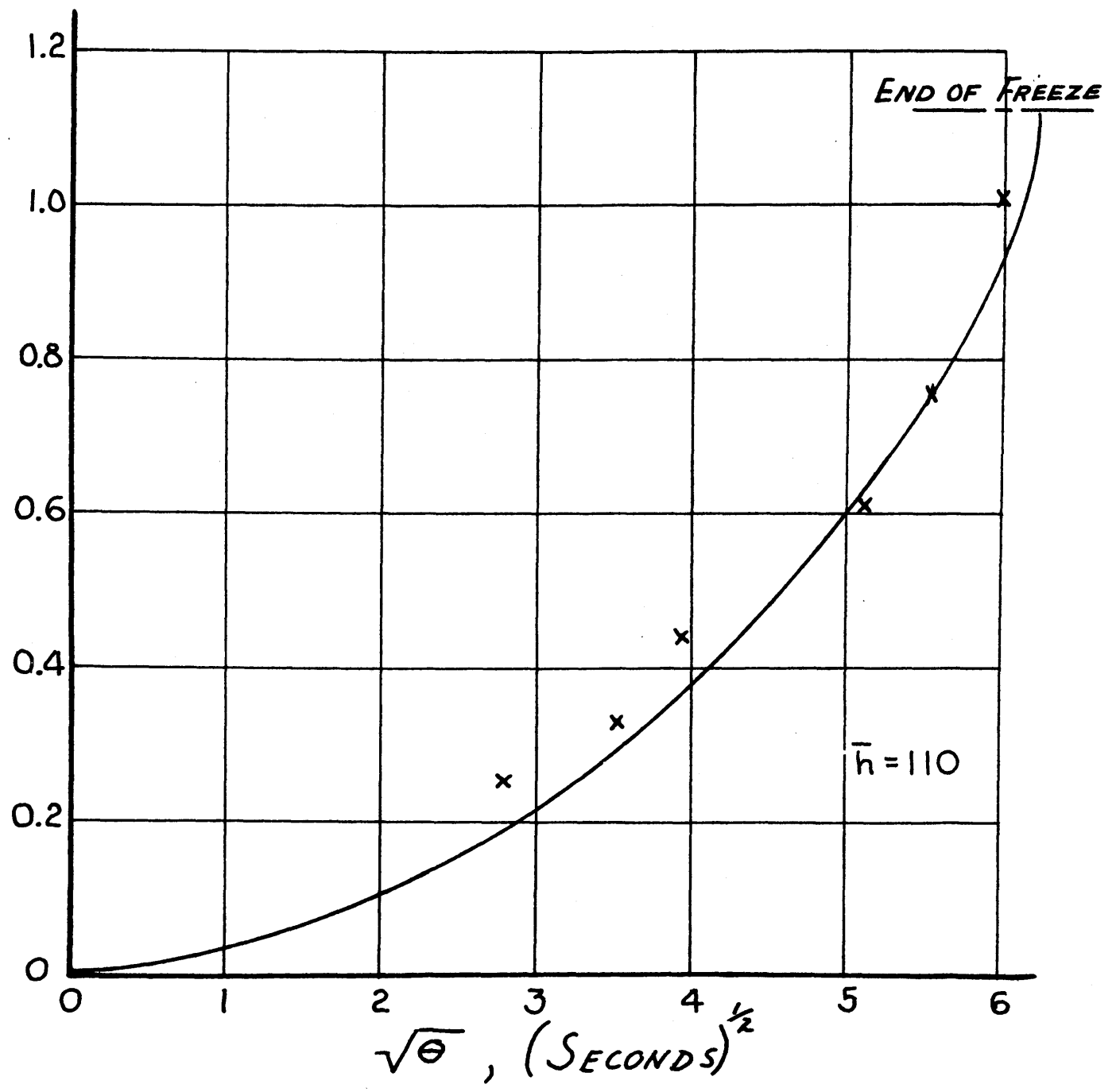


FIGURE 20

$(R-r')$, INCHES

COPPER FREEZING IN CAST IRON
CYLINDER

THICKNESS VS. \sqrt{TIME}

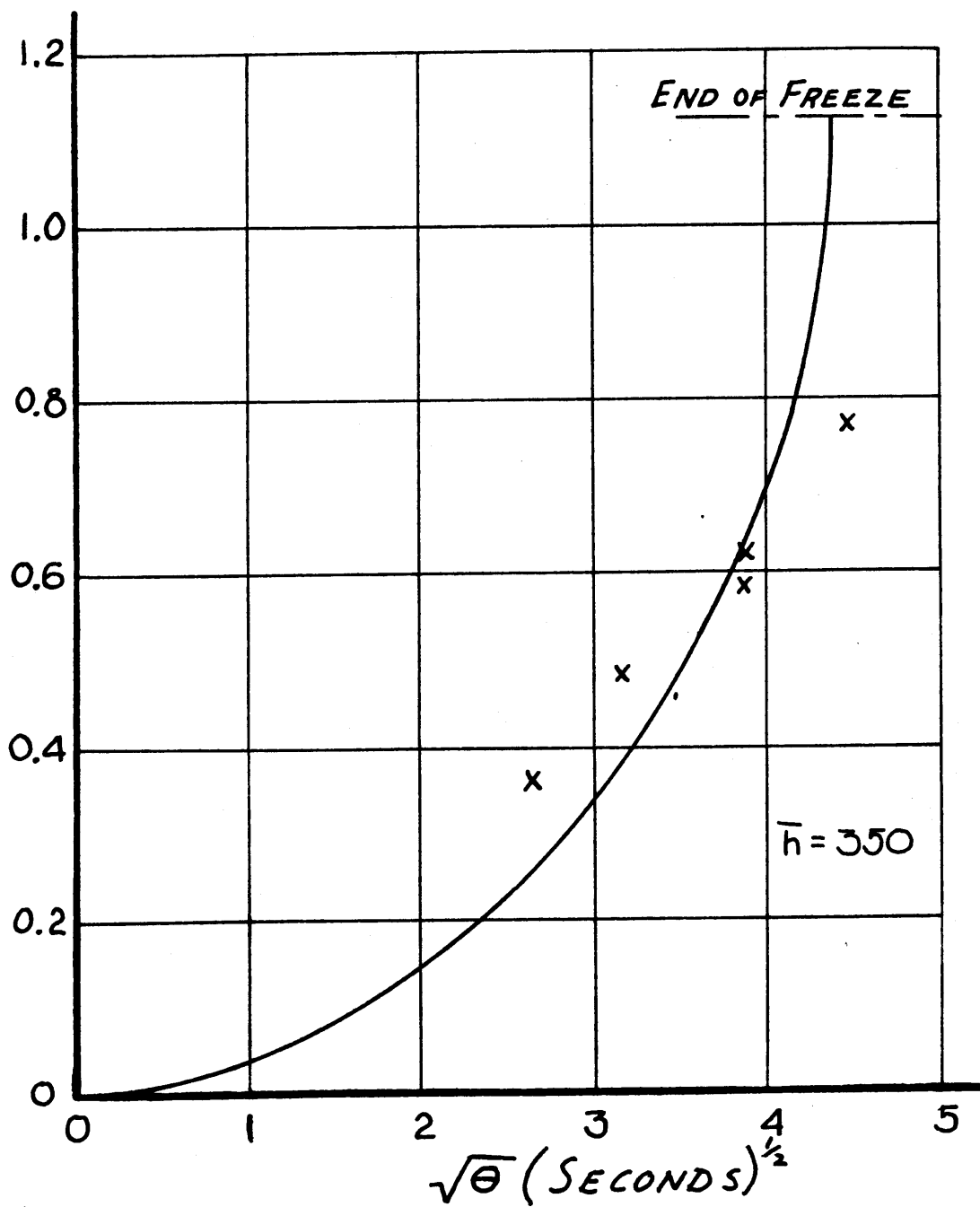


FIGURE 21

ALUMINUM FREEZING IN CAST IRON
CYLINDER

THICKNESS VS. \sqrt{t} TIME

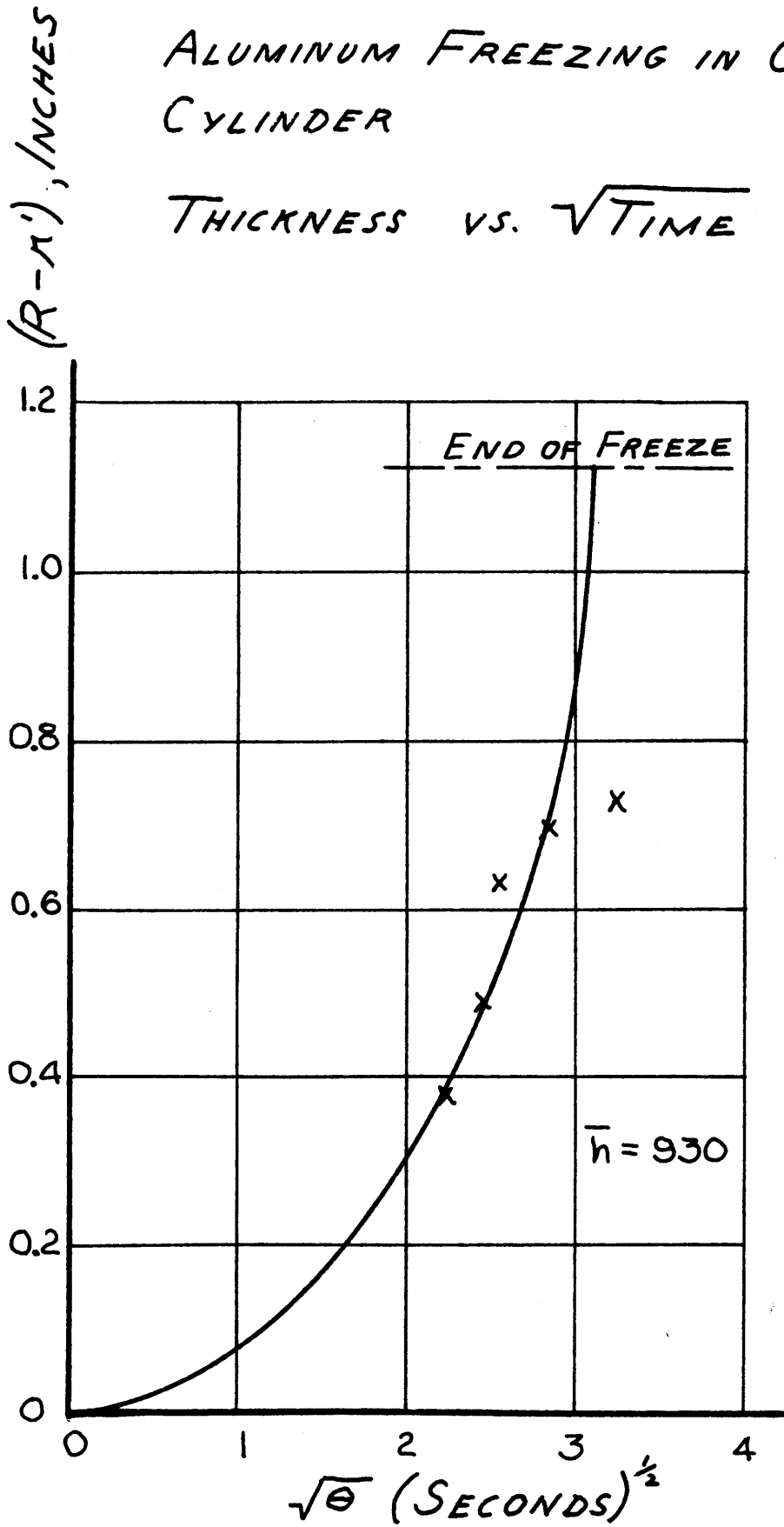


FIGURE 22

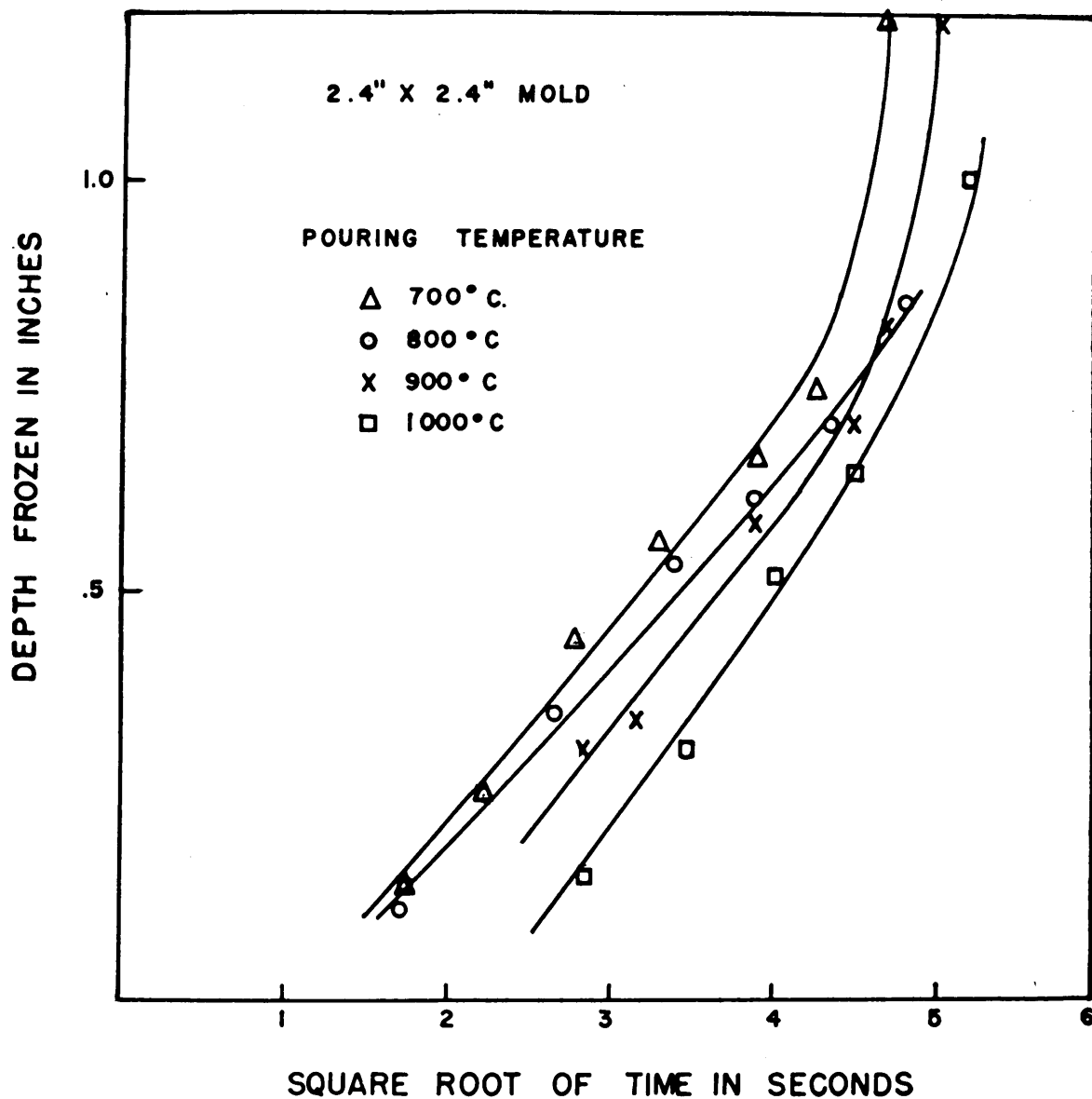


Fig. 23-Solidification curves for duralumin obtained at various pouring temperatures (2.4 in. x 2.4 in. mold).

VI. HEAT FLOW DURING SOLIDIFICATION OF CAST ALLOYS
WHICH FREEZE OVER WIDE TEMPERATURE RANGES

The purpose of this section is to provide a basis for applying the analytical results of preceding sections to the solidification of alloys.

A. Chilled Casting: Aluminum 4 Per Cent Copper Cast Against a Flat Copper Mold Wall.

In the solidification of an alloy of this type, latent heat of fusion is not evolved isothermally, but only upon cooling (except at invariant reaction temperatures, such as a eutectic). It is therefore possible to treat the latent heat of fusion, mathematically, as an increase in the apparent specific heat of the metal between the liquidus and solidus. When this is correctly done, the method of Neumann may be applied to the one-dimensional freezing of alloys.

A typical non-ferrous alloy cast against a copper mold has been chosen to exemplify the mathematics of alloy solidification. Before proceeding with the analysis, key physical constants must be known for the alloy, and an assumption made as to the mechanism of solidification. The physical constants which have been used are listed in Table VI, and these stem, in part, from the assumed mechanism of non-equilibrium solidification. Three premises are made in developing the required mechanism: (1) There is no diffusion of copper in the solid state. (2) There is no diffusion of copper in the liquid in a direction normal to the mold wall (no positive macrosegregation). (3) There is complete

TABLE VI.

Physical Values for Aluminum-4 Per Cent Copper Alloy

Terminal Solid Solubility	5.65% Cu
Eutectic Composition	33.0% Cu
Eutectic Temperature	1018°F
Liquidus Temperature	1193°F
Boundary Temperature Between Zones III and IV	1174°F
Zone IV, ρ_{4Cp4}	971 B.T.U./ $(\text{Ft.})^3(^{\circ}\text{F})$
Zone III, ρ_{3Cp3}	100.6 B.T.U./ $(\text{Ft.})^3(^{\circ}\text{F})$
Zone II, ρ_{2Cp2}	44.3 B.T.U./ $(\text{Ft.})^3(^{\circ}\text{F})$

diffusion of copper in the liquid in a direction parallel to the mold wall. On these bases, the fraction of metal solidified may be expressed as a function of the temperature for points between the liquidus and the non-equilibrium solidus. The method for making the calculation has been outlined by several investigators, including Scheil.²³

The proposed mechanism was felt to be the most realistic, and was chosen for this reason. However, the accuracy of the observations and conclusions which follow does not depend upon the assumed mode of freezing. The important objective is to set up a reasonable, coherent thermal picture for the solidification of an alloy, and examine its behavior under conditions of one-dimensional freezing. It will be seen that the purely thermal situation does not depend heavily upon the mechanism of solidification, although the metallurgical interpretation of thermal

$$\frac{1}{\alpha} \frac{\partial T}{\partial \theta} = \frac{\partial^2 T}{\partial x^2} \quad (T_1, T_2, T_3, T_4) \quad (1)$$

$$\frac{T_s - T_1}{T_s - T_n} = - \operatorname{erf} \frac{x}{2\sqrt{\alpha_1 \theta}} \quad (2)$$

$$\frac{T_2 - T_s}{T_2' - T_s} = \operatorname{erf} \frac{x}{2\sqrt{\alpha_2 \theta}} \quad (3)$$

$$\frac{T_3 - T_3''}{T_3' - T_3''} = \operatorname{erf} \frac{x}{2\sqrt{\alpha_3 \theta}} \quad (4)$$

$$\frac{T_4 - T_4''}{T_4' - T_4''} = \operatorname{erf} \frac{x}{2\sqrt{\alpha_4 \theta}} \quad (5)$$

$$A_T \quad x=0, \quad K \frac{\partial T_1}{\partial x} = K' \frac{\partial T_2}{\partial x} \quad (6)$$

$$A_T \quad x=x_2', \quad T_2 = T_e \quad T_3 = T_e \quad (7,8)$$

$$\frac{\partial T_2}{\partial x} - \frac{\partial T_3}{\partial x} = \frac{e'H}{K'} \frac{dx_2'}{d\theta} \quad (9)$$

$$A_T \quad x=x_3', \quad T_3 = \bar{T} \quad T_4 = \bar{T} \quad (10,11)$$

$$\frac{\partial T_3}{\partial x} = \frac{\partial T_4}{\partial x} \quad (12)$$

information is vitally affected.

The results of the calculation for non-equilibrium solidification are summarized by Figure 24, which shows heat content as a function of the temperature. The heat content is taken as zero for solid metal at the solidus temperature, and, of course, both latent heat and specific heat contributions are included in the computation. The dotted curve represents the exact function; the straight lines approximate the curve for purposes of analysis. 9.2 per cent of the alloy freezes isothermally at the eutectic temperature. The slopes of the straight lines correspond to the apparent specific heats which the metal has in these temperature ranges, and are reported in Table VI. The temperature at which the straight lines intersect is 1174°F.

When the metal is poured against the copper mold, it is assumed that perfect wetted contact occurs, and solidification progresses. That portion of the metal between 1174°F and the liquidus is referred to as Zone IV; the portion between the eutectic and 1174°F is Zone III; the completely solid layer of cast metal is Zone II; the copper mold is Zone I. The metal is poured at the liquidus temperature. All symbols not previously introduced are defined in Table VII.

Equation (1): The partial differential equation for linear heat flow must be satisfied in all four zones.

Equations (2) through (5): Particular solutions of the differential equation. T_5 is unknown, and T_2^I , T_3^I , T_3^{II} , and T_4^{II} are arbitrary constants, also unknown.

$$\beta_2 \equiv \frac{x_2'}{2\sqrt{\alpha_2\theta}} \quad \beta_3 \equiv \frac{x_3'}{2\sqrt{\alpha_3\theta}} \quad (13)$$

$$\frac{K(T_s - T_r)}{\sqrt{\alpha_1}} = \frac{K'(T_2' - T_s)}{\sqrt{\alpha_2}} \quad (14)$$

$$\frac{T_e - T_s}{T_2' - T_s} = \operatorname{erf} \beta_2 \quad (15)$$

$$\frac{T_2' - T_s}{\sqrt{\pi\alpha_2}} e^{-\beta_2^2} - \frac{T_3' - T_3''}{\sqrt{\pi\alpha_3}} e^{-\frac{\alpha_2}{\alpha_3}\beta_2^2} = \frac{\rho' H \beta_2 \sqrt{\alpha_2}}{K'} \quad (16)$$

$$\frac{T_e - T_3''}{T_3' - T_3''} = \operatorname{erf} \beta_2 \sqrt{\frac{\alpha_2}{\alpha_3}} \quad (17)$$

$$\frac{\bar{T} - T_3''}{T_3' - T_3''} = \operatorname{erf} \beta_3 \quad (18)$$

$$\frac{T_3' - T_3''}{\sqrt{\alpha_3}} e^{-\beta_3^2} = \frac{T_l - T_4''}{\sqrt{\alpha_4}} e^{-\frac{\alpha_3}{\alpha_4}\beta_3^2} \quad (19)$$

$$\frac{\bar{T} - T_4''}{T_l - T_4''} = \operatorname{erf} \beta_3 \sqrt{\frac{\alpha_3}{\alpha_4}} \quad (20)$$

As before, the procedure is to try to fit the above equations to the required boundary conditions, and solve for the unknown constants. If this can be accomplished, Equations (2) through (5) are the solutions. The temperature of the mold-metal interface is tentatively assumed to be constant; if (2) through (5) are solutions, T_s is constant.

Equation (6): The rate of heat flow is continuous at the mold-metal interface.

Equations (7,8,9): At the locus of the eutectic temperature, temperature in Zones II and III is fixed. The rate at which the eutectic reaction progresses into the casting is proportional to the difference in temperature gradient between Zones II and III. "H" in Equation (9) equals 9.2 per cent of the heat of fusion of aluminum.

Equations (10,11,12): The temperature at the boundary between Zones III and IV is fixed, and the temperature gradient at this boundary is continuous since there is no heat produced, but merely a change in specific heat.

Equation (13): Parabolic rate constants for the eutectic and the boundary between Zones III and IV. That these are constant is demonstrated by inserting conditions (7) and (10) into Equations (3) and (4).

When Equations (2), (3), (4), (5), and (13) are introduced into

boundary conditions (6) through (11), a transcendental system of seven equations in seven unknowns is obtained, Equations (14) through (20). When this system of equations is solved numerically, all of the unknown constants are determined. The equations are written in such an order that they may be easily solved by trial and error, using the following system:

- (a) Guess at β_3 .
- (b) Solve (20) for T_4'' .
- (c) Solve (19) for $T_3' - T_3''$.
- (d) Similarly solve (18), (17), (16), (15).
- (e) Plot the difference between the right- and left-hand sides of (14) versus the trial value of β_3 .
- (f) Repeat (a) through (e) for several trial values. Draw a curve through the points; where this curve crosses the zero axis is the solution.

The results of the above calculation for aluminum-4 per cent copper cast against a copper mold (perfect contact) is shown in Figure 25. Superposed on this figure is the corresponding temperature distribution for pure aluminum. Several features are noteworthy: (1) Because of the assumption of perfect contact, this abstract problem involves a more drastic chill than is ever realized in practice, except conceivably in continuous casting. Even with such steep gradients, the liquid-solid zone is as wide as the all-solid zone. (2) The discontinuity of the slope at the eutectic temperature is very slight. (3) In form, the curve for pure aluminum is closely similar to that for the alloy. This

observation is the most significant from a purely thermal standpoint. Solutions of more complex problems, such as were considered in previous sections, can be obtained for pure aluminum, and the results interpreted in terms of alloy solidification. Agreement between the two curves in Figure 25 becomes even closer, if the melting point of the pure aluminum is artificially lowered to the point where the alloy is half solid. The conclusion is that temperature gradients are much more dependent upon the total heat of fusion of an alloy than upon the mechanism of solidification.

$$\frac{T - T_n}{T_o - T_n} = e^{w^2} \operatorname{erfc} w \quad (21)$$

$$W \equiv \frac{\sqrt{KPC_p}}{\rho' C_p'} \frac{\sqrt{\theta}}{l} \quad (22)$$

$$\frac{T_e - T_n}{T_l - T_n} = e^{\bar{w}^2} \operatorname{erfc} \bar{w} \quad (23)$$

$$\bar{W} \equiv \frac{\sqrt{KPC_p}}{\rho' C_p''} \frac{\sqrt{\theta_f}}{l} \quad (24)$$

$$C_p'' \equiv \frac{H + C_p'(T_l - T_e)}{T_l - T_e} \quad (25)$$

$$Q_f = \frac{2 A_s K (T_m - T_n) \sqrt{\theta_f}}{\sqrt{\pi \alpha}} = C_p'' (T_l - T_e) A_s l \rho' \quad (26)$$

$$\frac{T_l - T_e}{T_m - T_n} = \frac{2}{\sqrt{\pi}} \bar{W} \quad (27)$$

$$\frac{T_m - T_e}{T_l - T_e} = \frac{\sqrt{\pi}}{2 \bar{W}} - \frac{e^{\bar{w}^2} \operatorname{erfc} \bar{w}}{1 - e^{\bar{w}^2} \operatorname{erfc} \bar{w}} \quad (28)$$

$$\frac{T_l - T_e}{T_l - T_n} < 0.25, \quad \frac{T_m - T_e}{T_l - T_e} \cong 0.20 \quad (29)$$

B. Sand Casting

When an alloy which freezes over a wide temperature range is poured into a sand mold, solidification takes place almost uniformly throughout the entire casting, since temperature gradients are very small. The casting freezes by cooling, and the heat flow problem is different than for a pure metal, since there is no "melting point". Again consider that the latent heat of fusion may be thought of as an increase in the apparent specific heat of the metal. The problem then approaches that of a fluid having high conductivity, and high specific heat which is cooling in contact with a sand mold. Consider that such a fluid is poured into a slab-type mold at zero time.

Equations (21,22): The temperature of the liquid as a function of time, Carslaw.¹⁹

Equations (23,24,25): Adapt the above solution to give the time θ_f required for an alloy, poured at the liquidus, to cool from the liquidus to the solidus, assuming that the latent heat is evolved as a linear function of temperature.

It is convenient to use the above result to determine an effective melting point for the alloy, which will give the correct solidification time.

Equation (26): Repeat the expression presented earlier giving the time required to freeze a pure-metal sand casting in terms of its melting point. The total heat removed is equated to that which leaves the alloy in cooling from the liquidus to the solidus.

Equation (27): Combine Equations (26) and (24).

Equation (28): Combine Equations (27) and (23).

Equation (29): If the solidification range is less than one-fourth the difference between the liquidus and room temperature, the right-hand side of Equation (28) is nearly constant. This is verified by the following brief table of values:

\bar{W}	$\frac{T_l - T_e}{T_l - T_r}$	$\frac{T_m - T_e}{T_l - T_e}$
0	0	0.215
0.1	0.1035	0.200
0.2	0.1910	0.196
0.3	0.2654	0.186

Equation (29) covers all the important alloys insofar as temperature ranges of solidification are concerned, but might be in error for castings poured into heated molds, since "room temperature" would then be raised. Errors introduced by using the melting point given by (29) will be less than one per cent, within the limitations indicated. The error from simply using the solidus temperature will be less than ten per cent.

An important side-development of the above analysis is the justification of a statement made in the section on sand castings: Superheat may be added calorifically to the latent heat with very small error. The cooling of a liquid metal, above its melting point, is the same problem as outlined above.

TABLE VII.

Definition of Terms Not Included in Tables I, II, and V.

- α_1 = Thermal diffusivity in mold.
 α_2 = Thermal diffusivity in solid cast metal.
 α_3 = Thermal diffusivity in Zone III.
 α_4 = Thermal diffusivity in Zone IV.
 C_p'' = Apparent specific heat of metal between liquidus and solidus, defined by Equation (25).
 T_1 = Temperature in the mold.
 T_2 = Temperature in solid cast metal.
 T_3 = Temperature in Zone III.
 T_4 = Temperature in Zone IV.
 $T_2^{\circ}, T_3^{\circ}, T_3'', T_4''$ = Integration constants.
 T_l = Liquidus temperature.
 T_e = Eutectic (or solidus) temperature.
 \bar{T} = Constant temperature of boundary between Zones III and IV.
 T_0 = Initial temperature of high-conductivity fluid in Equation (21).
 x_2° = Thickness of solid metal.
 x_3° = Distance from interface to boundary between Zones III and IV.
 $\beta_2 = \frac{x_2'}{2\sqrt{\alpha_2}\theta}$
 $\beta_3 = \frac{x_3'}{2\sqrt{\alpha_3}\theta}$
 W = Defined by Equation (22).
 \bar{W} = Defined by Equation (24).

HEAT CONTENT, $\frac{B.T.U.}{(FT.)^3}$

HEAT CONTENT OF AL-4% CU ALLOY VS. TEMPERATURE

REFERENCE: SOLID METAL AT EUTECTIC TEMP., HEAT CONTENT = 0

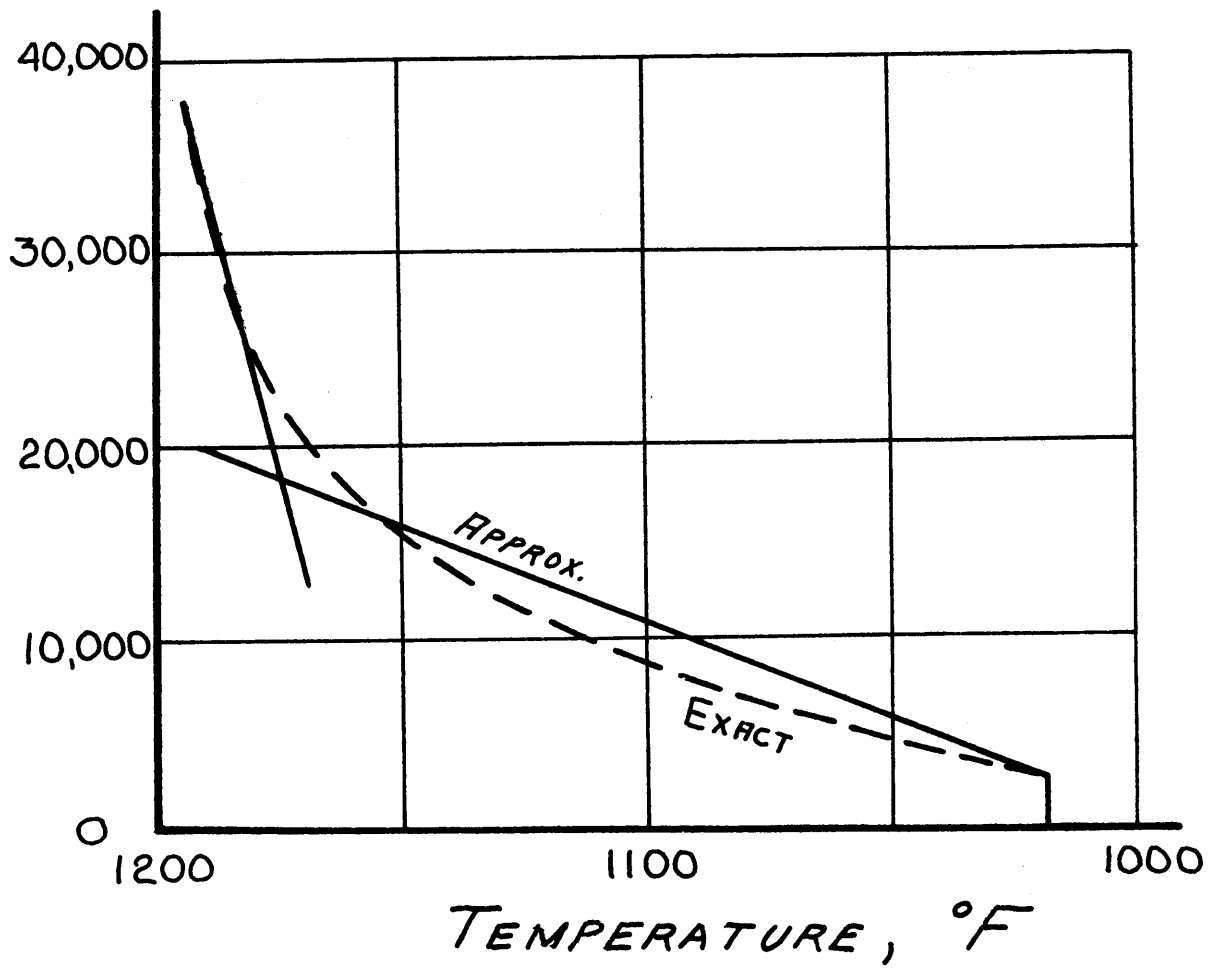


FIGURE 24

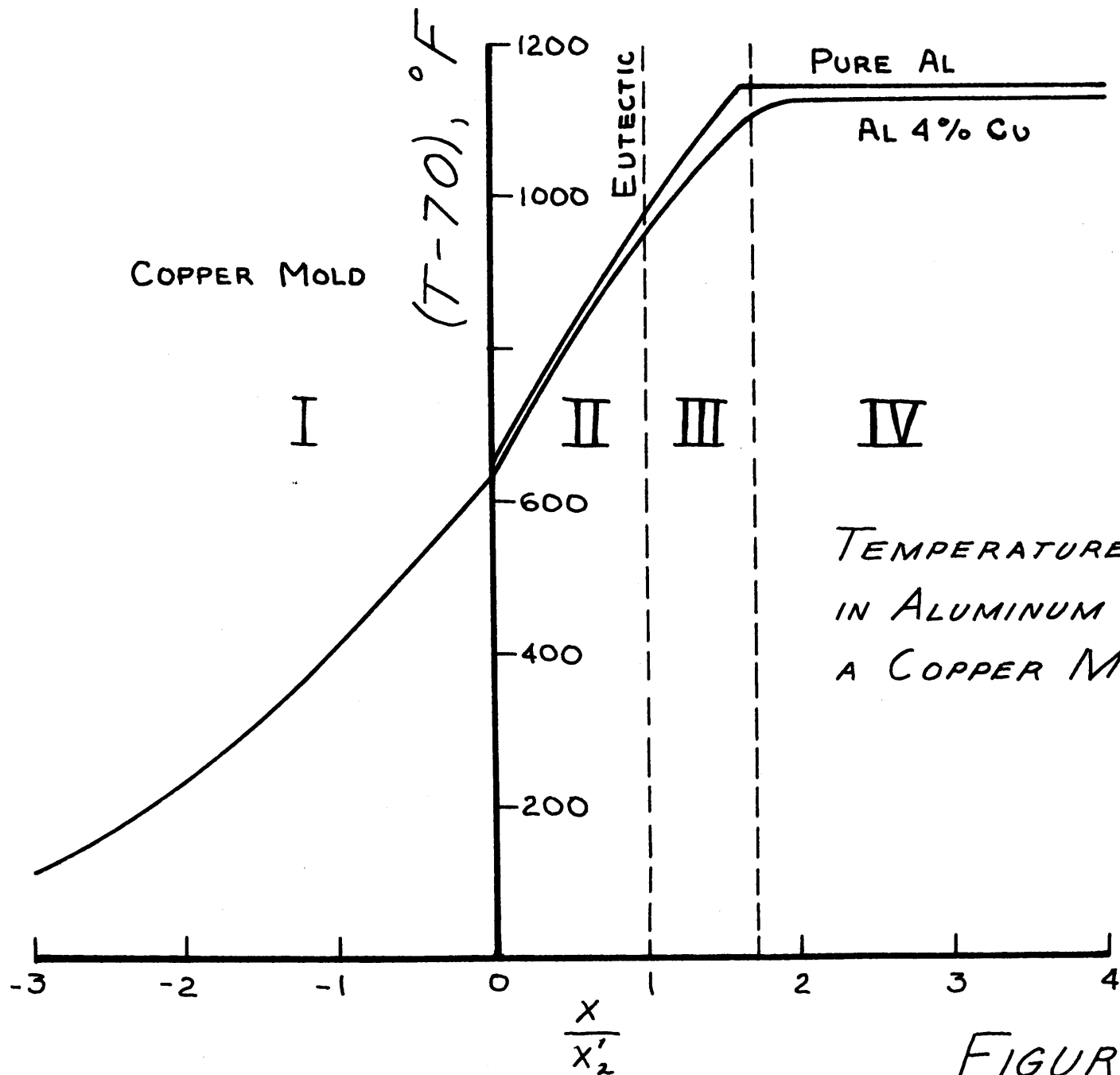


FIGURE 25

VII. CONCLUSIONS

A. Sand Castings

1. The heat which enters a sand mold may be expressed analytically as a function of time for plane, spherical, and cylindrical mold cavities. The development depends upon the metal being a much better conductor than the mold.

2. Chvorinov's Rule (freezing time proportional to the square of the ratio of volume to surface area) applies with some accuracy to castings having similar shape. Large errors may occur if the freezing times of slabs are compared with those of spheres or cylinders, using the Chvorinov relationship.

3. In calculating freezing times, superheat may be added calorifically to the latent heat of fusion, unless the superheat is abnormally high.

4. A sand cast alloy, which evolves its latent heat uniformly over the temperature range of freezing, is considered to have an "effective" melting point, and can so be adapted to the equations developed for pure metals. The "effective" melting point is one-fifth of the way from the solidus (or the temperature in question) to the liquidus.

B. Chilled Castings

1. An iterative method can be used to build power series solutions of simplified chilled casting problems: The freezing rates of plane,

spherical, and cylindrical castings with constant surface temperature and no superheat may be so studied. The method can also be applied when Newton's Law of Cooling prevails at the casting surface.

2. For metals cast into metal molds, an exact solution is known for only one situation: a flat, thick mold wall in perfect thermal contact with the metal. In this case, the physical interface temperature is constant.

3. Extending the concept of the interface temperature makes possible a judicious study of one-dimensional freezing in the presence of contact resistance at the mold-metal interface. The iterative method is used, and the results agree with experiment.

4. An approximate, relaxation procedure, which takes as a reference the casting surface temperature, yields information on the freezing of spherical and cylindrical castings, poured into metal molds.

5. Contact resistance is of determinative importance in the solidification of small chilled castings; it has only a minor effect on large steel ingots. The coefficient of heat transfer across a chill-metal interface may vary from 100 to 1,000 B.T.U./ $(\text{Ft.})^2(\text{Hr.})(^\circ\text{F})$, and depends upon the interface temperature (radiation) and the independent tendencies of the casting to contract and the mold to expand.

6. Small copper-, magnesium-, and aluminum-base chilled castings, made in ferrous molds, lend themselves to an accurate, simplified analysis which hinges upon a relatively constant casting surface

temperature.

7. Analysis of the one-dimensional freezing of an alloy in perfect contact with a chill mold, is feasible. The temperature distribution in an alloy freezing from a chill, is largely a function of its total heat of fusion and thermal conductivity. The mechanism of solidification has little net effect upon thermal conditions.

VIII. SUGGESTIONS FOR FURTHER WORK

1. Because of the importance of contact resistance in the solidification of small chilled castings, the properties of mold dressings used in permanent mold and die castings should be assessed from this standpoint. The success of flame-deposited lampblack in prolonging die-life, for example, is possibly related to its opaqueness and insulating properties.

2. Other problems in potential theory which involve the complication of change in phase, and which are important metallurgically, might be treated theoretically by an extension and broadening of the iterative procedures presented herein. The growth of a second phase, precipitated from a solid solution, where the rate is controlled by diffusion, is an example. The adaptation of some of these problems, through an iterative approach, to machine methods of computation, would be extremely valuable.

3. The measurement of high-temperature thermal properties, under casting conditions, is sorely needed.

4. The metallurgical characteristics of cast structures, as related to freezing rate and temperature gradients, should be studied using experimental techniques which permit sound thermal interpretation.

BIBLIOGRAPHY

1. H. S. Carslaw and J. C. Jaeger, Conduction of Heat in Solids, Oxford, 1947, p. 72.
 - 1a. Ibid, p. 41.
 - 1b. Ibid, p. 209.
 - 1c. Ibid, p. 280.
 - 1d. Ibid, p. 70.
 - 1e. Ibid, p. 71.
 - 1f. Ibid, p. 210.
 - 1g. Ibid, p. 248.
2. "Solidification of Steel in the Ingot Mold", A. L. Feild, Trans. Amer. Soc. Steel Treat., 11, 1927, p. 264.
3. "The Solidification of Molten Steel", N. M. H. Lightfoot, Proc. Lond. Math. Soc., 31, 1930, p. 97.
4. "Mathematics of Solidification Processes in the Casting of Metals", C. Schwarz, Z. angew. Math. u. Mech., 13, 1933, p. 202.
5. "Control of the Solidification of Castings by Calculations", N. Chvorinov, Giesserei, 27, 1940, pp. 177, 201, 222.
6. V. Paschkis, Trans. A.F.S., 52-61, 1945-53.
7. R. W. Ruddle, The Solidification of Castings, Institute of Metals, 1950.
8. "The Solidification and Crystallization of Steel Ingots", B. Matuschka, J. Iron Steel Inst., 124, 1931, p. 361.
9. "Solidification of Steel in Ingot Molds", L. H. Nelson, Trans. A.S.M., 22, 1934, p. 193.

10. "Rate of Solidification of Rimming Ingots", J. Chipman and C. R. FonDersmith, Trans. A.I.M.E., 125, 1937, p. 370.
11. "Kinetics of Solidification of Killed Steel Ingots", J. W. Spretnak, Trans. A.S.M., 39, 1947, p. 569.
12. "Solidification of Ingots", B. H. Alexander, Trans. A.F.S., 58, 1950, p. 270.
13. "Studies on Solidification and Contraction in Steel Castings", C. W. Briggs and R. W. Gezelius, Trans. A.F.A., 43, 1935, p. 274.
14. E. C. Troy, Steel Foundry Facts, 1943, p. 2.
15. "Methods Employed to Obtain Rates of Solidification", K. L. Clark, Trans. A.F.A., 53, 1945, p. 88.
16. "Solidification Rates of Aluminum in Dry Sand Molds", H. Y. Hunsicker, Trans. A.F.A., 55, 1947, p. 68.
17. "Reclaiming Steel Foundry Sands", Trans. A.I.M.E., 90, 1930, p. 83.
18. "Solidification of Metals", H. F. Bishop and W. S. Pellini, The Foundry, 80, 1952, p. 86.
19. "A Short Table of $\int_0^{\infty} \frac{e^{-\alpha u^2 \theta}}{\sqrt{J_0^2(uR) + Y_0^2(uR)}} \frac{du}{u}$ ", J. C. Jaeger and M. Clarke, Proc. Roy. Soc. Edinburgh, 61, 1942, p. 223.
20. W. H. McAdams, Heat Transmission, McGraw Hill, 1942, p. 380.
21. K. K. Kelley, Bureau of Mines Bulletin No. 476, U. S. Government Printing Office, 1949.
22. Metals Handbook, American Society for Metals, 1948.
23. "Bemerkungen zur Schichtkristallbildung", E. Scheil, Zeitschrift für Metallkunde, 34, 1942, p. 70.

BIOGRAPHICAL NOTE

The author was born in Detroit, Michigan on August 13, 1925, where he received primary and secondary school education. He entered the Massachusetts Institute of Technology in June, 1943, receiving his S.B. degree in June, 1949 and S.M. degree the following year. Service in the Naval Construction Battalions interrupted the author's education from 1943 to 1946. He has spent summers working for the Falk Corporation, Ingersoll-Rand, and the Steel Founders' Society of America, and was the recipient of a Foundry Educational Foundation undergraduate fellowship. The author is a member of Tau Beta Pi and Sigma Xi. Since 1950, the author has been in continuous residence at the Institute, where he was appointed Assistant Professor of Metallurgy in June, 1952.